HONOKIOL AND MAGNOLOL AS RENEWABLE RESOURCES FOR THE SYNTHESIS OF POLYMERS TOWARDS BIOMEDICAL AND ENGINEERING APPLICATIONS

A Dissertation

by

KEVIN T. WACKER

Submitted to the Office of Graduate and Professional Studies of
Texas A&M University
in partial fulfillment of the requirements for the degree of

DOCTOR OF PHILOSOPHY

Chair of Committee,	Karen L. Wooley
Committee Members,	Lei Fang
	Jaime C. Grunlan
	David C. Powers
Head of Department,	Simon W. North

May 2018

Major Subject: Chemistry

ABSTRACT

This dissertation has focused on the design, synthesis, and characterization of novel polymers derived from the renewable resources honokiol and magnolol. These natural products – isolated from *magnolia officinalis* – are highly functional and, thus, amenable to a broad range of synthetic organic transformations. The transformations explored in this work have yielded diverse monomers and, subsequently, polymer types which have included polycarbonates, thermosets, and olefin-based polymers that were studied for potential engineering or biomedical materials. A guiding theme in the development of polymers from honokiol and magnolol has been to control and vary the final polymer properties through the monomer design and polymerization chemistry. This work has used scalable syntheses, well-known chemistries, and, as the first examples of polymers synthesized from these natural products, it has laid the foundation to further explore material applications and new polymers based on honokiol and magnolol.

Poly(honokiol carbonate) (PHC) was synthesized in one step from honokiol using step-growth polycondensation techniques. Synthetic conditions were screened to yield polymers of varying molecular weight and the resulting polymers were studied in their thermomechanical and biological properties. PHC shares comparable thermomechanical properties with established engineering materials, both renewable- and petroleum-based, with which it was compared. Additionally, PHC serves as a good substrate for cell growth over an extended period of time.

In an effort to take advantage of both the phenolic and alkenyl functionalities of magnolol, thermoset syntheses *via* thiol-ene chemistry were performed directly from magnolol and with a library of magnolol-based monomers. The thermomechanical and hydrolytic degradation properties were controlled *via* monomer design in order to leverage beneficial biological effects, namely radical scavenging, in future biomedical applications. Degradation products and model compound studies showed antioxidant behavior similar to what has been observed for the natural product, magnolol.

A similar approach in controlling polymer properties through monomer design was realized in the synthesis of olefin-based polymers from magnolol through acyclic diene metathesis (ADMET) chemistry. Magnolol is an alkene-containing natural product and, as such, avoids the necessity to install alkene moieties that other renewable resources often require before metathesis chemistry. The rigid polymers displayed a wide range of glass transition temperatures (T_g) up to 180 °C after the initial polymerization. Additionally, several strategies were employed for post-polymerization modification and further tuning of the thermomechanical and physical properties.

DEDICATION

To my family and educators for providing the foundation to complete this work.

ACKNOWLEDGEMENTS

I would first like to acknowledge my advisor, Professor Karen Wooley. Her encouragement and support have allowed me to pursue my passion and the science that I have found most interesting over these last four years. The drive she instills to pursue more in my work has shaped this dissertation and, more broadly, my development as a scientist. Karen has shown me that, towards my chemistry, I should be constantly curious, never "hope" in scientific matters, to consistently use the Oxford comma (or don't), and to avoid sounding "pedestrian".

Secondly, I would like to thank my dissertation committee: Drs. Lei Fang, Jaime Grunlan, David Powers, and formerly, Daniel Romo. Their technical expertise, advice, and questioning, especially during the major milestones of my dissertation, have provided new approaches and lenses with which to analyze both the minutia and broader impacts of my work. This dissertation has also required expertise and know-how in a number of disciplines including chemistry, biochemistry, materials, and engineering. I am indebted particularly to my friend and collaborator Dr. Andrew Weems (TAMU, Biomedical Engineering & University of Warwick, Chemistry) who has helped me through numerous projects and problems, taught me about shape memory polymers and polyurethanes, and was never overly-critical of my ignorance in engineering and material matters. My dedicated collaborators, Soon Mi Lim and Sarosh Khan, were particularly helpful in carrying out all of the cell studies and their perseverance in the development and improvement of the biological areas of this work is appreciated. I am

also extremely thankful for my friends and confidants in the Wooley lab: Yi-Yun Timothy Tsao, Simcha Felder, and Samantha Kristufek, as well as the rest of the Wooley Lab, who have all been helpful in navigating both the science and trials of graduate school. Finally, I would like to thank the Wooley staff and managers (Justin Smolen, Andy Moutray, Sherry Melton, and Jeff Raymond) for all their help not just in teaching but in keeping the Wooley lab going. It has been fulfilling to work with so many researchers on problems we have found mutually interesting and I am thankful for their help, direction, and patience in teaching me.

Additionally, I would be remiss to not acknowledge all of the Administrative and Support Staff in the Chemistry Department, particularly the Graduate Office (Sandy Horton, Valerie McLaughlin, Dr. Joanna Goodey-Pellois, and Dr. Simon North), Business Operations (Ron Carter, Curtis Lee, Angie Stickley, Judy Ludwig, Julie Zercher, Angie Medina, and Melvin William), NMR facilities (Drs. Greg Wylie, Vladimir Bakhmoutov), Mass Spectrometry (Drs. Bo Wang, Doyong Kim, Yohannes Rezenom, and Ms. Vanessa Santiago), X-Ray Diffraction Laboratory (Joe Reibenspies), Electronics (Tim Pehl), Glass Blowing (Bill Merka), Machine Shops (Bill Seward), and IT (Steve Tran and Mike Green) – I am thankful for all that you have done, especially the work that often goes unnoticed by the students but keeps the Chemistry Department at Texas A&M running.

Finally, I want to thank to my mother and father for their support and guidance in life and throughout my education and to Christine for her continued patience and love over these past years of graduate school.

CONTRIBUTORS AND FUNDING SOURCES

Contributors

This dissertation was supervised by a committee of researchers at Texas A&M: Prof. Karen L. Wooley (advisor) of the Departments of Chemistry, Chemical Engineering, and Materials Science and Engineering; Prof. Lei Fang (committee member) of the Departments of Chemistry, and Materials Science and Engineering; Prof. Jaime Grunlan (committee member) of the Departments of Mechanical Engineering, Chemistry, and Materials Science and Engineering; Prof. David Powers (committee member) of the Department of Chemistry; Prof. Daniel Romo (former committee member) formerly of the Department of Chemistry.

In Chapter II, synthesis of poly(honokiol carbonate) and dynamic mechanical analysis was performed with the help of Dr. Samantha Kristufek of the Department of Chemistry. All cell culturing, confocal imaging, and cytotoxicity (MTT) assays were performed by Dr. Soon-Mi Lim and Ms. Sarosh Khan of the Department of Chemistry. Prof. Cynthia J. Meininger and Prof. Andreea Trache of the Texas A&M Health Science Center provided the coronary venular endothelial cells (CVECs).

In Chapter III, tensile testing was performed by Dr. Andrew Weems of the University of Warwick under the supervision of advisor Prof. Andrew Dove of the University of Warwick, both of the Department of Chemistry. Wet dynamic mechanical analysis was performed with the help of Dr. Andrew Weems. Cell culturing, confocal imaging, cytotoxicity assays, and reactive oxygen species assays were performed by Dr.

Soon-Mi Lim and Ms. Sarosh Khan. Degradation studies were performed, in part, by Ms. Simcha Felder. Drs. Bo Wang and Doyong Kim of the Laboratory for Biological Mass Spectrometry obtained mass spectra. Prof. Cynthia J. Meininger and Prof. Andreea Trache of the Texas A&M Health Science Center provided the coronary venular endothelial cells (CVECs).

In Chapter IV, all computational calculations were performed by Mr. Yi-Yun Timothy Tsao.

All other experiments were carried out independently by the student.

Funding Sources

The work in Chapter II was made possible by financial support from the National Science Foundation (CHE-1410272) and the Welch Foundation through the W. T. Doherty-Welch Chair in Chemistry (A-0001).

The work in Chapters III and IV was funded by the National Science Foundation (CHE-1610311) and the Welch Foundation through the W. T. Doherty-Welch Chair in Chemistry (A-0001).

The contents are solely the responsibility of the authors and do not necessarily represent the official views of the National Science Foundation or the Welch Foundation.

NOMENCLATURE

ADMET	Acyclic diene metathesis
ATR	Attenuated total reflectance
BHT	Butylated hydroxytoluene
BPA-PC	Poly(bisphenol A carbonate)
CDI	1,1'-Carbonyldiimidazole
CVEC	Coronary venular endothelial cell
DCFDA	2',7'-dichlorofluorescin diacetate
DCM	Dichloromethane
DFT	Density functional theory
DIPEA	*N*,*N*-Diisopropylethyl amine
DMA	Dynamic mechanical analysis
DMF	*N*,*N*-Dimethylformamide
DMPA	2,2-Dimethoxy-2-phenylacetophenone
DMSO	Dimethyl sulfoxide
DP_n	Degree of polymerization
$DPPH^{\bullet}$	2,2-diphenyl-1-picrylhydrazyl radical
DSC	Differential scanning calorimetry
EtOAc	Ethyl acetate
FTIR	Fourier-transform infrared
G1	Grubbs Catalyst™ 1st generation

G2	Grubbs Catalyst™ 2nd generation
IC_{50}	Half maximal inhibitory concentration
M_n	Number average molecular mass
MA	Magnolol acetonide
MAG	Magnolol
MBAC	Magnolol di(allylcarbonate)
MBAE	Magnolol di(allylether)
MEE	Magnolol ethylether
MeOH	Methanol
MPE	Magnolol propylether
MTS	3-(4,5-dimethylthiazol-2-yl)-5-(3-carboxymethoxyphenyl)-2-(4-sulfophenyl)-2H-tetrazolium, inner salt
NMR	Nuclear magnetic resonance
PETMP	Pentaerythritol tetrakis(3-mercaptoproprionate)
PHC	Poly(honokiol carbonate)
PIC	Poly(isosorbide carbonate)
PLA	Poly(lactic acid)
PMA	Poly(magnolol acetonide)
PMEE	Poly(magnolol ethylether)
PMPE	Poly(magnolol propylether)
PTFE	Polytetrafluoroethylene
ROMP	Ring-opening metathesis polymerization
SEC	Size-exclusion chromatography

tBHP	*tert*-Butyl hydroperoxide
T_d	Thermal degradation onset temperature
T_g	Glass transition temperature
T_m	Melting transition temperature
TEA	Triethylamine
TGA	Thermogravimetric analysis
UV	Ultraviolet
VIS	Visible
5-HMF	5-Hydroxymethylfurfural

TABLE OF CONTENTS

LIST OF FIGURES

Page

LIST OF TABLES

Page

CHAPTER I

INTRODUCTION

1.1 Background and Motivation

In August 2016, 60 academic, government, and industry leaders in polymer science and engineering met for a NSF Workshop entitled "Frontiers in Polymer Science and Engineering" to address both global challenges and opportunities for the community, as well as to put forth ideas to tackle these opportunities and advance the polymer science field. Renewable polymers – broadly, polymers containing renewable elements at some stage of their life cycle – were significant components of the program. This workshop was but one piece of a much larger international movement addressing renewability in the chemical industry. Currently efforts and pressures from government, society, and academics in the form of review boards, special interest groups, and regulations are driving chemical industry[1-3] (not just the field of polymer science and engineering,) to work in a sustainable and renewable manner. "Renewable" thus has come to take on a number of meanings and components of renewability may be incorporated at many points during polymer lifetime. For example, renewable resources such as natural products[4-5] or metabolites[6] that are produced by nature may be used as raw materials in the synthesis of renewable polymers. Other efforts towards renewability focus on using enzymatic- and microbial-based synthetic methods[7-9] or to recycle gases such as carbon dioxide and carbon monoxide[10-14] in the synthesis of

renewable polymers. Finally, understanding the timescale on which a polymer may be useful in an application is quite important. Subsequently incorporating degradation features[15-19] into the design of the renewable polymer or identifying bacterial species or enzymes that degrade particular polymers[20] could allow for recycling[21-22] and reuse[23-24] of renewable polymer components.

There has been a long history of using natural products or renewable resources in the synthesis of polymers or using biopolymers produced in nature. Cellulose, the most common biopolymer on earth, has been used as a chemical raw material for over 150 years in applications for cotton, fibers, polymer supports, films, and composites.[25] Other biopolymers, such as natural rubber, or 1,4-polyisoprene, have been a foundation for entire industries like those that rely on elastomers.[26] Similarly, with improvements in synthetic chemistry and industrial technology relating to the extraction, processing, and production of small molecules from renewable resources[27-29], many new, renewable building blocks are now used in the synthesis of polymers with interesting architectures, thermomechanical, and physicochemical properties in both academia and industry. The renewable feedstocks that are currently of great interest on an industrial scale include sugars, lignin, and oils.[30-31] In response to the availability and potential of these feedstocks, government has funded initiatives in the United States, including the Department of Energy's $12.9B contract (Contract ID: DEAC0576RL01830) with Battelle Memorial Institute, to continue developing process technology toward the production of "Top Value Added Chemicals from Biomass". Industry leaders have similarly taken steps to develop new products from these defined value added chemicals

(Figure 1-1): BASF, Avantium, Avalon, and Eastman are developing polymers from 5-Hydroxymethylfurfural (5-HMF) – one application being the replacement of PET used in packaging.[32] Mitsubishi Chemical currently offers poly(isosorbide carbonate)[33] with improved optical properties compared to well-established, industry standard bisphenol A polycarbonate. Itaconix, a long-time producer of itaconic acid-based products, partnered with AkzoNobel in 2017 to bring itaconic acid polymers to the coatings and construction industries.[34] Meanwhile, Succinity[35], BioAmber[36], and Reverdia[37] have commercialized processes to produce bio-based succinic acid from fermentation of sugar as a drop in replacement of petrochemically-based succinic acid commonly used in polyesters, polyamides, and polyurethanes.[38]

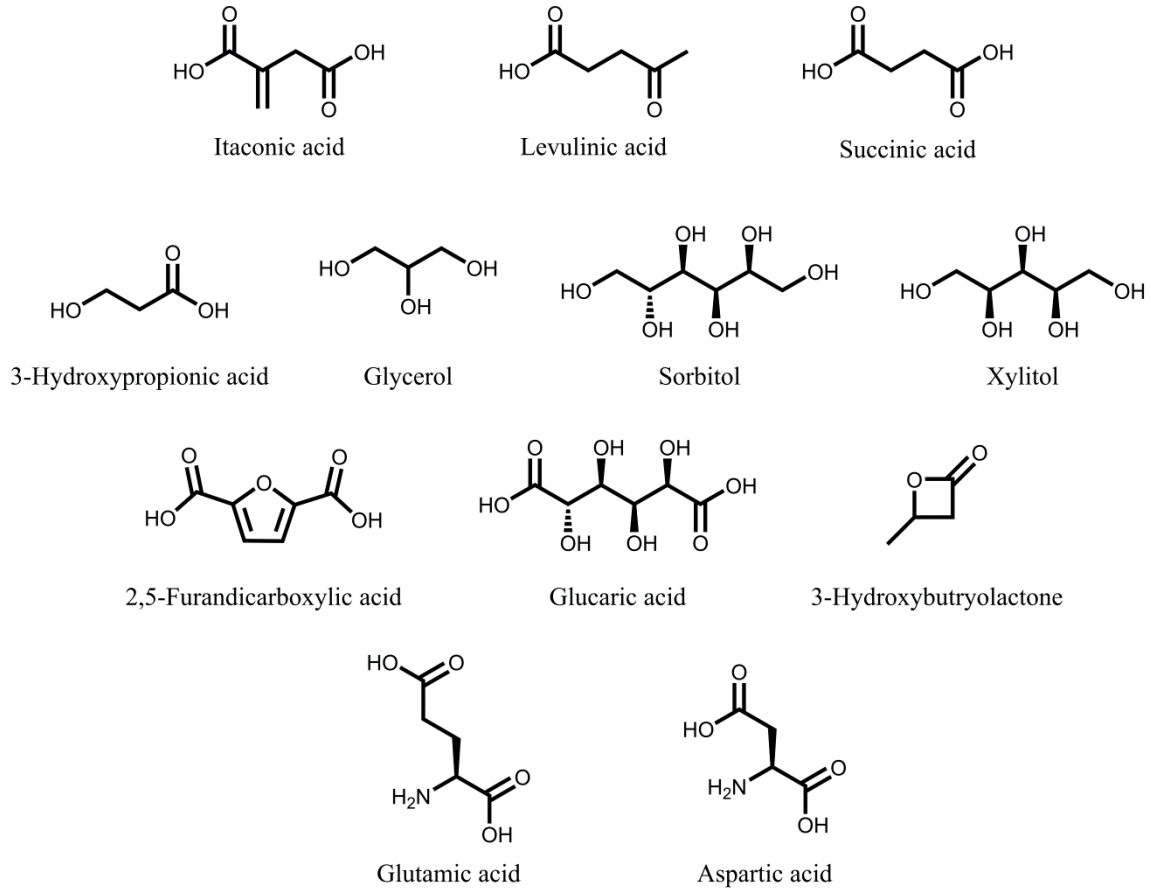

Figure 1-1. Structures of Twelve "Top Value Added Chemicals from Biomass" Identified by the Department of Energy Through the Pacific Northwest National Lab and the National Renewable Energy Lab.

The volume of production in industry requires straightforward chemistry, scalable technologies, and competitive costs compared to the more fundamental developments of renewable polymers at an academic level. At the academic level, higher-cost natural products and chemistries may be used in multistep syntheses of new monomers and polymers based on terpenes[39] or flavonoids[40], for example. These academic forays into lower volume, higher cost raw materials serve several important

purposes: (1) they add to chemical knowledge through fundamental understanding and application of reactions[41,42] to natural product substrates, (2) help elucidate and expand upon polymer structure-property relationships, and (3) ultimately introduce new monomers and polymers for which there may be no petrochemically-based equivalent by taking advantage of the breadth of natural product chemical and structural diversity. This last point is the foundation by which new, renewable resources may one day be converted into beneficial products for society and reduce reliance on petrochemically-derived polymers. Furthermore, it would be advantageous to translate the therapeutic or biochemical properties of a renewable resource into a polymer in its final application.

One important distinction should be made and, that is, although this aim to replace petrochemically-based resources with natural products/renewable resources for polymer production is a goal in and of itself, it does not necessarily mean that all renewable polymers are degradable or will have no net effect on polymer waste or the environment.[43] However, when it is desired, polymeric materials may also incorporate degradable features by harnessing the chemical diversity of natural product starting materials and introducing these properties with synthetic polymer chemistry techniques. Degradable and bioresorbable, renewable polymers are certainly aims in the field as it has been estimated in 2012 that over one hundred million metric tons of plastic end up littered and unrecycled per year.[2] In the same vein, not all choices of chemical reagents in the synthesis of new, renewable polymers will be either economical or waste-minimizing with respect to large scale applications. However, this is yet another aim that is also eventually required to advance the ideals of renewability in polymer science.

1.2. Neolignans – Honokiol and Magnolol

Although the chemical and structural diversity of natural products is exceptionally large – it is estimated that there are over one million natural products produced in plants alone[44] – their potential use in polymeric materials, even at an academic level, requires easy access to quantities sufficient to produce bulk materials. The Wooley lab has identified renewable resources which are amenable to bulk material production including polyols and phenols such as glucose[45-47], quinic acid[48], isosorbide[49], ferulic acid[50], tyrosine[51], quercetin[40], and other peptide-based[52,53] structures. Polymers from these renewable resources are possible on account of their availability from both plant and food sources[54-56], as well as their chemical functionality which makes them amenable to synthetic organic transformations into readily-polymerized monomers.

Two classes of natural products that have not been investigated previously for the production of renewable polymers are lignans and neolignans. (Neo)lignans are structurally diverse scaffolds that are synthesized through the oxidative dimerization of a core phenylpropanoid (C_6-C_3) unit and exist in nature in the stem, leaf, bark, root, and seeds of over seventy plant families[57] both in free form and as glycoside derivatives.[58] Neolignans are structurally different from lignans and classified by the dimerization linkage (Figure 1-2): when dimerization occurs at C_8 (also referred to as the β-carbon of the propyl moiety) of both phenylpropanoid cores, the natural product belongs to the "lignin" class. Any structure that does not contain a C_8-C_8' bond is broadly classified as

a "neolignan".[59] Lignans and neolignans are synthesized from cinnamic acid derivatives originating from chorismic acid produced *via* the Shikimate metabolic pathway.[54] Based upon the structural connectivity and variations in oxidation along the backbone, lignans are further subdivided into eight groups while neolignans contain fifteen subgroups, only two of which are shown in Figure 1-2.

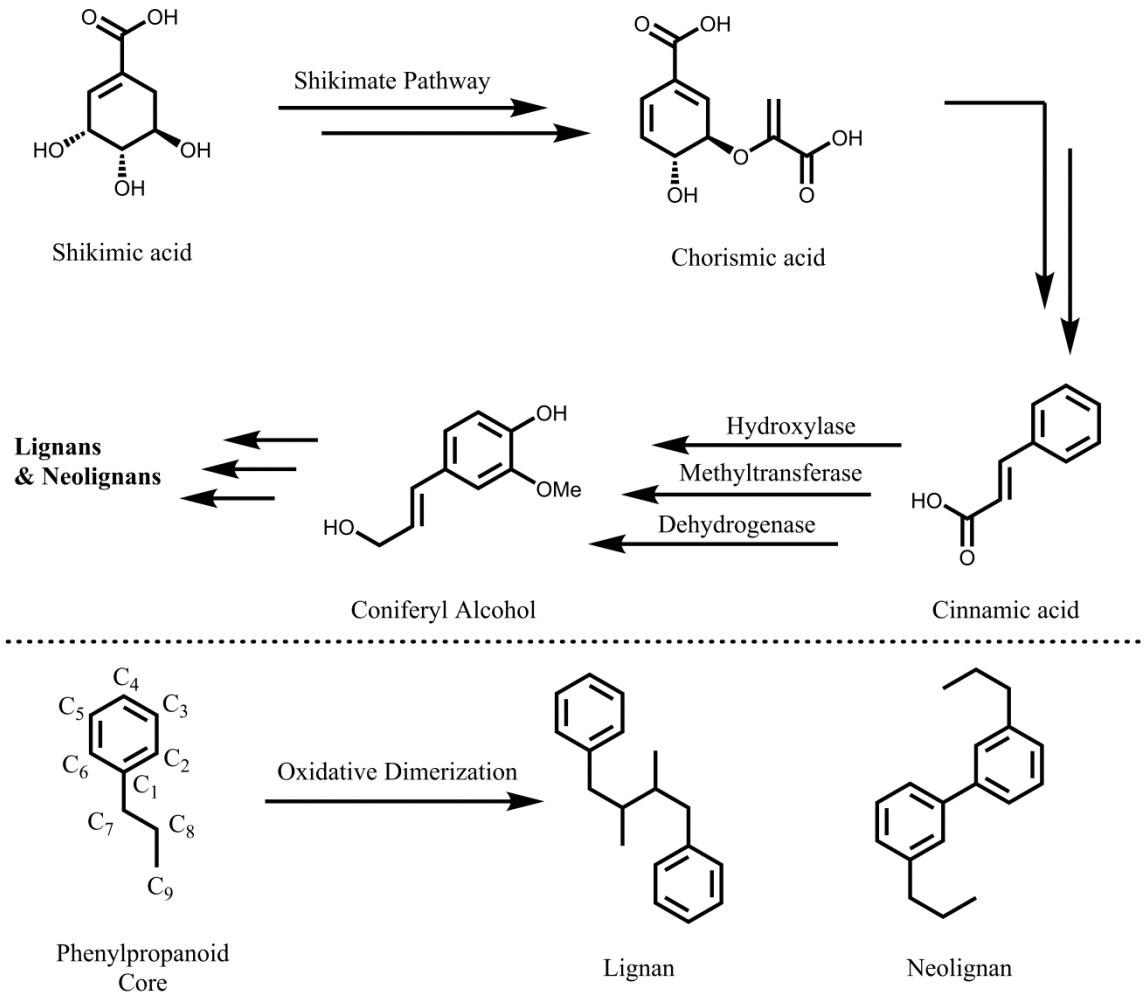

Figure 1-2. General Biosynthetic Pathway to Lignans and Neolignans

Of the neolignans, honokiol and magnolol can be found in relatively high concentrations of several percent by weight throughout a number of plants in the *Magnolia* family.[60-61] Currently, honokiol and magnolol are harvested from the bark of *Magnolia officinalis*, *Magnolia obovata*, and *Magnolia grandiflora* which are native to China, Japan, and the United States. Typically found as mixtures, advances in separation[62-65] have led to efficient isolation of single, pure compounds. Their longstanding use in traditional Chinese medicine have led to studies for a number of therapeutic applications, while total syntheses[66-70], as well as derivative syntheses[71-75] particularly for biochemical assays, are reported.

One potential advantage of using a natural product, such as honokiol or magnolol, in polymeric materials is to leverage therapeutic benefits in a targeted application. In this way, the therapeutic potential of the natural product[76-80] may present in the polymer itself, or the designed degradation of a honokiol- or magnolol-based polymer would produce a small molecule to exert a beneficial biological effect. In a similar fashion, the designed degradation of the polymer back to the unadulterated natural product would not add to polymer waste or microparticle accumulation in waterways. This would be possible particularly in cases where hydrolytically labile carbonyl backbones, *i.e.* polyester or polycarbonate, are present.

From a synthetic polymer chemistry perspective, honokiol and magnolol are extremely attractive for monomer and polymer design given that they are highly functional, containing both allylic and phenolic moieties. Both the allylic and phenolic moieties are suitable for selective transformations and both are amenable to broad

number and types of chemical transformations, in general. For example, in this thesis, only a small subset of these transformations are outlined in Figure 1-3 wherein polycarbonates, olefin materials, and thermosets may be accessed in short synthetic sequences. Honokiol and magnolol are also readily available to apply these synthetic sequences with current pricing $ 0.75/gram (on kilogram batches) in 98% purity.

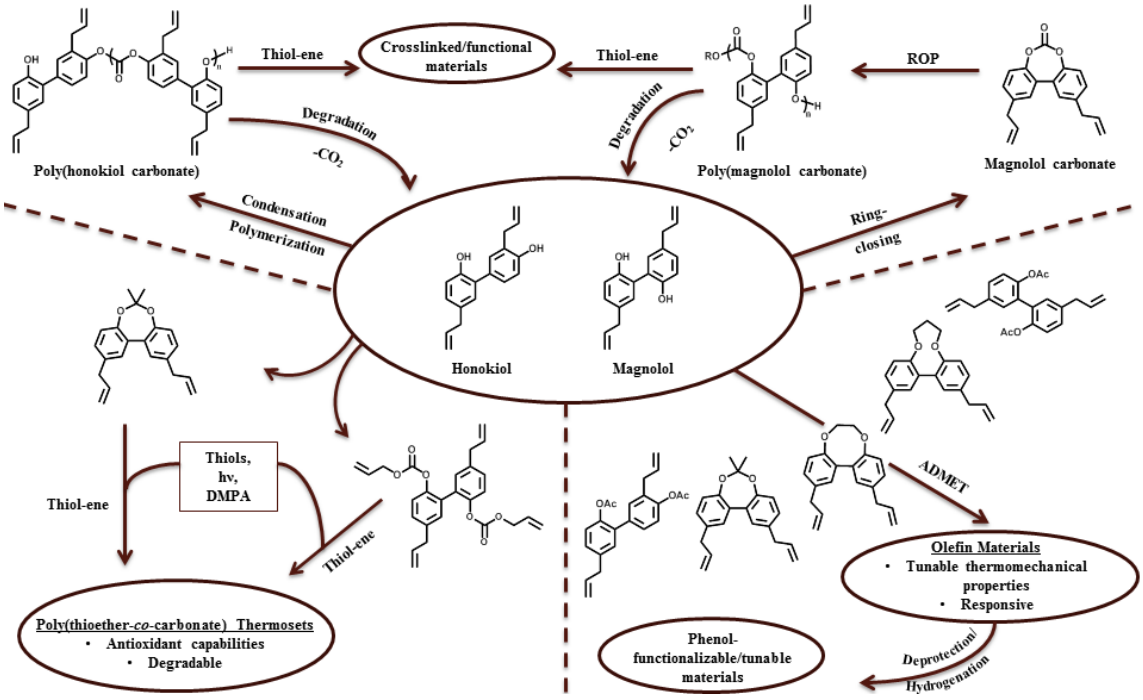

Figure 1-3. Synthetic Outline from Honokiol and Magnolol to Three Different Polymer Classes: Polycarbonates, Thiol-ene Thermosets, and Olefin Materials.

This dissertation focuses on the synthesis, characterization, and development of polymeric materials from the neolignans honokiol and magnolol. Several guiding principles have encompassed the synthesis of both renewable monomers and polymers including the use of straightforward, scalable, and translatable chemistries. The monomers and polymers are designed such that the resulting material properties are easily controlled and manipulated while also incorporating modalities that allow for further functionalization and fine tuning. To our knowledge, this work is the first instance of honokiol and magnolol raw materials incorporated as polymers. As such, it was an aim of this work to effectively introduce new raw materials into the field of polymer science and lay a foundation from which new chemistries and engineering or biomedical applications may be explored with honokiol and magnolol.

CHAPTER II

BIO-BASED POLYCARBONATES DERIVED FROM THE NEOLIGNAN HONOKIOL*

2.1 Overview

Honokiol, a highly functional phenolic- and alkenyl-containing neolignan natural product isolated from several *Magnolia* plant species, is an interesting bio-based resource, which is shown to be useful directly as a monomer for the rapid and scalable synthesis of poly(honokiol carbonate) (PHC). PHC was synthesized in one step from the natural product using condensation polymerization methods. Polymers of number average molecular weight (M_n) ranging from 10–55 kDa were obtained on gram scales in yields up to 80%. Thermal analysis demonstrated high thermal stability, with degradation temperatures in excess of *ca.* 450 °C. Mechanical testing of several PHC polymers indicated a generally increasing storage modulus with increasing M_n and a similar trend with T_g. With an interest toward cardiovascular applications, initial cytotoxicity and fluorescence cell imaging studies were conducted and showed no cytotoxicity toward coronary venular endothelial cells (CVECs), which proliferated on PHC thin films up to a month. Bulk PHC is a robust material, as it underwent slow

---

*Adapted from "Bio-based polycarbonates derived from the neolignan honokiol", by Kevin T. Wacker, Samantha L. Kristufek, Soon-Mi Lim, Sarosh Khan, and Karen L. Wooley, **2016**, *RSC Advances*, 6, 81672-81679, Copyright 2016 by the Royal Society of Chemistry.

hydrolytic degradation under basic conditions (*ca*. 0.1%/day under 1 M $NaOH_{(aq)}$), and no observable degradation under acidic and neutral conditions, each at 37 °C over 130 days. These polycarbonates serve as potential specialty engineering- or bio-materials derived from a commercially-available natural product monomer.

2.2 Introduction

There has been a keen interest in developing renewable resources to supplement or replace petroleum-based feedstocks used in the production of specialty engineering plastics, as well as, materials for biomedical applications.[81-83] This interest stems primarily from suggested dwindling resources of petroleum-based feedstocks[84-85] and the health[86] and environmental[2, 87-88] risks associated with non-degradable polymer waste. On an industrial scale, products such as the Tritan™ line of polymers from Eastman Chemical Company and Durabio™ from Mitsubishi are being used to replace materials associated with potential endocrine disrupting properties.[89,90] Currently, lignin and polysaccharide-based[91-93] raw materials dominate as renewable sources for production of small molecules used in sustainable and renewable polymer manufacture processes.[94] These renewable sources yield a variety of monomers that can be used in polyester, polyurethane, polyamide, and polycarbonate – including poly(isosorbide carbonate), (PIC) – production, among others.[95-101] However, renewable polymers constitute less than 1% of the yearly production of polymers worldwide.[81] Of the polymer classes

derived from renewable sources, polycarbonates have shown promise as materials that could reduce waste in aqueous environments, as they have potential to yield CO_2 and alcohols or phenols upon hydrolytic degradation. This attractive feature has led to the interest in developing new natural product- and bio-based polycarbonates for a number of applications, such as biomedical applications.[102,49] For example, glucose has been utilized as a monomer, where biocompatibility and biodegradability could be desirable.[45,103] In addition, bio-based polycarbonates for specialty engineering materials such as PIC have potential toward replacing poly(bisphenol A carbonate), BPA-PC, and other bisphenol A-containing materials,[97-99, 104] which have been linked to potential carcinogenic and toxic effects.[105,106] Although it is important to develop new, renewable, biocompatible, and potentially (bio)degradable materials, it will be imperative not to compromise performance in comparison to current petrochemical-derived standards. From a performance aspect, yet another aim in utilizing renewable materials is to develop polymers that are unique in having characteristics for which there are no current comparable petrochemically-derived equivalents. The vast chemical and structural diversity of renewable materials is ideal for the development of polymers for new technologies.

Currently, many interesting classes of natural products, such as lignans and neolignans, remain undeveloped for use in material or polymer applications. Lignans and neolignans are structurally diverse secondary plant metabolites produced through oxidative dimerization of a core phenylpropanoid unit.[57] Of the neolignans, honokiol and its isomers have been widely studied, as they are readily extracted from several

Magnolia plant species and have shown promise for a number of therapeutic applications in cancer, neuronal disease, inflammation, and cardiovascular disease, among others.[60, 79, 107-110] In addition, honokiol has been used as a therapeutic in several drug delivery and nanoparticle formulations for *in vitro* studies.[111,112] These features, along with the potential to synthesize a number of structurally- and chemically-diverse materials directly from honokiol or its derivatives, prompted our initial investigation into the synthesis and characterization of the linear polymer, poly(honokiol carbonate), PHC. Furthermore, we envisioned that the development of a new monomer from a renewable resource may further the replacement of non-renewable, petroleum-based feedstocks. For applications as a potential natural product-based biomaterial, particularly in cardiovascular diseases, we examined cellular responses to PHC with cytotoxicity assays and fluorescence cell imaging. We anticipate that this initial demonstration of honokiol as a highly functional phenolic- and alkenyl-containing bio-based resource for the direct, rapid, and scalable production of polycarbonates will lead the efforts toward expansion to other (neo)lignans as starting materials/monomers for the synthesis of polymeric materials.

2.3 Experimental Section

2.3.1 Materials

Pyridine (>99.8%), *N*,*N*-Diisopropylethylamine (99.5%), triethylamine (≥99%), poly(bisphenol A carbonate) (M_w = 42.1 kDa, M_n = 21.4 kDa), poly(lactic acid) (M_w = 60 kDa, M_n = 30 kDa), dimethyl sulfoxide, fetal bovine serum (FBS), penicillin-streptomycin, 1.5% bovine gelatin, Phalloidin-Alexa488, and anti-vinculin antibody were purchased from Sigma Aldrich (St. Louis, MO). *N*,*N*-Diisopropylethylamine, triethylamine, and pyridine were distilled over CaH_2 prior to use unless otherwise noted; all other materials was used as received. Diphosgene (98%) was purchased from Alfa Aesar (Ward Hill, MA) and triphosgene (98%) was purchased from Oakwood Chemical (West Columbia, SC), and both were used as received. *Caution: Special precautions should be taken when working with phosgene precursors, including diphosgene and triphosgene. They are highly toxic by inhalation and ingestion; use of appropriate personal protective equipment is strongly recommended*. Solvents were purchased from EMD Millipore (Darmstadt, Germany) and used as received. All solvents were of ACS grade or higher. Honokiol (>98%) was purchased from Stanford Chemicals (Irvine, CA) and stored in a desiccator prior to use. Bovine coronary venular endothelial cells (CVECs) were kindly gifted by Professors Cynthia J. Meininger and Andreea Trache at Texas A&M Health Science Center. Glass-bottom cell culture dishes used in PHC thin film coatings were obtained from MatTeck (MatTeck, Ashland, MA) and ninety-six-well plates for cytotoxicity assays were purchased from Argos Technologies (Illinois, USA).

2.3.2 Characterization

NMR spectra (500 MHz for ^{1}H and 125 MHz for ^{13}C) were recorded on a Varian Inova 500 spectrometer. Chemical shifts were referenced to $CHCl_3$ at 7.26 ppm (^{1}H) and 77.16 ppm (^{13}C), respectively. IR spectra were recorded on a Shimadzu IR Prestige attenuated total reflectance Fourier-transform infrared spectrometer (ATR-FTIR) and analyzed using IRsolution v. 1.40 software. Size exclusion chromatography (SEC) measurements were performed on a Waters Chromatography Inc. (Milford, MA) system equipped with an isocratic pump model 1515, a differential refractometer model 2414, and a four-column set of 5 μm Guard (50 × 7.5 mm), Styragel HR 4 5 μm DMF (300 × 7.5 mm), Styragel HR 4E 5 μm DMF (300 × 7.5 mm), and Styragel HR 2 5 μm DMF (300 × 7.5 mm) using DMF (0.05 M LiBr) as the eluent (1.00 mL/min) at 40 °C. Polymer solutions were prepared at concentrations of 5-10 mg/mL and an injection volume of 200 μL was used. Analysis was performed using Empower 2 v. 6.10.01.00 software (Waters, Inc.). The system was calibrated with polystyrene standards (Polymer Laboratories, Amherst, MA) ranging from 580 to 1,233,000 Da. Glass transition temperatures (T_g) and the melting transition temperature (T_m) were measured by differential scanning calorimetry (DSC) on a Mettler-Toledo DSC822 (Mettler-Toledo, Inc., Columbus, OH) under N_2 with a heating rate of 10 °C/min unless otherwise noted. The glass transition and melting transition temperatures of honokiol were measured by heating the sample to 100 °C and immediately transferring the sample into a liquid nitrogen bath before scanning from -50 °C to 100 °C. The measurements were analyzed using Mettler-Toledo STAR^{e} v.10.00 software. The T_g was taken on the third heating

cycle as the extrapolated onset temperature from the intersection of the tangent drawn from the transition curve with the greatest slope with the extrapolated baseline before the transition. Thermogravimetric analysis (TGA) was performed using a Mettler-Toledo model TGA/DSC 1, with a heating rate of 10 °C/min under an Ar atmosphere. The measurements were analyzed using Mettler-Toledo STAR^{e} v.10.00 software. Rectangular dynamic mechanical analysis (DMA) samples were prepared using poly(honokiol carbonate) powder, which was ground with a mortar and pestle and pressed into an aluminum mold (2.0 cm × 0.5 cm × 0.2 cm). The powder was then heated in a VWR Symphony Vacuum Oven at ambient pressure using a heating cycle optimized for each number-average molecular weight polymer for a total heating cycle of no more than 48 hours. Samples were then allowed to cool to room temperature before being removed from the mold. Samples were sanded using 100 or 150 grit sandpaper to uniform dimensions. DMA was performed on a Mettler-Toledo TT-DMA system (Mettler-Toledo AG, Schwerzenbach, Switzerland). Sample dimensions were *ca.* 7 × 5 × 0.6 mm. Samples were analyzed in tension *via* thermal scan (3 °C/min) from 0 ºC to 200 ºC or 20 ºC to 250 ºC in autotension mode, with a frequency of 1 Hz, a preload force of 1 N, and a static force of 2 N. DMA data were obtained from Triton Laboratory software and exported to Origin Pro 8.0 for analysis.

2.3.3 Poly(honokiol carbonate) – PHC

The following consist of general procedures for the optimized syntheses of poly(honokiol carbonate) at varying initial molar concentrations of honokiol:

2.3.3.1 Procedure 1

Honokiol (1.104 g, 4.063 mmol), dry *N*,*N*-Diisopropylethylamine (1.00 mL, 5.74 mmol), and pyridine (3.00 mL) were added to a flask, which was then placed in an ice bath and purged with nitrogen. Diphosgene (0.45 mL, 4.5 mmol) was then added to the flask over *ca.* 35 min and the reaction was allowed to proceed for *ca.* 60 h while warming to room temperature before being quenched with saturated aqueous sodium bicarbonate solution. The mixture was then diluted in dichloromethane (40 mL) and washed (deionized water) (40 mL × 2), followed by extraction of the aqueous phase with dichloromethane (10 mL). The combined organic layers were then dried over $MgSO_4$, filtered, and concentrated. The crude polymer was then precipitated into cold methanol (30 mL), centrifuged (10k RPM, 15 ºC, 10 min), and decanted twice. The polymer was dried *in vacuo* to afford poly(honokiol carbonate). ATR-FTIR υ_{max} (cm^{-1}) 3085-2820, 1771, 1639, 1608, 1484, 1432, 1234, 1173, 1112; ^{1}H NMR (500 MHz, $CDCl_3$) δ 7.60-6.60 (br, 6H), 6.10-5.70 (br, 2H), 5.30-4.90 (br, 4H), 3.60-3.10 (br, 4H) ppm; ^{13}C NMR (125 MHz, $CDCl_3$) δ 151.9, 151.8, 151.7, 151.4, 149.0, 148.9, 148.8, 148.7, 146.4, 146.3, 139.0, 138.7, 136.9, 135.5, 133.8, 133.4, 132.1, 131.9, 131.3, 130.9, 129.1, 128.4, 122.1, 116.9, 116.6, 39.6, 34.6, 34.2 ppm.

2.3.3.2 Procedure 2

Honokiol (1.110 g, 4.086 mmol), dry triethylamine (0.85 mL, 6.1 mmol), and pyridine (4.15 mL) were added to a flask then placed in an ice bath and purged with

nitrogen. Diphosgene (0.45 mL, 4.5 mmol) was then added to the flask over *ca.* 35 min and the reaction was allowed to proceed for *ca.* 60 h while warming to room temperature before being quenched with saturated aqueous sodium bicarbonate solution. The mixture was then diluted in dichloromethane (40 mL) and washed (deionized water) (40 mL × 2), followed by extraction of the aqueous phase with dichloromethane (10 mL). The combined organic layers were then dried over $MgSO_4$, filtered, and concentrated. The crude polymer was then precipitated into cold methanol (30 mL), centrifuged (10k RPM, 15 ºC, 10 min), and decanted twice. The polymer was dried *in vacuo* to afford poly(honokiol carbonate).

2.3.4 Cell Culture

Coronary venular endothelial cells (CVECs) were kindly provided by Profs. Cynthia J. Meininger and Andreea Trache (Texas A&M Health Science Center, College Station, TX, USA). CVECs were cultured in GIBCO® Dulbecco's Modified Eagle Medium: Nutrient Mixture F-12 (DMEM/F-12) from Invitrogen (Invitrogen, Carlsbad, CA), along with 10% FBS, 100 U/mL penicillin - 100 U/mL streptomycin - 0.25 mg/mL amphotericin B (Lonza, Walkersville, MD), and 20 units/mL heparin (Midwest Vet Supply, Lakeville, MN). For subculture and experiments, cells were trypsinized and quenched with media. Trypsin was removed after centrifugation at 250 G for 4 minutes. Resuspended cells were plated on 1.5 % bovine gelatin-coated flasks for subculture or 50×10^3 cells were plated on glass-bottom dishes coated with 1.5 % bovine gelatin or polymer coated glass-bottom dishes for experiments.

2.3.5 MTT Assay

Cells (10 x 10^3 cells/well) were plated in 96-well plate (coated with 1% gelatin) and incubated at 37 °C in a humidified atmosphere containing 5% CO_2 for 24 h to adhere. Then, the medium was replaced with a fresh medium 1 h prior to the addition of 20 μL of poly(honokiol carbonate) stock solution (DMSO) to 100 μL of the medium (final concentrations ranged from 10 - 0.0048 μM). The cells were incubated with the formulations for 72 h, and then the medium was replaced with 100 μL of the fresh complete media. MTS combined reagent (20 μL) was added to each well (Cell Titer 96® Aqueous Non-Radioactive Cell Proliferation Assay, Promega Co., Madison, WI). The cells were incubated with the reagent for 2 h at 37 °C in a humidified atmosphere containing 5% CO_2 protected from light. Absorbance was measured at 490 nm using SpectraMax M5 (Molecular Devices Co., Sunnyvale, CA). The cell viability was calculated based on the relative absorbance to the control-untreated cells. IC_{50} values of the polymer could not be determined because high cell-viabilities were observed at the range of the tested concentrations (10 - 0.0048 μM).

2.3.6 Polymer Thin Films for Cell Culture

A PHC thin film was prepared by solvent casting from polymer solutions in dichloromethane (DCM) on glass-bottom cell culture dishes. A 1% solution was prepared by dissolving 10 mg of PHC in 1.0 mL of DCM, and diluted to 0.1 % and 0.01

% in DCM. Dried dishes were sterilized under UV for 1 h in the biosafety cabinet and washed with sterile PBS before plating cells. Cells were plated on polymer-coated glass-bottom dishes for experiments. As a control, cells were plated on glass-bottom dishes coated with 1.5 % bovine gelatin. Cell media was replaced with fresh media every 2-3 d, and proliferation and morphology of cells were continuously monitored up to one month.

2.3.7 Immunofluorescence and confocal imaging

Cells were fixed with 2% paraformaldehyde and stained with Alexa Fluor 488® phalloidin & anti-vinculin with secondary antibody conjugated with Alexa Fluor 647® after 24 h, 1 week, and 1 month from plating to stain actin proteins in cytoskeleton and vinculin protein in focal adhesions, respectively. Laser scanning confocal microscopy was used to acquire fluorescence images. Excitation and emission filter settings were adjusted according to fluorophore spectra provided by the manufacturer. 3D confocal images were acquired as stacks of 15-18 planes with 0.5 μm step size. Overall, cell population was identified from the large filter view with a 10x objective. Details of cell morphology were investigated from fluorescence images acquired with a 20x objective with 2x zoom (40x magnification equivalent).

2.3.8 Degradation of Poly(honokiol carbonate)

Samples were prepared from a home-built silicon cylindrical mold and were *ca.* 2.0 mm × 1.5 mm diameter and *ca.* 100 mg. Five to six samples (M_n = 21 kDa) were used for each set of degradation conditions: 1 M $NaOH_{(aq)}$, 1 M $HCl_{(aq)}$, and 1x PBS. All samples were placed in 1 dram vials and set in an incubating shaker at 37 °C at 60 RPM. For the $HCl_{(aq)}$ and $NaOH_{(aq)}$ samples, each solution was replaced every 2-3 days in order to maintain constant concentration of reagent, while 1x PBS was replaced every week. At predetermined times, samples were removed from the shaker, blotted dry, weighed, dried under vacuum at 45 °C to constant weight and reweighed. Swelling percentage was taken as the mass difference between wet and dry sample relative to the dry sample mass.

2.4 Results and Discussion

The condensation polymerization of honokiol required optimization of the carbonylation agent and the conditions to obtain high molecular weight polycarbonates. The condensation reaction of honokiol was first attempted with relatively mild carbonylation reagents including 1,1'-carbonyldiimidazole (CDI), ethyl chloroformate, and 4-nitrophenyl chloroformate with triethylamine in *N,N*-dimethylformamide at 70 °C for 60 h or in bulk at elevated temperatures with diethyl- or diphenylcarbonate under dynamic vacuum. Upon workup, there was no precipitation of polymer from cold

methanol and only starting material and small molecules were recovered. Subsequently, the polymerization was attempted with phosgene analogues triphosgene and diphosgene (Figure 2-1). *Caution: Special precautions should be taken when working with phosgene precursors, including diphosgene and triphosgene. They are highly toxic by inhalation and ingestion; use of appropriate personal protective equipment is strongly recommended.* Polymers of number average molecular weight, M_n, of up to 82 kDa (DP_n = 280) were obtained using triphosgene in dichloromethane with pyridine, but yields were markedly low – typically less than 10% – and produced, largely, an intractable gel upon workup. Similar results were obtained when switching to diphosgene in pyridine without any additional base at reaction times of 60 h – the reaction mixture became increasingly viscous as the reaction volume decreased, and vigorous stirring was required to prevent gelation.

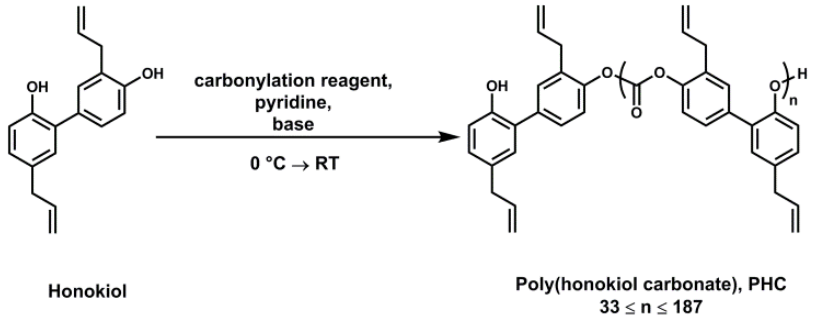

Figure 2-1. General Poly(honokiol carbonate) Synthesis

Conditions were then screened with the aim of reducing the viscosity of the reaction mixture and increasing isolated yield by addition of organic co-bases and reduction in the molarity of the monomer at t_0. *N*,*N*-Diisopropylethylamine (DIPEA) and triethylamine (TEA) proved most successful with an optimal ratio of 0.75 eq. DIPEA or TEA/phenol moiety (Table 2-1). Reaction conditions utilizing 1 M initial honokiol concentration in pyridine and DIPEA with phosgene precursor (1.0 eq./hydroxyl) and no additional solvent yielded poly(honokiol carbonate) in up to 80% yield.

Table 2-1. Synthesis of Poly(honokiol carbonate) with Phosgene Analogues

Reagents	**Honokiol Conc. (M)**	M_n **(kDa)**	**Đ**	**Yield (%)**
Triphosgene	1.0	82	2.3	5
Diphosgene	1.0	37	3.3	3
Triphosgene/DIPEA[a]	1.0	20	2.0	79
Diphosgene/DIPEA	1.0	55	2.5	80
Diphosgene/DIPEA	0.5	43	2.6	77
Diphosgene/DIPEA	0.3	27	2.8	79
Diphosgene/DIPEA[b]	1.0	15	2.5	44

[a]All polymers were comparable when DIPEA was replaced with TEA. [b]DIPEA not distilled.

When reducing the initial concentration of honokiol by dilution with pyridine, high yields were still obtained while the M_n of poly(honokiol carbonate) varied as expected with all other reaction conditions being equal: 0.50-0.80 M, *ca.* 42 kDa; 0.35 M, 27 kDa. The polycondensation was also fairly susceptible to moisture, as using non-distilled base resulted in polymers with lower molecular weights and yields (Table 1, final entry). The M_n and polydispersity, Đ, of all polymers were calculated using size exclusion chromatography (SEC) in *N*,*N*-dimethylformamide (0.05 M LiBr) eluent and compared to polystyrene standards (Figure 2-2). (PHC also showed markedly good solubility in many organic solvents, including chloroform, dichloromethane, tetrahydrofuran, dimethylsulfoxide, *etc*.) Confirmation of polymer formation was also noted with ATR-FTIR through disappearance of the O-H stretch of the hydroxyl moieties at 3300 cm^{-1} and appearance of the carbonate moiety with a carbonyl stretch at 1771 cm^{-1} and the symmetric and asymmetric C-O stretches at 1173 and 1234 cm^{-1} (Figures 2-3 & A-1).

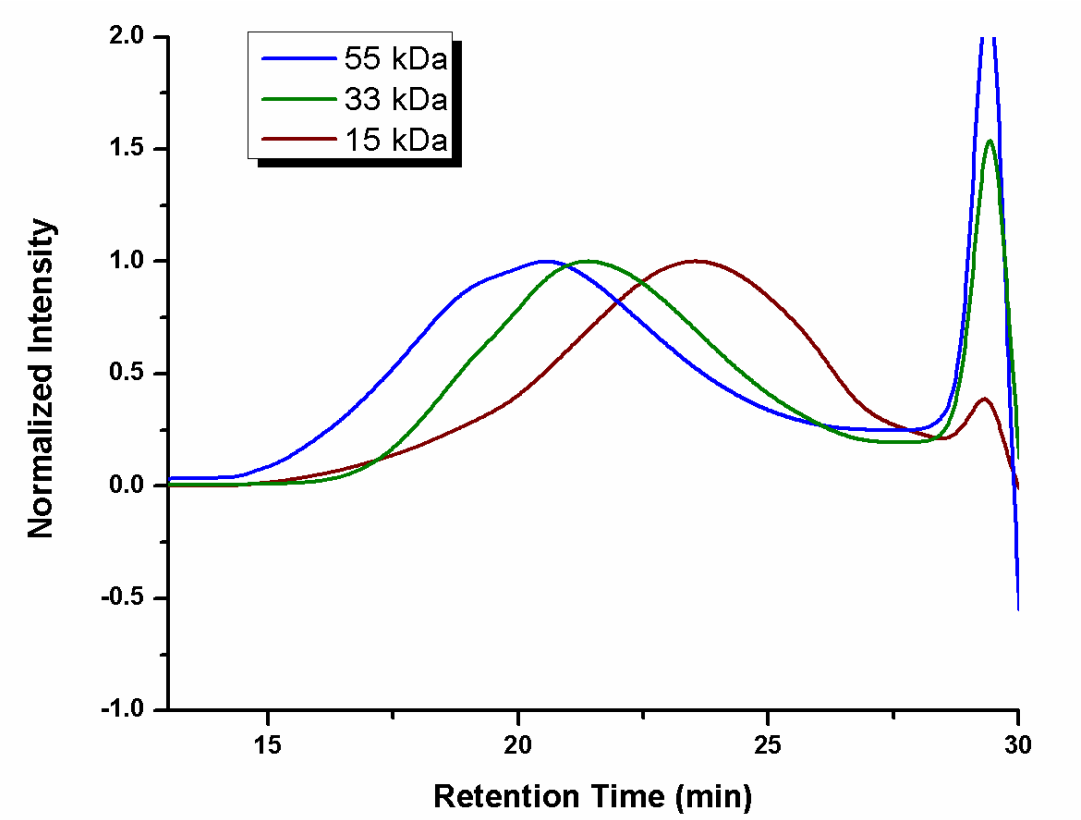

Figure 2-2. SEC Traces of PHC in DMF (0.05 M LiBr) Eluent.

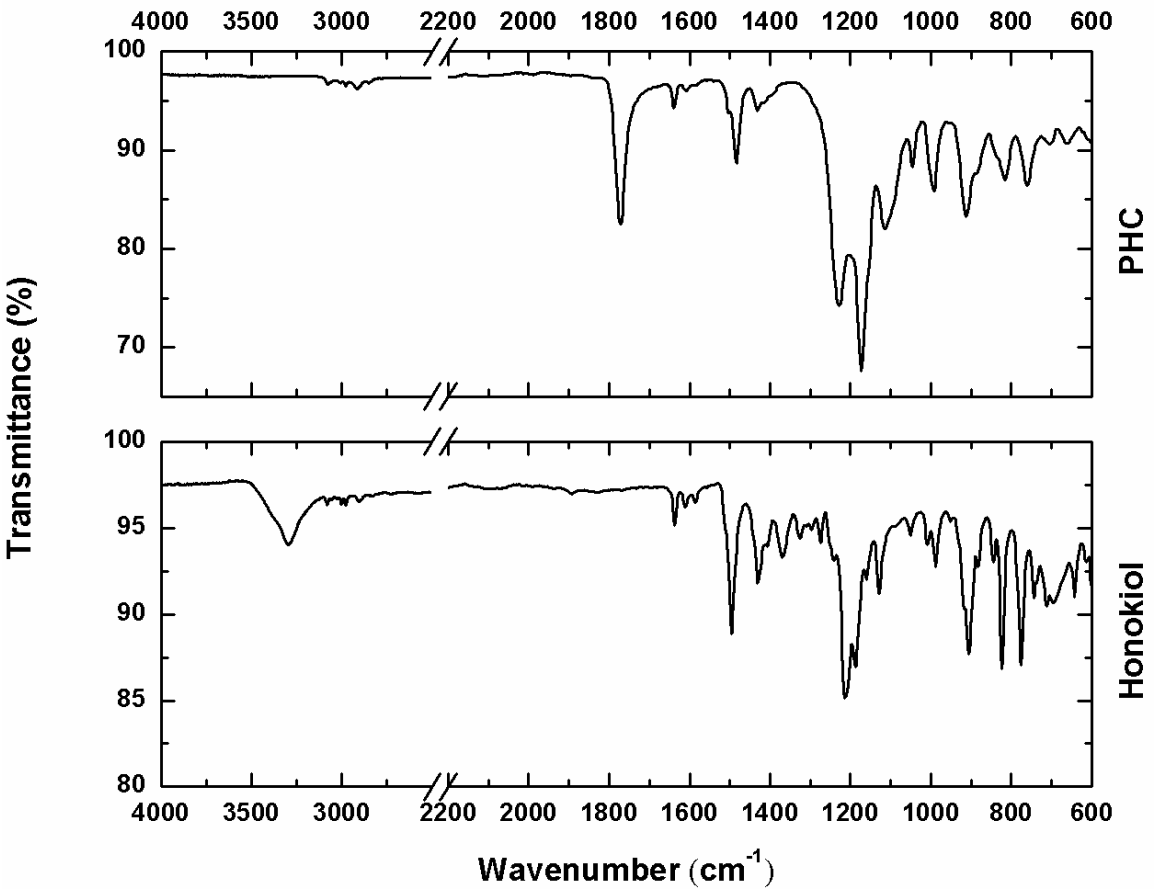

Figure 2-3. ATR-FTIR Spectra Comparing PHC-55 kDa and Honokiol.

Initial thermal analyses had indicated high thermal stability yet relatively low glass transition temperatures, therefore, extensive thermal analyses were conducted for the series of PHCs, with comparisons to honokiol, a poly(bisphenol A carbonate) standard, M_n = 21.4 kDa, Đ = 2.0, literature reports for PIC under similar conditions, and a poly(lactic acid) standard, M_n = 30 kDa, Đ = 2.0. Thermal stabilities were evaluated by thermogravimetric analysis (TGA). PHCs of varying M_n all showed markedly good thermal stability in comparison to the poly(bisphenol A carbonate), poly(lactic acid), and

poly(isosorbide carbonate) (Figure 2-4), as noted by high onsets of thermal degradation (PHC: 454-462 °C *vs* BPA-PC: 504 °C, PLA: 338 °C, and PIC: 346 °C [97, 113]). The onsets of thermal degradation for the BPA-PC and PLA standards were in good agreement with other reports.[114-115] Interestingly, the side chain alkenyl groups did not cause a significant reduction in thermal stability relative to BPA-PC and no degradation of the PHC carbonate backbone was observed prior to reaching the onset temperature of degradation for the monomer, honokiol (Figure 2-5). While both standards, PLA and BPA-PC, showed one mass loss event, the PHCs exhibited two-stage degradation profiles with a second mass loss event *ca.* 600 °C. Complete degradation of the PHCs, as noted by remaining char mass or total mass loss, was observed only at temperatures above 700 °C. Both PHC and BPA-PC have shown much higher thermal stability than reports for PIC (340-346 °C).[97, 113]

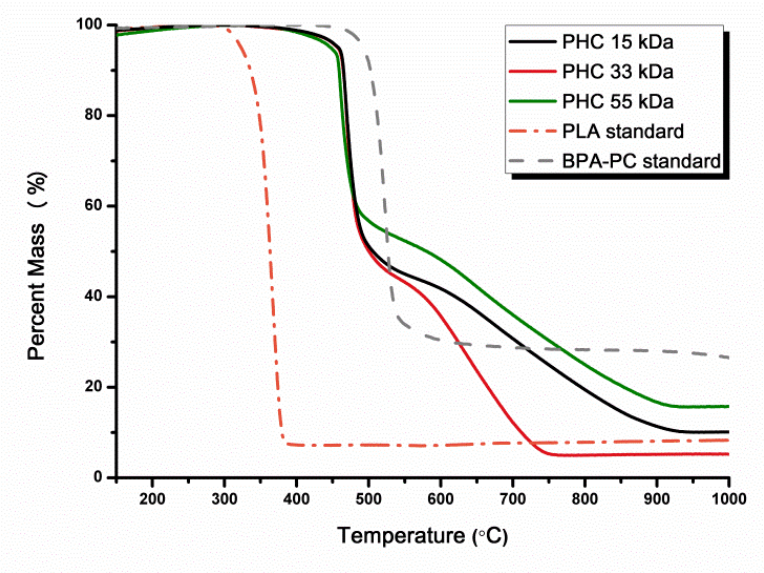

Figure 2-4. PHC Thermal Degradation Compared with Standards.

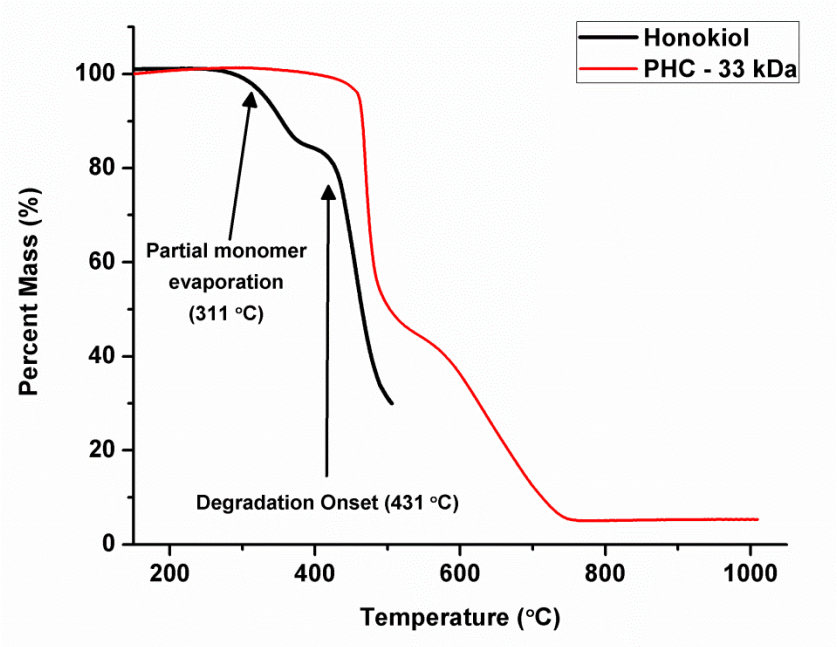

Figure 2-5. TGA – Thermal Degradation of Honokiol and PHC Having a M_n of 33 kDa.

Differential scanning calorimetry (DSC) showed one thermal transition for each PHC polymer when using temperature sweeps ranging from 0-200 °C with a single transition and onset in the range of 60-65 °C, corresponding to the glass transition temperature, (T_g) (Table 2-2). Further analysis up to 400 °C provided no additional thermal transitions corresponding to a melting transition, which suggests PHC to be non-crystalline. The amorphous nature was further confirmed by X-ray powder diffraction (data not shown). We initially predicted the glass transitions of PHC to be lower compared to our BPA-PC standard (T_g = 146 °C) and literature precedence for PIC ($T_g \approx$ 165 °C)[97] as honokiol contains two allylic side chains which are absent in both BPA-PC and PIC and can increase the free volume between the polymer chains of PHC. However, as measured by DSC, the T_g for the original, powder PHC samples were lower than expected, and comparable to current, widely used biomaterial polymers such as poly(lactic acid) (T_g = 57 °C, in agreement with the literature[,116]).

Table 2-2. Thermal Data of Honokiol, PHC, and Standards, as Measured by DSC and TGA

Monomer/Polymer	T_g (°C) – powder	T_g (°C) – bar[a]	T_m (°C)	T_d (°C)
Honokiol	-24	–	86	431
PHC-15 kDa	64	–	–	460
PHC-23 kDa	63	67	–	454
PHC-31 kDa	66	76	–	458
PHC-33 kDa	63	–	–	462
PHC-37 kDa	67	88	–	459
PHC-55 kDa	65	–	–	454
BPA-PC-21 kDa	146	–	–	504
PIC-28 kDa[b]	167	–	–	346
PLA-30 kDa	57	–	177	338

[a] Bar samples were fabricated from powder as in experimental [b] Ref. 18

Additional thermomechanical properties of the bio-based poly(honokiol carbonate) were determined by dynamic mechanical analysis, DMA, with further comparison to BPA-PC, PIC, and PLA. Samples of PHC with M_n = 23, 31, and 37 kDa were analyzed in tension using temperature sweeps ranging from 0 °C to 200 °C or 20 °C to 250 °C at 1 Hz in triplicate. As shown in Figure 2-6, there is an increase in the

glass transition temperature as measured by the peak of the loss modulus, E″, for poly(honokiol carbonate) with increasing M_n at room temperature, as well as a general increase in the storage modulus, E′. Most notably, E′ of all PHC (1.1 – 1.7 GPa) were comparable to reported values for PLA (1.6 GPa), PIC (2.7 GPa), and BPA-PC (2.2 GPa), as reported using DMA under similar conditions.[113, 117-119] Furthermore, it was intriguing to note the T_g of the highest M_n PHC tested (37 kDa, T_g = 106 °C) was substantially higher than values observed by DSC – all consistently in the range of 60-65 °C – while the T_g of the 23 kDa PHC (76 °C) was in good agreement with the DSC measurements. The DMA samples were then submitted to DSC characterization to compare thermomechanical changes between the original powder samples and the heat processed bars prepared for DMA. By DSC, similar trends were observed for the bar samples as with DMA, wherein PHC of increasing M_n showed steady increases in T_g and higher values than those observed for powder samples (Figure 2-7 and 2-8). For example, by DSC when bar samples were heated at the same rate as powder samples (10 °C/min), PHC-31 kDa and PHC-37 kDa displayed T_gs of 76 and 88 °C, respectively. These values are, at least, 10 °C higher than powder samples of any molecular weight. PHC-23 kDa had a T_g similar to the powder sample (67 °C). These effects are more noticeable when bars were heated at a faster rate (40 °C/min) (Figure 2-9). It is evident that the heat annealing process to form the bars allowed for reorganization of the polymer chains and results in T_gs with higher values than powder samples, more in line with other aromatic and rigid polycarbonates. It is hypothesized that polymers of these M_n and degree of polymerization values, $77 < DP_n < 126$, have not yet reached the

theoretical glass transition temperature limit of an infinite molecular weight polymer. Furthermore, difficulties were encountered with processing of uniform sample bars that could survive DMA measurement. In fact, several samples were prone to failure before the full temperature scan completed (Figure A-14). Future work will expand upon the relationship of these bulk thermomechanical properties, E′ and T_g, with M_n,[120,121] as well as modification of synthetic conditions to allow access to higher molecular weight PHC in large quantities and processing conditions to afford uniform DMA samples.

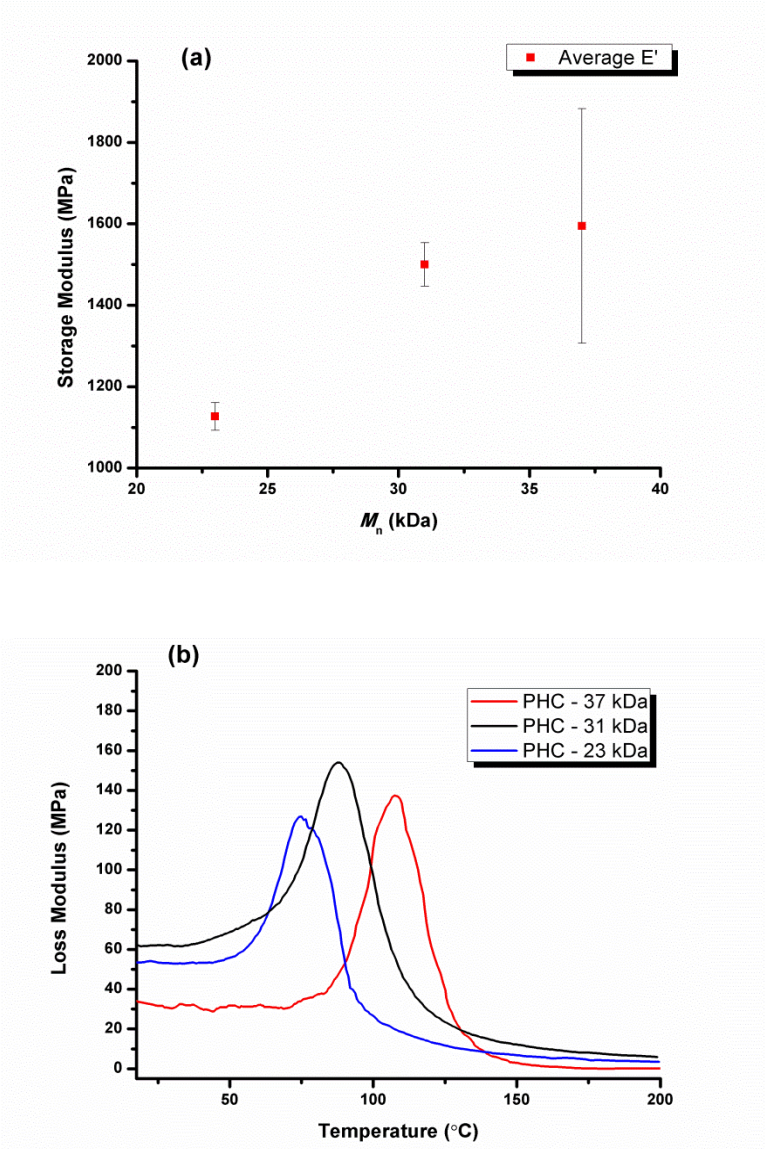

Figure 2-6. Preliminary DMA Results of PHC. (a) Average E′ (25 °C) Scaled with M_n. Scale Bars Represent Standard Deviation; n = 3. (b) Increasing T_g with M_n as Measured by Peak of the Loss Modulus. $T_{g,\ 23kDa}$ = 75 °C, $T_{g,\ 31\ kDa}$ = 87 °C, $T_{g,\ 37\ kDa}$ = 106 °C.

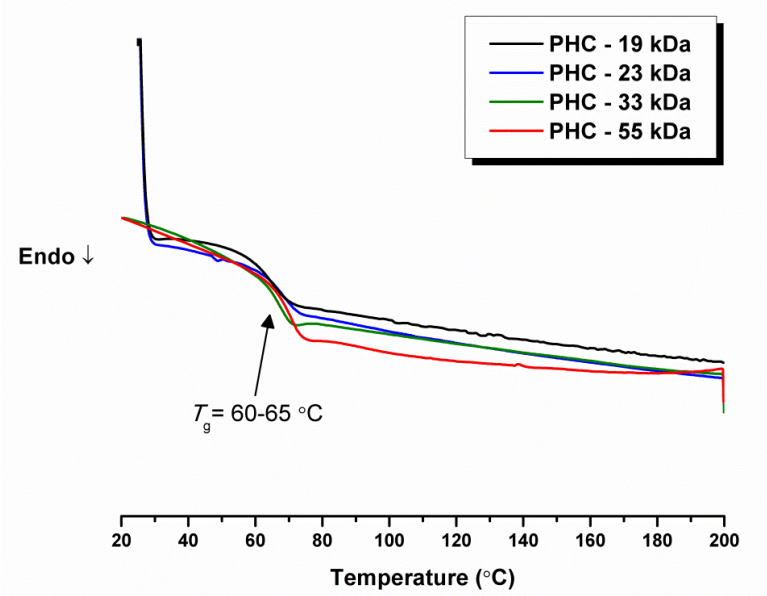

Figure 2-7. DSC Traces of Powder PHC Samples Showing T_gs All in the Range of 60-65 °C.

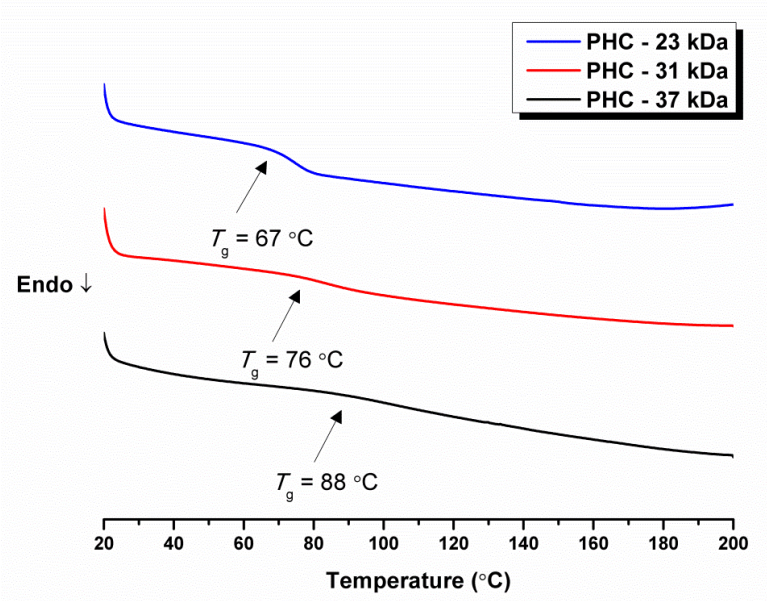

Figure 2-8. DSC Traces of PHC Bars Used in DMA Analyses Showing an Increase in T_g Higher Than Powder Samples. Heating Rate: 10 °C/Min.

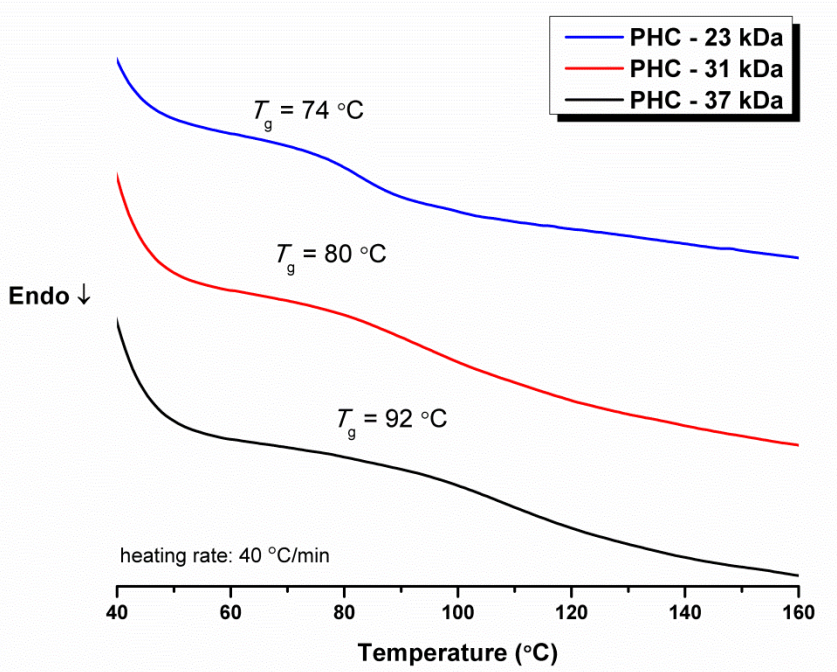

Figure 2-9. DSC Traces of PHC Bars Used in DMA Analyses Showing an Increase in T_g with Increase in Molecular Weight. Heating Rate: 40 °C/Min.

As honokiol has been well studied as a potential therapeutic, particularly in cardiovascular applications,[107,60] several assays were used to assess biocompatibility and cytotoxicity of PHC to coronary venular endothelial cells (CVECs). The endothelium is the inner-most layer of the blood vessel and functions as a barrier between the blood lumen and vessel wall. Malfunction in the endothelium leads to hyperpermeability of the blood vessel that is often associated with cardiovascular diseases and tumor vessel leakage.[122] Therefore, we sought to test adaptability of endothelial cells to PHC, especially for long-term culture, using fluorescence imaging and cytotoxicity assay. Four polymers of M_n = 20, 28, 31, 37 kDa were used in MTS assays and showed no

cytotoxic effects to CVECs at all concentrations tested (10 - 0.0048 μM). IC_{50} values of the polymers could not be determined because high cell-viabilities were observed at the range of the tested concentrations and PHC promoted cell growth at the higher concentrations (Figure 2-10). PHC effect on cell morphology was tracked with fluorescence imaging (Figure 2-11). CVECs were plated and cultured up to one month, and actin fibers and focal adhesions were visualized by staining with fluorophores. Cell sensitivity to the extracellular environment and effects on actin fibers and focal adhesion distribution were monitored.[123-124] CVECs plated on PHC-coated cell culture dishes proliferated to reach confluency and maintained the monolayer with refreshed medium every 2-3 days. CVECs cultured on PHC were compared to the cells on gelatin-coated dishes, which is a common substrate for endothelial cell culture. Cells on PHC showed an intact monolayer with well-structured actin fibers and punctate focal adhesions comparable to the cells on the control surface.

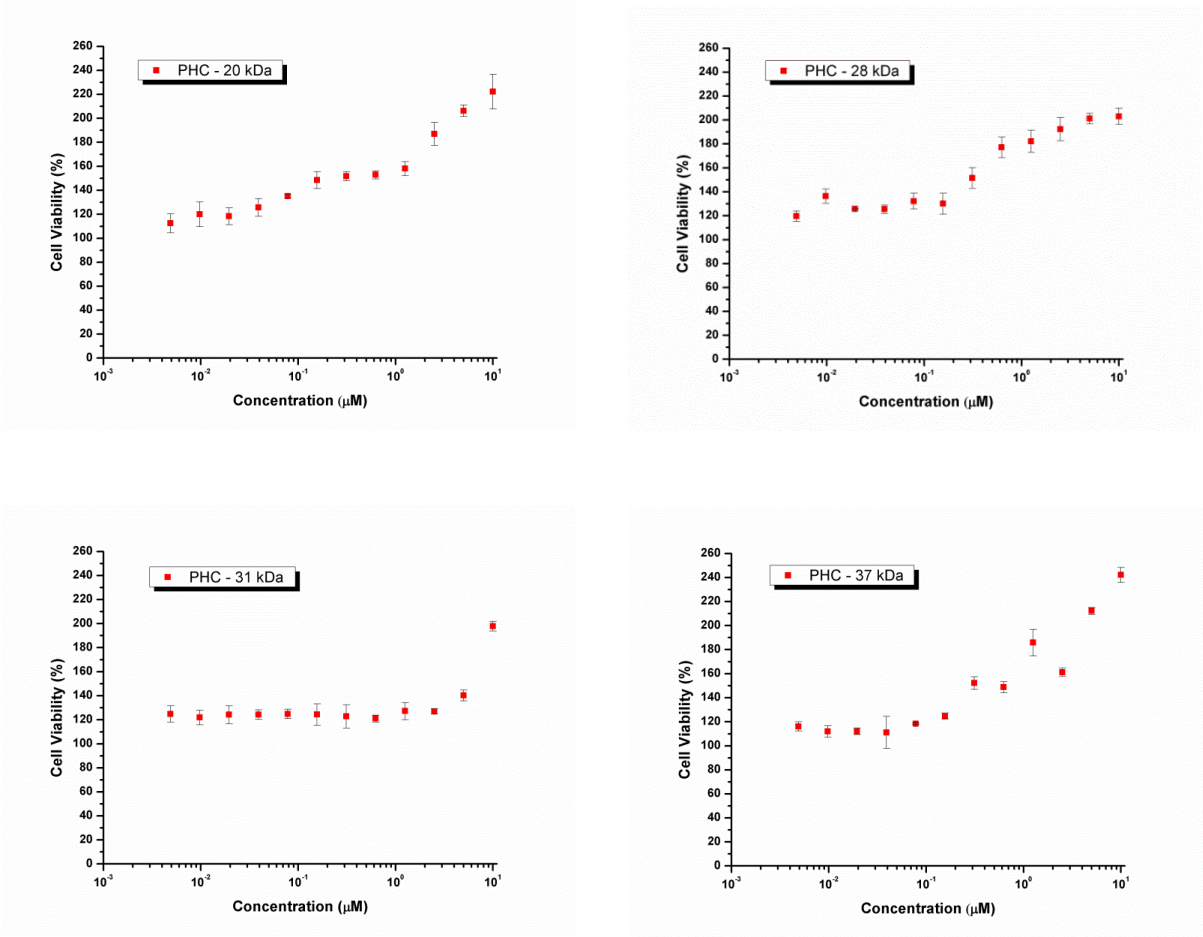

Figure 2-10. MTS Cytotoxicity Assays Comparing Cell Viability to Control Group.

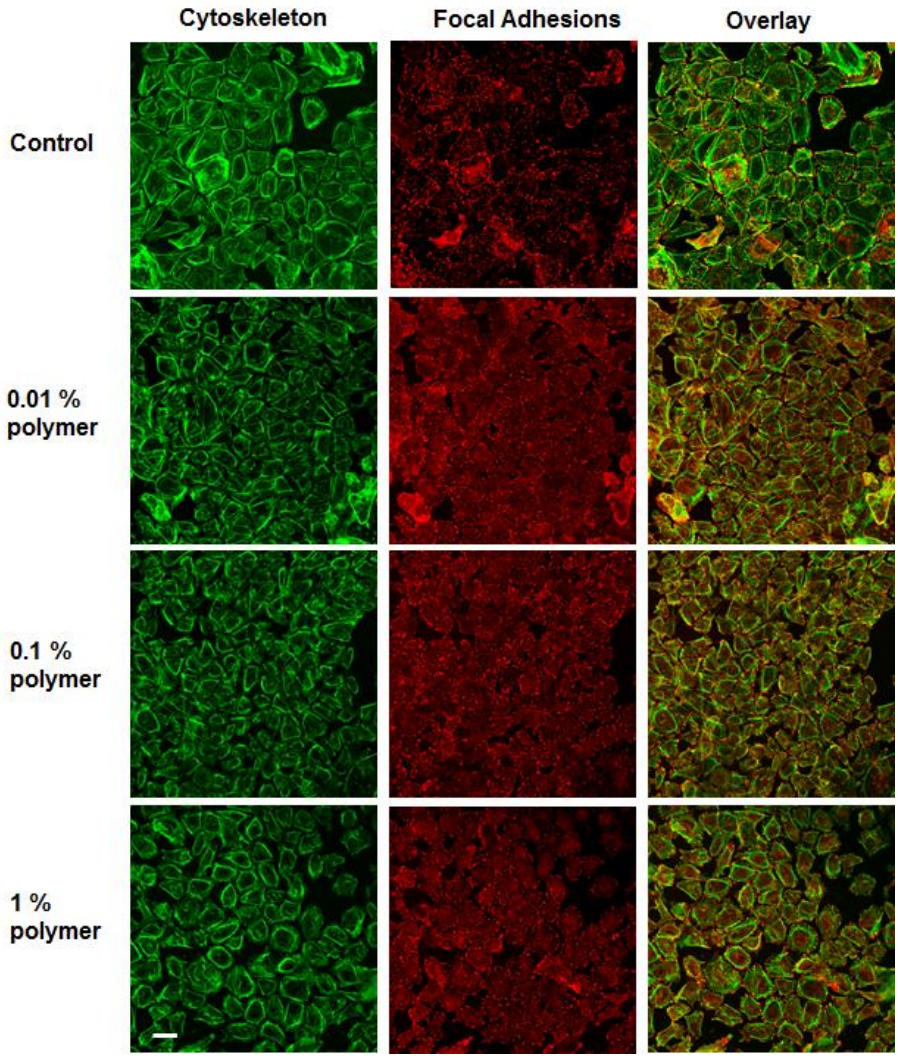

Figure 2-11. Bovine Coronary Venular Endothelial Cells (CVECs) on Poly(honokiol carbonate). Cells Were Fixed After 1-Month of Culture on the Polymer and Stained with Phallodin-Alexa488® (Green) and Vinculin Antibody and Secondary Antibody Conjugated with Alexa647® to Show Cytoskeleton and Focal Adhesions, Respectively. Images were Acquired with a Laser Scanning Confocal Microscope with 20x Objective and 2x Magnification. Scale Bar 30 mm.

To assess the stability and response of bulk PHC to physiological and accelerated degradation conditions, five or six cylindrical samples were prepared and immersed in acidic (1 M $HCl_{(aq)}$), basic (1 M $NaOH_{(aq)}$), and PBS solutions and allowed to stir in an incubator shaker at 37 °C. Degradation of the samples was followed for 130 days (Figure 2-12), while the acidic & basic solutions were replaced every 2-3 days and every week for PBS solutions. Weights remained constant for the samples in PBS and acidic solutions, however, the samples swelled gradually to maxima of *ca.* 5 and 10% at 130 days in PBS and $HCl_{(aq)}$ solutions, respectively. In the case of samples subjected to 1 M $NaOH_{(aq)}$, slow, but steady degradation occurred at a mass loss rate *ca.* 0.1% day^{-1}. At the completion of the study, 18% average total mass loss was observed under basic environment. Analogous to the acidic and PBS samples, swelling increased with time, yet reached a higher relative percentage, *ca.* 15%. These results suggest PHC could serve as a robust biomaterial in most aqueous environments.

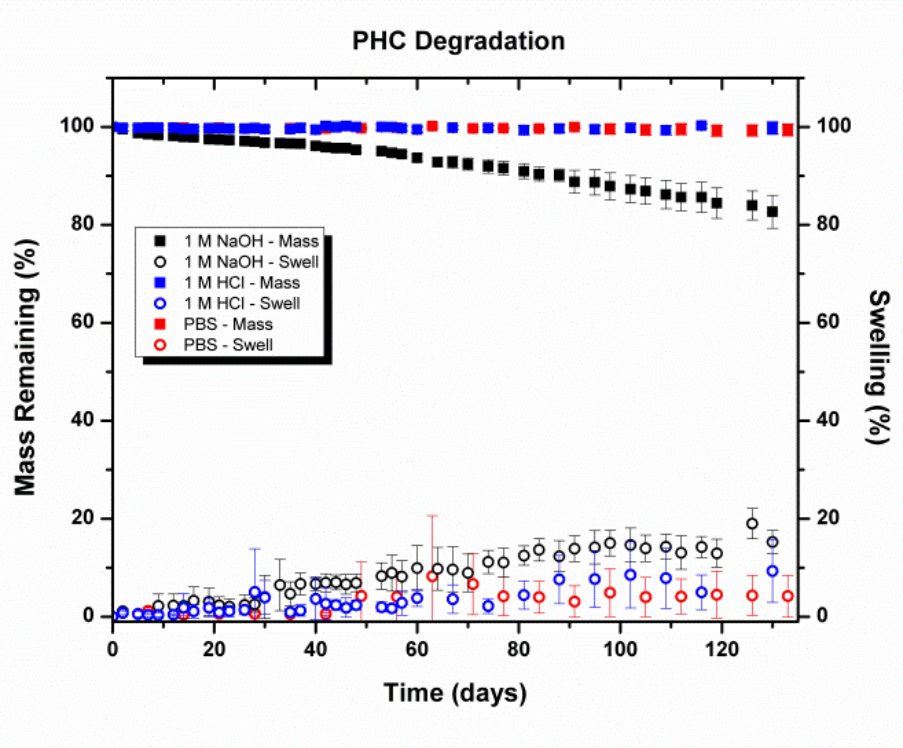

Figure 2-12. Stability and Swelling of PHC in Aqueous Media.

2.5 Conclusions

In summary, we have presented a short, straightforward synthesis of a polycarbonate from a renewable resource, honokiol. Unlike other renewable feedstocks, neolignans have been undeveloped until now and additionally do not compete with food production. Thermal characterization of the polymers yielded degradation and glass transition temperatures comparable to industry standards. Thermomechanical characterization has shown generally increasing moduli and T_g as M_n increases and an E′ for PHC that is comparable to reported values for BPA-PC, PIC, and PLA at ambient

conditions. In addition, the bulk polymers are robust and stable under physiological and acidic conditions yet also biocompatible to endothelial cells *in vitro*. These results suggest potential application of poly(honokiol carbonate) as an engineering or biomedical material where robust features and biocompatibility may be necessary.

CHAPTER III

HARNESSING THE CHEMICAL DIVERSITY OF THE NATURAL PRODUCT MAGNOLOL FOR THE SYNTHESIS OF RENEWABLE, DEGRADABLE NEOLIGNAN THERMOSETS WITH TUNABLE THERMOMECHANICAL CHARACTERISTICS AND ANTIOXIDANT ACTIVITIES

3.1 Overview

Magnolol, a neolignan natural product with antioxidant properties, contains inherent, orthogonal, phenolic and alkenyl reactive groups that were used in both direct thermoset synthesis, as well as, the stepwise synthesis of a small library of monomers followed by transformation into thermoset materials. Each monomer from the small library was prepared *via* a single step functionalization reaction of the phenolic groups of magnolol. Thermoset materials were realized through solvent-free, thiol-ene reactions, and the resulting crosslinked materials were each comprised of thioether and ester linkages, with one retaining the hydrophilic phenols from magnolol, another having the phenols protected as an acetonide, and two others incorporating the phenols into additional crosslinking sites via hydrolytically-labile carbonates or stable ether linkages. With this diversity of chemical compositions and structures, the thermosets displayed a range of thermomechanical properties including glass transition temperatures, T_g, 29-52 °C, onset of thermal degradation, T_d, from *ca.* 290-360 °C, and ultimate strength up to 50 MPa. These tunable materials were studied in their degradation and biological

properties with the aim of exploiting the antioxidant properties of the natural product. Hydrolytic degradation occurred under basic conditions (pH = 12) in all thermosets, but with kinetics that were dependent upon their chemical structures and mechanical properties: 20% mass loss was observed at 5, 7, 27, and 40 weeks. Isolated degradation bproducts and model compounds displayed antioxidant properties similar to magnolol, as determined by both UV-vis and *in vitro* reactive oxygen species (ROS) assays. As these magnolol-based thermosets were found to also allow for extended cell culture, these materials may serve as promising degradable biomaterials.

3.2 Introduction

There is a great interest to incorporate renewable resources into monomers and polymers in order to reduce use of petroleum-based materials, comply with legal and societal standards, and to develop advanced polymeric materials with emergent properties, particularly for engineering or biomedical applications.[32, 125-127] Concurrently, thiol-ene reactions have become pervasive methods for the development of polymeric materials on account of the inherent chemoselectivity, high yields, and often solvent-free reaction conditions associated with their chemistry.[128-130] The union of these two areas has been the subject of much attention recently and has resulted in the synthesis of natural product-based monomers from eugenol,[131-132] isosorbide,[49, 133-134] limonene,[23, 135-136] phenolic acids,[137] polyols,[48] and others[125] *en route* to polymers *via*

thiol-ene chemistry. There is particular interest in polymers that retain the biological properties of the natural products from which they are made, as is the case of antibacterial networks from linalool and isosorbide.[134] Natural products and their derivatives that are amenable to thiol-ene polymerization may serve as starting points in the design of polymers that include interesting biological properties. Furthermore, the potential to produce new materials with emergent properties for which there may be no close petrochemical equivalent drives the exploration of new natural products for polymeric materials.

One class of natural products that has been underdeveloped for renewable monomers and polymers is neolignans. Neolignans are structurally-diverse natural products synthesized through oxidative dimerization of a core phenylpropanoid unit[57] and have been well-studied for their anti-inflammatory and antioxidant properties, among others.[60] A recent example of a neolignan-based polycarbonate developed in our lab from honokiol, a natural product containing both phenolic and alkenyl functionalities, showed excellent cell compatibility and cell culturing capabilities.[138] The regioisomeric neolignan, magnolol, was unable to undergo carbonylation of the phenolic groups to establish an analogous linear polycarbonate, likely due to steric constraints. However, the 2,2'-biphenolic structure of magnolol provides opportunities for chemical modification or protection via ring closure to afford tricyclic structures that retain the alkenyl moieties. Magnolol is of particular interest, therefore, not only for potential biological properties, but also in that it is highly functional, allowing for either direct polymerization, or the rapid and scalable syntheses of diverse libraries of both

renewable monomers and polymers. Because the antioxidant properties[139] of magnolol involve intriguing redox chemistry of the phenols in the presence of peroxyl radicals,[140] without reliance on the allylic moieties, we designed a strategy whereby the alkenyl moieties could be used in forming a polymer network *via* thiol-ene chemistry, with variation in the chemistry conducted upon the phenolic groups to allow for monomer and polymer diversification and investigation of the physicochemical, thermomechanical, and biological properties.

Herein, we present the scalable syntheses of thermoset materials based on magnolol by solvent-free polymerization with a commercially-available, multifunctional thiol comonomer through photo-initiated thiol-ene chemistry. The partially bio-based, tunable thermosets were thoroughly characterized and differences in the resulting key thermomechanical properties were rationalized by the structure-property relationships of the magnolol-based monomers. Selective thermoset degradation, as well as cytotoxicity studies of both pristine thermosets and degradation compounds, directed radical scavenging and antioxidant assays. These studies have shown promising results for use of magnolol-based thermosets in biomedical applications where tunable polymer properties, including degradation, are desired and where beneficial biological activity of the degrading thermoset might be leveraged without the need for additional small molecule therapeutics.

3.3 Experimental Section

All chemicals were commercially available and used without further purification unless otherwise stated. Solvents were of ACS grade or higher. Magnolol (>98%) was purchased from Stanford Chemicals (Irvine, CA) and purified by silica column chromatography (15% EtOAC in hexanes) prior to direct thermoset synthesis and model reactions. NMR spectra (500 MHz for ^{1}H and 125 MHz for ^{13}C) were recorded on a Varian Inova 500 spectrometer. Chemical shifts were referenced to $CHCl_3$ at 7.26 ppm (^{1}H) and 77.16 ppm (^{13}C) or DMSO at 2.50 ppm (^{1}H) and 39.52 ppm (^{13}C), respectively. IR spectra were recorded on a Shimadzu IR Prestige attenuated total reflectance Fourier-transform infrared spectrometer (ATR-FTIR) and analyzed using IRsolution v. 1.40 software. Glass transition temperatures (T_g) were measured by differential scanning calorimetry (DSC) on a Mettler-Toledo DSC822 (Mettler-Toledo, Inc., Columbus, OH) under N_2 with a heating rate of 10 °C/min. The measurements were analyzed using Mettler-Toledo STAR^{e} v.10.00 software. The T_g was taken on the third heating cycle as the extrapolated onset temperature from the intersection of the tangent drawn from the transition curve with the greatest slope with the extrapolated baseline before the transition. Thermogravimetric analysis (TGA) was performed using a Mettler-Toledo model TGA/DSC 1, with a heating rate of 10 °C/min under an Ar atmosphere. The measurements were analyzed using Mettler-Toledo STAR^{e} v.10.00 software and the temperature for onset of thermal degradation, T_d, is reported. Rectangular dynamic mechanical analysis (DMA) samples were prepared in an aluminum mold (2.0 cm × 0.5

cm × 0.2 cm). Samples were sanded using 100 or 150 grit sandpaper to uniform dimensions. DMA was performed on a Mettler-Toledo TT-DMA system (Mettler-Toledo AG, Schwerzenbach, Switzerland). Samples were analyzed in tension *via* thermal scan (3 °C/min) from -40 ºC to 120 ºC in autotension mode, with a frequency of 1 Hz, a preload force of 1 N, and a static force of 1 N. Submersion DMA was performed by submerging samples directly into phosphate-buffered saline (PBS) at 37 °C and following the storage modulus decay isothermally over time. Three samples were used in each analysis. DMA data were obtained from Triton Laboratory software and exported to Origin Pro 8.0 for analysis. Exponential fitting was performed, as appropriate, to determine average storage modulus lifetimes. Chi-square and adjusted r-square were used to determine fit and the average storage modulus lifetimes for multiexponential kinetics which are given as $t_{avg} = \Sigma(a_i \bullet t_i^2) / \Sigma(a_i \bullet t_i)$. Mechanical testing was conducted to failure on ASTM type V dog bone samples ($n = 5$) using a dual column Instron model 5965 tensile tester with a 500 N load cell and 1000 N high temperature S5 pneumatic grips. The dog bone samples were cut from a film with a 40 W Gravograph LS100 CO_2 laser. Ultraviolet-visible spectroscopy (UV-vis) absorption measurements were made on a Shimadzu UV-2550 spectrophotometer using matched quartz cuvettes and the spectra were analyzed with UV-Probe v. 2.33 software.

3.3.1 Cell culture

Bovine coronary venular endothelial cells (CVECs) were gifted from Professors Cynthia J. Meininger and Andreea Trache at Texas A&M Health Science Center. CVECs and MC3T3 cells were cultured in Dulbecco's Modified Eagle Medium: Nutrient Mixture F-12 (DMEM/F-12) from Invitrogen (Invitrogen, Carlsbad, CA) supplemented with 10% Fetal Bovine Serum, 100 U/mL penicillin - 100 U/mL streptomycin - 0.25 mg/mL amphotericin B (Lonza, Walkersville, MD), and 20 units/mL heparin (Midwest Vet Supply, Lakeville, MN). Cells were plated on polymer coated round glass coverslips or on 1.5% bovine gelatin (Sigma-Aldrich, St. Louis, MS) for control. Polymer-coated coverslips were placed in a 35-mm glass-bottomed dish, sterilized under UV for 1 h in the biosafety cabinet, and washed with sterile PBS before cell placement. Cells were trypsinized, quenched with media, centrifuged to remove trypsin, and resuspended in fresh medium prior to plating as 25,000 cells per each dish. Cell medium was changed to fresh medium every 2 – 3 days and proliferation and morphology of the cells were monitored up to a month.

3.3.2 Dihydromagnolol-3,3'-bis(thioetherpropionic acid) (1)

3.3.2.1 Small Scale

Magnolol (0.1962 g, 0.7366 mmol) and 2,2-dimethoxy-2-phenylacetophenone (0.019 g, 0.074 mmol) were dissolved in 0.835 mL of deuterated dichloromethane in a

vial in the dark. 3-Mercaptopropionic acid (0.128 mL, 1.46 mmol) was then added and an aliquot of solution was transferred to an NMR tube prior to irradiation (λ = 352 nm, 40W). Starting material conversion was monitored by 1H NMR and reaction kinetics are shown in Figure A-15.

3.3.2.2 Large Scale

To a dry flask containing magnolol (2.3465 g, 8.810 mmol) and 2,2-dimethoxy-2-phenylacetophenone (0.2540 g, 0.9910 mmol) was added degassed dichloromethane (10 mL) under nitrogen. 3-Mercaptopropionic acid (1.55 mL, 17.6 mmol) was then added *via* syringe and the solution was irradiated (λ = 352 nm) in the dark. Aliquots were removed *via* syringe and conversion was monitored by 1H NMR. Upon total conversion of magnolol, the solution was concentrated and purified by column chromatography (15% → 100% EtOAc in hexanes). The viscous oil was dried *in vacuo* and allowed to solidify in a chemical fume hood at room temperature (3.7769g g, 7.891 mmol, 90% yield). ^{1}H NMR (DMSO, 500 MHz) δ 12.25 (br, 2H), 8.98 (br, 2H), 6.96 (br, 4H), 6.80 (d, *J* = 8.8 Hz, 2H), 2.67 (t, *J* = 7.1 Hz, 4H), 2.57 (t, *J* = 7.6 Hz, 4H), 2.50 (m, 8H), 1.77 (dt, *J* = 15.0, 7.6 Hz, 4H) ppm; ^{13}C NMR DMSO (125 MHz) δ 173.00, 152.36, 131.54, 131.32, 127.80, 125.76, 115.70, 34.54, 33.29, 31.22, 30.52, 26.34 ppm; FTIR (ATR): 3600-2400, 1692, 1615, 1510, 1497, 1435, 1420, 1378, 1343, 1302, 1259, 1239, 1198, 1150, 1116, 1066, 949, 933, 918, 891 cm^{-1}; ESI-MS $[M + Na]^{+}$ calculated: 501.1382, found: 501.1429.

3.3.3 Magnolol acetonide (2)

The synthesis was adapted from a previously reported procedure.[62] To a solution of magnolol (16.2128 g, 0.05965 mol) in 2,2-dimethoxypropane (70 mL) was added catalytic *p*-toluenesulfonic acid monohydrate (0.10 g). The reaction proceeded at room temperature overnight and was then concentrated, diluted with ether, and washed subsequently with aqueous sodium bicarbonate followed by water. The ether layer was then dried, filtered, and concentrated before purifying the orange-yellow oil by column chromatography (0→10% EtOAc in hexanes) to yield a clear oil (14.8780 g, 0.4855 mol, 81% yield). ^{1}H NMR ($CDCl_3$, 500 MHz) δ 7.32 (d, *J* = 2.2 Hz, 2H), 7.16 (dd, *J* = 8.1, 2.2 Hz, 2H), 7.04 (d, *J* = 8.1 Hz, 2H), 6.03 (ddt, *J* = 16.8, 10.0, 6.7 Hz, 2H), 5.17 – 5.09 (m, 4H), 3.46 (d, *J* = 6.7 Hz, 2H), 1.65 (s, 6H) ppm; ^{13}C NMR (125 MHz, $CDCl_3$) δ 150.16, 137.56, 136.86, 133.21, 128.80, 128.46, 123.26, 116.08, 115.40, 39.92, 25.25 ppm; FTIR (ATR): 3080-2800, 1638, 1493, 1423, 1381, 1371, 1254, 1247, 1219, 1201, 1134, 1115, 1041, 992, 975, 910, 894 cm^{-1}; ESI-MS $[M + Li]^+$ calculated: 313.1780, found: 313.1782.

3.3.4 Magnolol di(allylcarbonate) (3)

To a purged flask containing magnolol (15.6051 g, 0.05742 mol) and tetramethylethylenediamine (9.5 mL, ρ = 0.775 g/mL, 0.062 mol) in dichloromethane (110 mL) was added allyl chloroformate (18.0 mL, 0.164 mol) in DCM (30 mL) at 0 °C by addition funnel over 1 h. The reaction was allowed to stir for an additional hour

before the solution was washed with saturated sodium bicarbonate solution and then water. The organic was dried, filtered, and concentrated and subjected to column chromatography (5 → 10 % EtOAc in hexanes) to yield the monomer as a clear oil (15.2400 g, 0.03508 mol, 74% yield). ^{1}H NMR ($CDCl_3$, 500 MHz): δ 7.21 (dd, *J* = 8.2, 2.2 Hz, 2H), 7.17 (d, *J* = 8.2 Hz, 2H), 7.14 (d, *J* = 2.2 Hz, 2H), 5.96 (ddt, *J* = 16.9, 10.2, 6.7 Hz, 2H), 5.83 (ddt, *J* = 17.3, 10.6, 5.7 Hz, 2H), 5.24 (dd, *J* = 17.2, 1.4 Hz, 2H), 5.19 (dd, *J* = 10.5, 1.4 Hz, 2H), 5.09 (m, 4H), 4.57 (m, 4H), 3.40 (d, *J* = 6.7 Hz, 4H) ppm; ^{13}C NMR ($CDCl_3$, 125 MHz): δ 153.34, 146.87, 138.06, 137.02, 131.49, 131.36, 129.76, 129.36, 122.17, 118.88, 116.39, 69.02, 39.63 ppm; FTIR (ATR): 3080-2820, 1758, 1639, 1493, 1362, 1236, 1205, 1190, 1099, 1035, 992, 915 cm^{-1}; ESI-MS $[M + Na]^+$ calculated: 457.1627, found: 457.1622.

3.3.5 Magnolol di(allylether) (4)

To a flask containing magnolol (7.3326 g, 0.02698 mol) and potassium carbonate (17.9210 g, 0.1296 mol) in acetone (100 mL) was added allyl bromide (9.5 mL, 0.11 mol) before refluxing the mixture overnight. The filtrate was then collected, concentrated, and taken up in dichloromethane before washing with water. The organic was then dried, filtered, concentrated and the resulting crude oil was purified by column chromatography (5% EtOAc in hexanes) to yield the monomer as a clear oil (6.8225 g, 0.01969 mol, 73% yield). ^{1}H NMR ($CDCl_3$, 500 MHz): δ 7.12 – 7.07 (m, 4H), 6.87 (d, *J* = 8.1 Hz, 2H), 6.04 – 5.96 (m, 2H), 5.96 – 5.87 (m, 2H), 5.22 (dd, *J* = 17.3, 1.8 Hz,

2H), 5.14 – 5.03 (m, 6H), 4.48 (d, J = 4.8 Hz, 4H), 3.36 (d, J = 6.6 Hz, 4H) ppm; ^{13}C NMR ($CDCl_3$, 125 MHz): δ 154.61, 137.99, 133.89, 131.94, 131.91, 128.36, 128.33, 116.44, 115.58, 112.63, 69.29, 39.56 ppm; FTIR (ATR): 3100-2790, 1638, 1605, 1495, 1453, 1421, 1381, 1360, 1269, 1221, 1135, 1105, 1021, 993, 910 cm^{-1}; ESI-MS $[M + Na]^+$ calculated: 369.1831, found: 369.1858.

3.3.6 General procedure for thiol-ene polymerization with magnolol derivatives

To a covered vial containing magnolol-based monomer and pentaerythritol tetrakis(3-mercaptopropionate) (1:1 mol alkene:thiol) was added freshly ground 2,2-dimethoxy-2-phenylacetophenone (1 wt%:thiol). The resin was mixed in the dark until all photoinitiator was dissolved. The resin was then pipetted into molds or between PTFE-treated glass slides to generate rectangular bars, pellets, and films. The polymerization proceeded in a UV oven for 4-6 h followed by a postcure at 110 °C for 2 h.

3.3.7 Procedure for thiol-ene polymerization with magnolol

In a 20 mL scintillation vial was added magnolol, pentaerythritol tetrakis(3-mercaptoproprionate) (1:1 mol alkene:thiol), and 2,2-dimethoxy-2-phenylacetophenone (3 wt%:thiol). The thick tan solid mixture was then heated at 110 °C for several minutes until a clear, colorless, homogenous oil was produced. The oil, still warm, was pipetted into molds or between PTFE-treated glass slides to generate rectangular bars, pellets,

and films. The polymerization proceeded in a UV oven for 2 h followed by a post-cure at 110 °C for 2 h.

3.3.8 Hydrolytic degradation

Thermosets were prepared from a home-built silicon cylindrical mold and were *ca.* 2.0 mm × 1.5 mm diameter. The cylindrical pellets were added to 1 dram vials, 3 samples for each degradation condition. 4 mL of appropriate PBS solution (acidic: pH = 3.0, basic: pH = 12.0, physiological: pH = 7.4) were added to each vial and the vials were placed in an incubator shaker at 37 °C, 60 RPM. Swelling and degradation measurements were taken by removing the pellet, blotting dry, and then weighing the pellet. Pellets were then dried to constant weight at 50 °C under vacuum and reweighed. The samples were added back to the appropriate vials and degradation solutions were replaced. Degradation solutions were lyophilized and saved for use in later experiments. Swelling percentage was taken as the mass difference between wet and dry samples relative to the dry sample mass.

3.3.9 Antioxidant/Radical Scavenging (DPPH$^{\bullet}$) assay

The procedure to assess radical scavenging was adapted from Scherer and Godoy[141] using the 2,2-diphenyl-1-picrylhydrazyl (DPPH$^{\bullet}$) radical. Methanol (HPLC grade, ≥ 99.9%) solutions of DPPH$^{\bullet}$ were first prepared to assess linearity and stability

before a calibration curve and the time necessary for the reaction to reach the steady state was determined (S4). Samples used in the assay included model degradation compound **(1)** and degradation compounds which were prepared separately by lyophilization of the degradation solutions obtained from hydrolytic degradation. Briefly, the lyophilized degradation product was dissolved in 10 mL of MeOH, sonicated for two minutes, and filtered through a syringe filter (Pall Life Science, Acrodisc® syringe filter with nylon membrane, 0.45 μm). Antioxidant activity was determined by adding 100 μL of model degradation compound (4.95×10^{-4} M stock solution) or degradation solutions to 3.9 mL of DPPH$^{\bullet}$ stock solution (3.0×10^{-4} M) and were analyzed by UV-vis spectroscopy at 0 h and 3 h. The reaction solutions were kept in the dark otherwise. The experiments were performed in triplicate for each compound and degradation solution. The radical scavenging ability was determined by following the change in absorbance of DPPH$^{\bullet}$ at 514 nm over time compared to a reference blank (0.1 mL MeOH and 3.9 mL DPPH$^{\bullet}$ stock solution).

3.3.10 Immunofluorescence and Confocal Imaging

Cells were fixed with 4% paraformaldehyde with 5% sucrose prior to membrane permeabilization with Triton X-100. Cytoskeleton structure was visualized by staining with phalloidin-Alexa 488® (Invitrogen, Carlsbad, CA). Focal adhesions were stained with vinculin antibody (Sigma-Aldrich, St. Louis, MS) followed by secondary antibody conjugated with Alexa 647® (Invitrogen, Carlsbad, CA). Fluorescence images were

acquired with a FV1000 confocal microscope (Olympus, Center Valley, PA) with an IX-81 inverted base and PMT detectors. Alexa 488® and Alexa 647 fluorophores were excited with 488 nm from an Ar laser and 635 nm from a diode laser, and emissions were collected from 500 – 550 nm and 660 – 710 nm simultaneously. Cell populations on polymer substrate were compared to cells cultured on 1.5% gelatin from a large filter view with a 10× objective lens (Olympus). Details of cell morphology were investigated with 4× zoom with the same objective lens (equivalent to 40× magnification). 3D confocal images were acquired as stacks of 4 - 8 planes with 3 μm step size for 1× zoom and stacks of 16 - 20 planes with 1μm step size for 4× zoom. Images were acquired and contrast was adjusted using Fluoview Viewer software.

3.3.11 In Vitro Reactive Oxygen Species (ROS) Scavenging Assay

Model degradation compound (**1**) was used to test as a ROS scavenger by co-culturing the CVECs in the presence of 1% FBS and peroxide reagent. Cells were plated at a density of 30,000/well and were then incubated at 37 °C in a humidified atmosphere containing 5% CO_2 for 24 h to adhere. **1** and magnolol were dissolved in DMSO, sterilized under UV for 1 h in the biosafety cabinet, and then further diluted with DMEM/F-12 – phenol free 1% FBS medium to desired concentrations. After incubating the CVECs with **1** or magnolol solutions for 24 h, the medium was replaced with the formulations in phenol-free 1% FBS medium with the addition of 1 μL of 0.5 mM of *tert*-butyl hydroperoxide (tBHP) (Sigma-Aldrich, St. Louis, MO) in 100 μL of cell

medium and incubated for 2 h at 37 °C with 5% CO_2. The medium was finally replaced with 50 μM of 2',7'–dichlorofluorescin diacetate (DCFDA) (Sigma-Aldrich, St. Louis, MO) in phenol-free 1% FBS medium and incubated for 30 min at 37 °C with 5% CO_2. ROS levels were measured from the fluorescence of DCFDA at 529 nm with excitation at 495 nm.

3.4 Results and Discussion

Because the antioxidant characteristics of magnolol are due to the radical scavenging ability of its phenolic groups, our original aim to employ the alkenyl functionalities for thiol-ene copolymerization of magnolol with multi-functional comonomers necessitated a study of its reactivity in a model photo-initiated thiol-ene reaction (Figure 3-1, lower left). A mono-functional thiol was used for these model studies to be able to monitor the reaction and isolate the products as small molecules for detailed analyses to confirm that the thiol-ene reaction would proceed in high conversion without significant radical scavenging by the phenols that could lead to cyclohexadienone formation and other side reactions. In addition, the mono-functional thiol was selected to be 3-mercaptopropionic acid, specifically, as the bis(thioetherpropionic acid) adduct **1** and its mono-thioether analog have the chemical structures of the hydrolytic degradation products from the thiol-ene copolymerization of magnolol with pentaerythritol tetrakis(3-mercaptoproprionate) (PETMP). In the

presence of *ca.* 0.05 mol% photoinitiator (2,2-dimethoxy-2-phenylacetophenone, DMPA, m.p. = 70 °C), two equivalents of 3-mercaptopropionic acid were allowed to undergo reaction with magnolol under ultraviolet irradiation (λ = 352 nm, 40W) in deuterated dichloromethane at room temperature. The reaction was monitored by 1H NMR spectroscopy and found to reach 100% conversion at 10 m, with no undesirable by-product formation noticed (Figure A-15). The model reaction was then scaled up from *ca.* 100 mg magnolol to several grams in a round bottom flask with degassed dichloromethane to model the scale at which polymerizations would occur and to yield desirable quantities of this model compound for future studies. At this larger scale but under identical conditions, full alkene conversion required 2 h. The viscous oil was purified by column chromatography (15→100% ethyl acetate in hexanes) and then allowed to solidify under atmospheric conditions to afford **1** in 90% yield.

Although the phenols of magnolol did not significantly impede the model thiol-ene reaction in solution, direct thermoset synthesis in the bulk utilizing magnolol as an A_2 monomer and widely-available pentaerythritol tetrakis(3-mercaptoproprionate) (PETMP) as a tetra-functional B_4 comonomer encountered challenges. At room temperature, the solid magnolol monomer and photoinitiator did not dissolve well into the viscous thiol comonomer (Figure A-16). Attempts to realize bulk polymerization through photoinitiation at room temperature were unsuccessful. However, with manageably low melting points for DMPA and magnolol (m.p. = 102 °C), the mixture of comonomers and photoiniator were melted at 110 °C in an oven to produce a clear oil that was transferred hot into pre-shaped molds. The resins were then polymerized in a

UV oven (352 nm, 40W total) for 2 h followed by a post cure at 110 °C for an additional 2 h. Similar to the observed differences in the model reactions performed on small and large scales in solution, thermoset synthesis in bulk performed on scales up to several grams in molds (ca. 0.5 cm thick) necessitated a longer UV exposure for gelation. The resulting clear, colorless magnolol/PETMP (MAG/PETMP) thermosets were stiff but pliable after handling. Notably, attempts to thermally initiate DMPA and yield polymer in the absence of UV irradiation were unsuccessful, even after heating for 10 h at 110 °C – no gelation was observed and solid precipitated from the mixture upon cooling to room temperature.

Initial characterization was performed to determine the thermomechanical properties and chemical resistance under basic, acidic, and physiologically-relevant pH at physiological temperature (Figure 1). The MAG/PETMP thermoset was thermally stable (onset of thermal degradation, T_d = 350 °C) and showed modest storage modulus (E′ @ 25 °C = 1.10 ± 0.14 GPa). The glass transition temperature, T_g, was slightly above room temperature, as measured by dynamic mechanical analysis (DMA) (T_g = 29 ± 1 °C). The thermomechanical properties also appeared to have an effect on the hydrolytic stability in that, although hydrophobic, at physiological temperature, the MAG/PETMP thermoset immediately swelled and began hydrolytic degradation in basic PBS media (pH = 11.0) (Figure 3-2, bottom). Full degradation occurred by 18 weeks under basic conditions, while samples exposed to acidic and pH = 7.4 conditions displayed little swelling and no degradation over the course of the study. It is expected

that degradation occurred through hydrolysis of the ester moieties of the repeat units derived from PETMP.

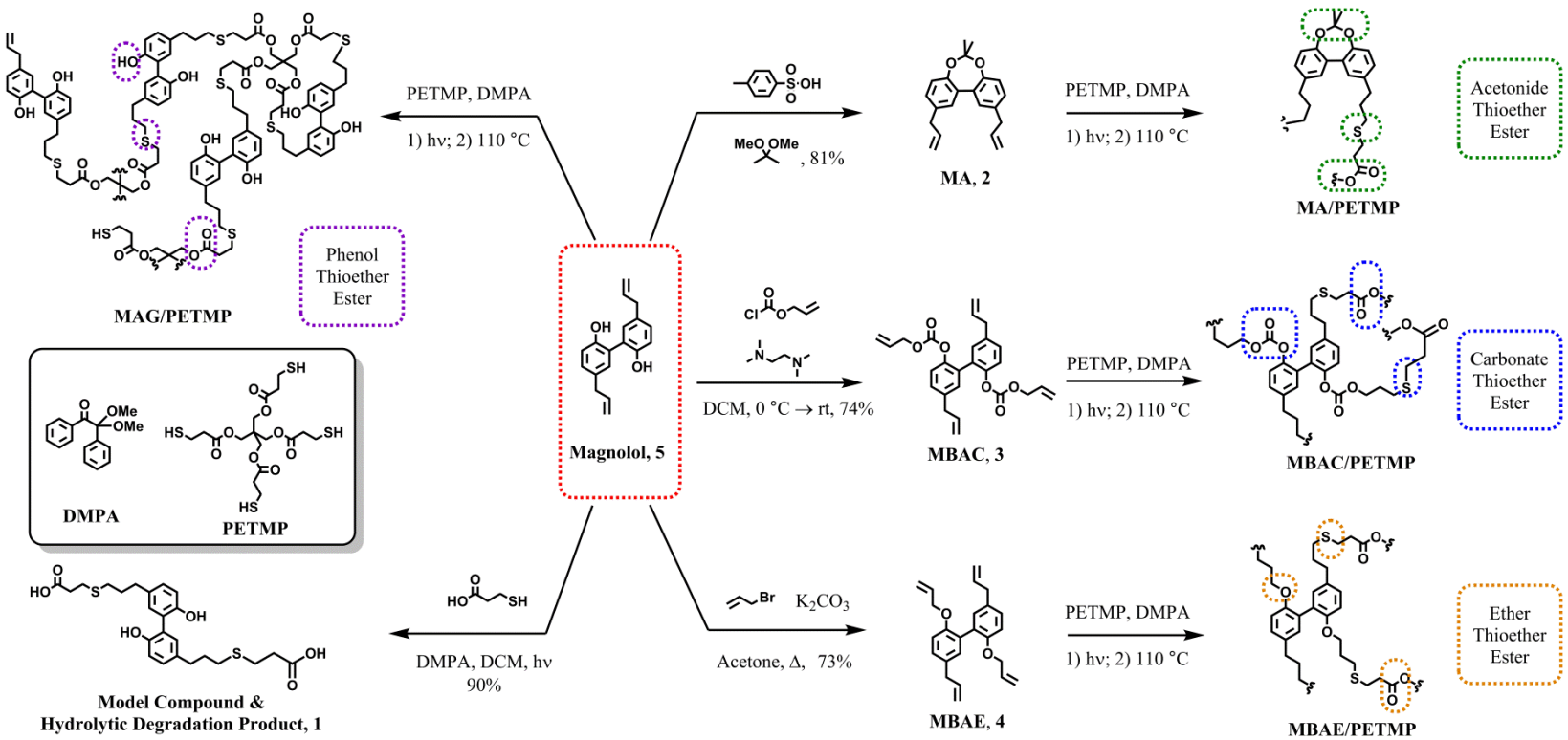

Figure 3-1. Synthetic Approach to Magnolol Monomers, Thermosets, and Model Compound.

To expand upon the performance of this initial thermoset, a small library of magnolol-based monomers was desired, wherein crosslinked polymer networks would be synthesized *via* thiol-ene polymerization and the resulting thermomechanical and degradation properties could be controlled through the initial monomer design and further exploited in material applications without requiring extensive synthetic procedures or processing. With this in mind, magnolol was functionalized in three separate reactions to yield di- or tetra-functionalized monomers on multigram (up to decagram) scales and > 70% yields. Magnolol acetonide, MA (**2**), a tricyclic, di-functional A_2 monomer containing an acid-labile phenolic protecting group was synthesized by organic acid-catalyzed acetonide formation with 2,2-dimethoxypropane in 81% yield through a procedure adapted from Schinazi and coworkers.[62] Of the tetra-functional A_4 monomers, magnolol bis(allyl carbonate), MBAC (**3**) – intended to serve as a base-labile monomer – was synthesized in 74% yield by addition of allyl chloroformate to a solution of magnolol in dichloromethane and tetramethylethylenediamine at 0 °C following a similar procedure from previously reported work in our group,[48] while magnolol bis(allyl ether), MBAE (**4**), a hydrolytically-stable monomer, was prepared in 73% yield using slight excess of allyl bromide with potassium carbonate in acetone under reflux (Figure 3-1).

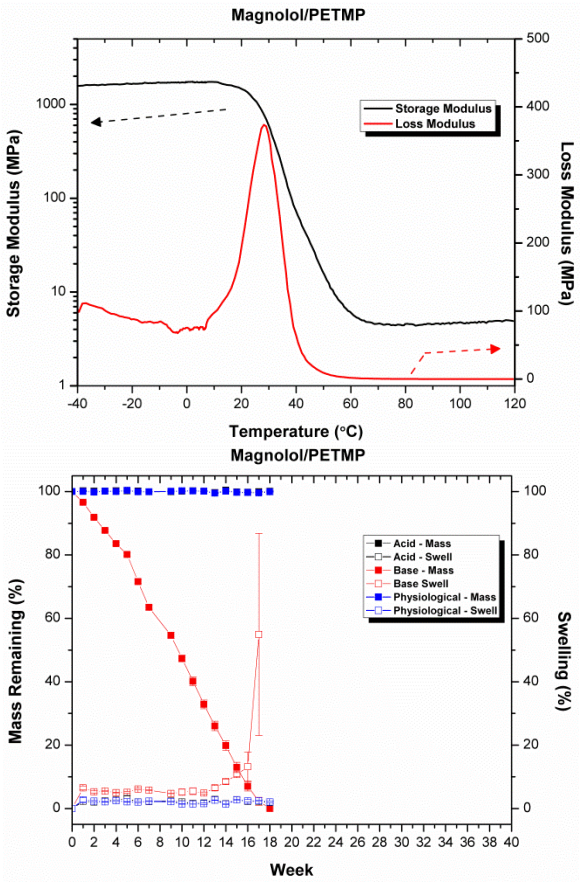

Figure 3-2. Characterization of Thermosets Synthesized Directly from Magnolol and PETMP. Dynamic Mechanical Analysis Exhibiting Loss in Mechanical Properties Near Room Temperature and T_g, as Measured by the Peak in the Loss Modulus, E″, at 29 °C (Top). Degradation of Thermoset Pellets (n = 3, *ca*. 110 mg each), in PBS Media (pH = 3.0, 7.4, and 11.0, Bottom).

Similar to the direct synthesis of thermosets from magnolol, highly-crosslinked thermosets were achieved through reaction of **2**, **3**, or **4** with PETMP using stoichiometric equivalences of functional group and in the presence of 1 wt% DMPA:thiol under UV irradiation followed by a post-cure at 110 °C. Although magnolol is a beige solid in its commercial form (> 98% purity), the magnolol-based

monomers **2**–**4** were transparent, colorless oils and mixed well with comonomer and photoinitiator. No heating was required to mix or transfer the resin to the molds and the solvent-free polymerizations ultimately yielded transparent films. Comparison of FTIR spectra of the films to the spectra of the monomers did not indicate the presence of free thiol (S-H stretch, *ca.* 2600 cm^{-1}) (Figure A-17) and showed good consumption of alkene (str. C-H bend, *ca.* 900 cm^{-1}) (Figure A-18) in the thermosets.

Table 3-1. Magnolol Thermosets Showing Tunable Thermomechanical Properties by TGA, DSC, DMA, and Tensile Testing

Thermoset	T_d (°C)	T_g – DSC (°C)	T_g – DMA[a] (°C)	E′ (GPa)[b]	E_r (MPa)[c]	Modulus (MPa)	Ultimate Strength (MPa)	Strain (%)
MAG/PETMP	350	23	29	1.10 ± 0.14	4	386 ± 65	28 ± 5	68 ± 25
MA/PETMP	359	30	33	1.25 ± 0.09	7	384 ± 37	26 ± 3	131 ± 29
MBAC/PETMP	293	46	52	1.33 ± 0.02	38	735 ± 48	48 ± 2	18 ± 6
MBAE/PETMP	361	47	52	1.21 ± 0.13	41	794 ± 91	50 ± 2	20 ± 7

[a]As measured by the peak of the loss modulus, E″. [b]Measured at 25 °C. [c]Measured at 100 °C.

As was expected, the thermoset compositions containing monomers with higher functionality (and a greater expected degree of crosslinking), MBAC/PETMP and

MBAE/PETMP, displayed higher T_gs by DSC (46 and 47 °C) as compared to the difunctional magnolol-based thermosets, MA/PETMP (30 °C) and MAG/PETMP (23 °C) (Table 3-1). Interestingly, the same trend was not observed thermogravimetrically, as MAG/PETMP, MA/PETMP, and MBAE/PETMP showed significantly higher thermal stabilities – 350, 359, and 361 °C, respectively – compared to MBAC/PETMP, which began degrading at *ca*. 295 °C (Figure 3-3). The MBAC/PETMP thermoset did display a second thermal degradation event near *ca.* 360 °C and a final thermal degradation event near *ca.* 425 °C as did the thermosets synthesized from monomers **2**, **4**, and **5**. All other variables equivalent, and given the high conversion of monomers to thioether, we hypothesize this difference in thermal stability amongst the polymers is a result of a more thermally-labile carbonate linkage in MBAC/PETMP. Similar degradation temperatures have been observed for other polycarbonate crosslinked networks synthesized *via* thiol-ene chemistry.[48-49]

With these results, we decided to further investigate by DMA (dry and submersion) and tensile testing analyses the fundamental materials properties and potential performance of the thermosets relevant to biomedical materials. The same T_g trend was observed by DMA as for DSC, whereby the MA thermoset showed a transition at 33 °C (as measured by the peak of the loss modulus, E″), just below physiological temperature, while MBAC and MBAE thermosets were *ca.* 20 °C higher (Figure 3-4). All T_gs were higher than the thermoset synthesized directly from magnolol (MAG/PETMP, 29 °C). Although containing the same degree of crosslinking, assuming a complete thiol-ene reaction, the slightly higher glass transition of MA/PETMP may be

attributed to the rigidity of this monomer with its tricylic structure compared to the thermoset from the magnolol monomer which is able to undergo rotation about the biphenyl C-C bond. Given the differences in T_g, there is a greater than 1000 MPa difference in the storage moduli, E′, between MBAE/PETMP (1250 MPa) or MBAC/PETMP (1210 MPa) and MA/PETMP (100 MPa) or MAG/PETMP (110 MPa) at 37 °C. These results are in contrast with the material properties at room temperature, which show little change in E′. Additionally, the degree of crosslinking was noticeably higher in A_4B_4 MBAC and MBAE thermosets compared to the A_2B_4 MA/PETMP and MAG/PETMP thermosets as measured by the rubbery modulus, E_r, in accordance with the theory of rubber elasticity.[142] These differences, although seemingly modest at room temperature, may have large effects under physiological conditions.

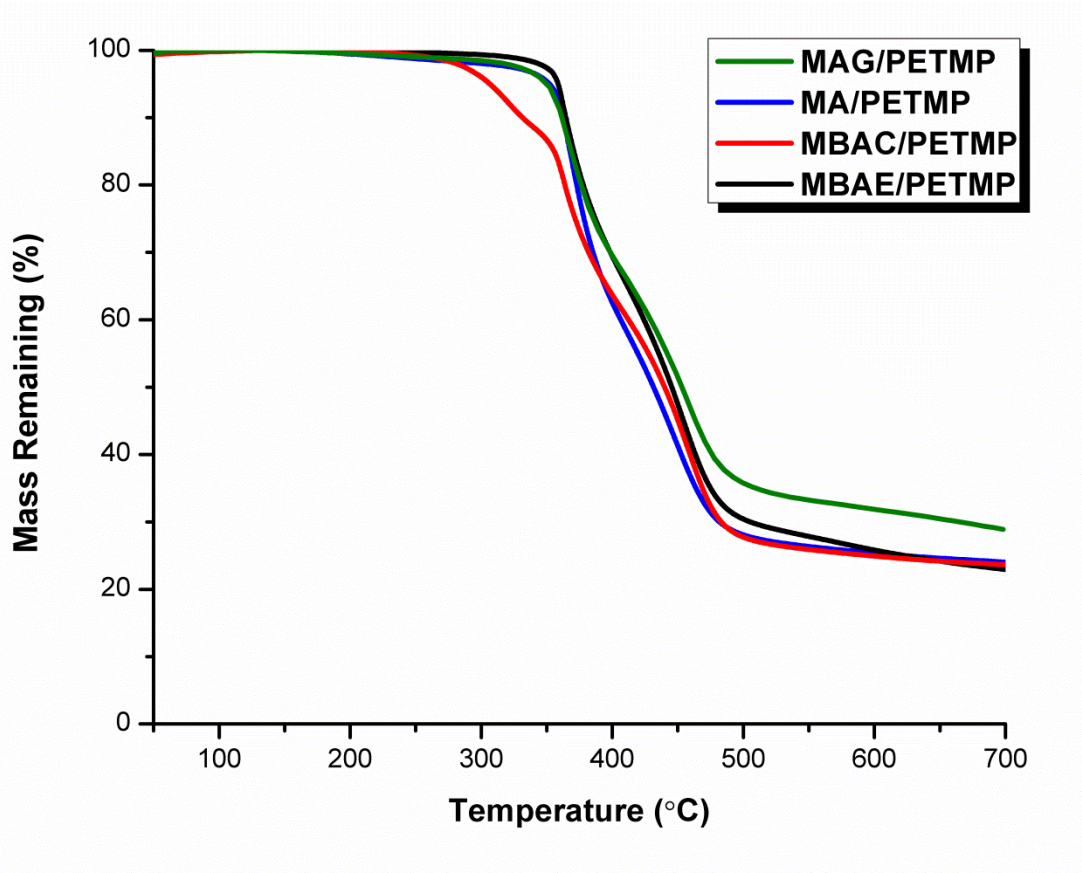

Figure 3-3. TGA Analyses of Thermosets Under Nitrogen Atmosphere.

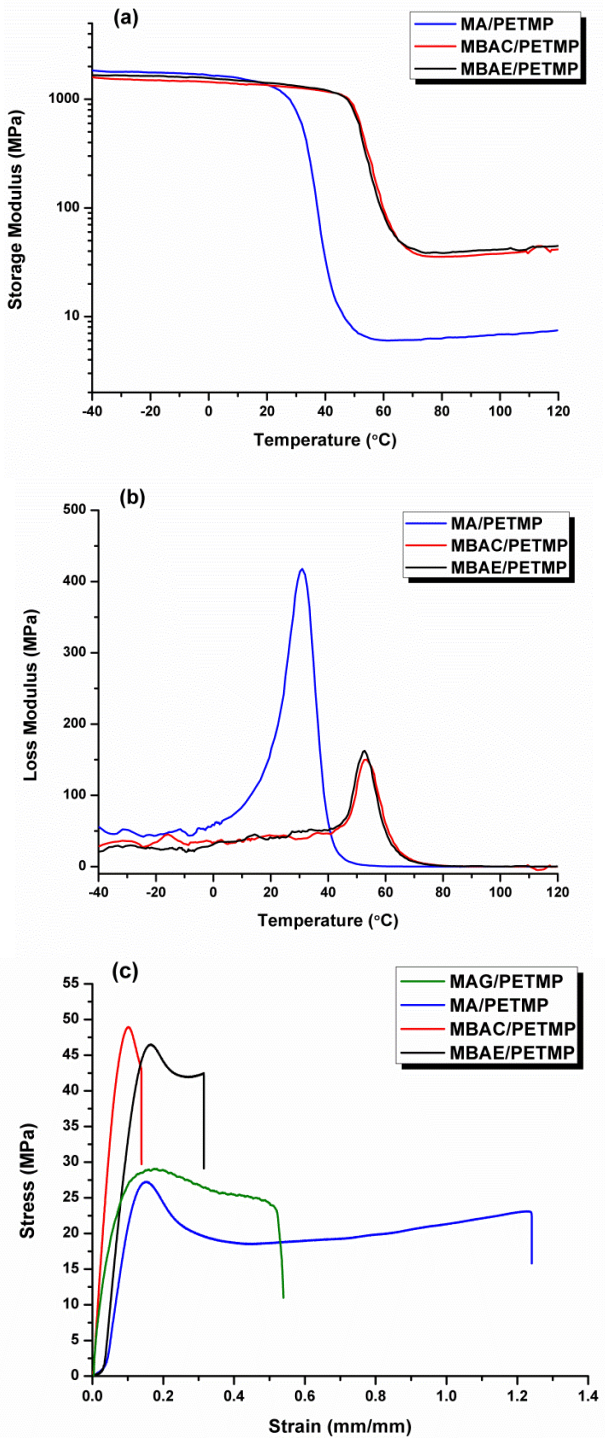

Figure 3-4. Thermomechanical Results Comparing MAG/PETMP, MA/PETMP, MBAC/PETMP, and MBAE/PETMP. (a) Storage Moduli, E′, Showing Distinct Differences Above Physiological Temperature, Particularly in Rubbery Modulus, E_r , Measured at 100 °C. (b) T_gs as Measured by the Peak in the Loss Modulus, E″. (c) Tensile Testing Performed at Room Temperature, 5 mm/min Strain Rate.

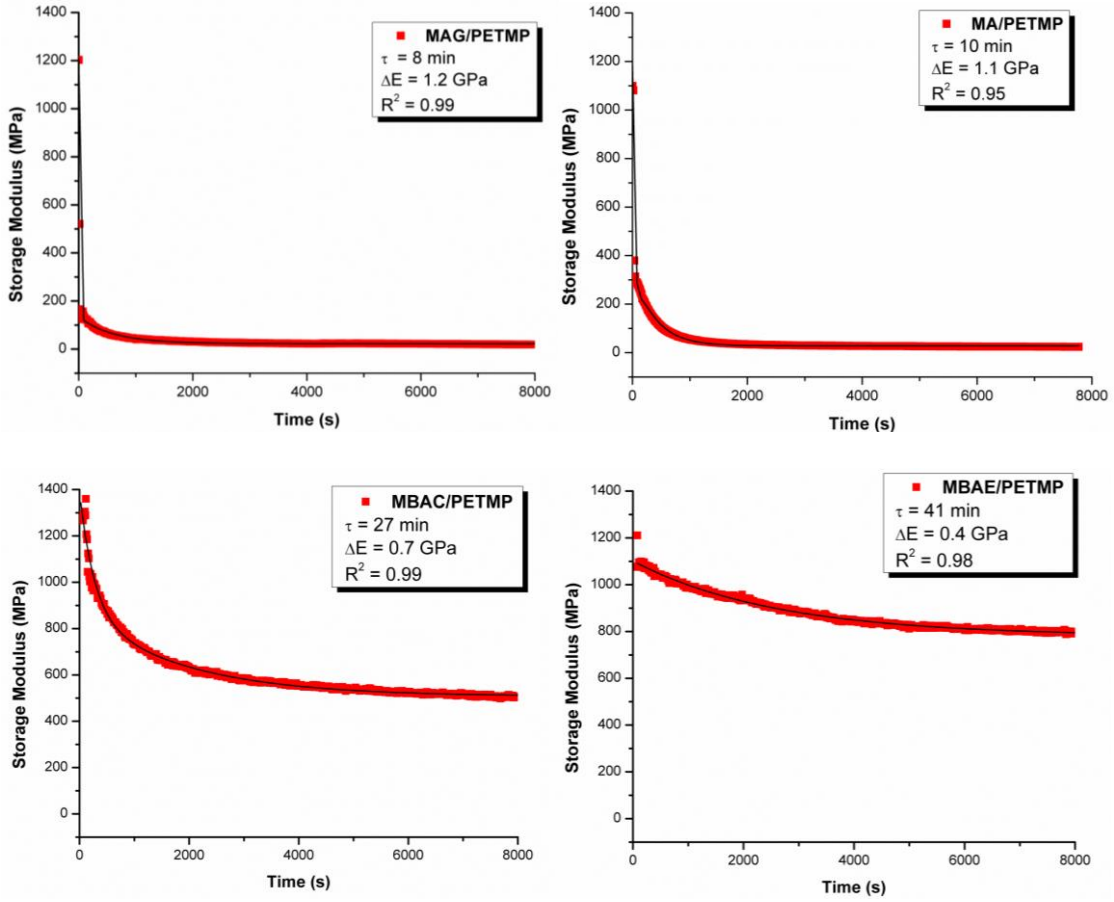

Figure 3-5. Submersion DMA (PBS, pH 7.4, 37 °C) and Lifetime Measurements.

The effects of compositional and structural differences of the thermosets on mechanical properties were also revealed by tensile testing. Each thermoset displayed a modest ductile behavior at a strain rate of 5 mm/min, however, MA/PETMP showed a drastically higher strain at failure and lower modulus and ultimate strength than the more highly-crosslinked counterparts. The mechanical behavior of MAG/PETMP was similar

to MA/PETMP, with the exception of having early strain at break. In addition to the chemical composition differences across this series of thermosets, the relatively lower crosslinking density for the MA- and MAG-derived A_2B_4 materials and their associated lower T_g values *vs*. the A_4B_4-based structures may have contributed to the mechanical properties effects, due to the testing conditions (room temperature ≈ 27 °C) being near their glass transitions but still 25 °C lower than thermosets from MBAC and MBAE (Figure 3-4c).

As the dry thermoset properties may be altered in response to plasticization under physiological conditions, in situ matrix relaxation DMA was also performed in PBS at 37 °C. The wet material properties may yield additional insight into the ultimate material performance in a biological application. The change in E′ over time followed a similar trend to the T_g of the dry thermosets. The results were fitted to dual-exponential decay models which yielded average storage moduli lifetimes, τ, of 8 min (MAG/PETMP), 10 min (MA/PETMP), 27 min (MBAC/PETMP), and 41 min (MBAE/PETMP) (Figure 3-5). The dual-exponential fit accounts for the response of the thermosets to both temperature change (room temperature to physiological temperature, Δ 12 °C) followed by solvent plasticization of the thermosets. The overall loss in mechanical properties, as measured by the change in the storage moduli, ΔE′, followed an inverse relationship, whereby MAG/PETMP had the largest loss over time (ΔE′ = 1200 MPa) while MBAE/PETMP showed the least significant change (ΔE′ = 400 MPa). MA/PETMP similarly displayed a large and quick change in mechanical properties when placed under physiological conditions and we anticipated that swelling and subsequent

hydrolysis might occur most readily in this thermoset (compared to MBAC and MBAE thermosets) at a rate comparable to the degradation observed for MAG/PETMP. Interestingly, the surface chemistry did not appear to have a substantial effect on the plasticization and loss in mechanical properties upon submersion in PBS. Furthermore, there was not a significant effect of the chemical composition on the water contact angles, other than the phenol-containing MAG/PETMP was slightly more hydrophilic (θ_{water} = 75°) than the thermosets having the phenolic groups consumed (θ_{water} = 88 - 94°) (Figure 3-6).

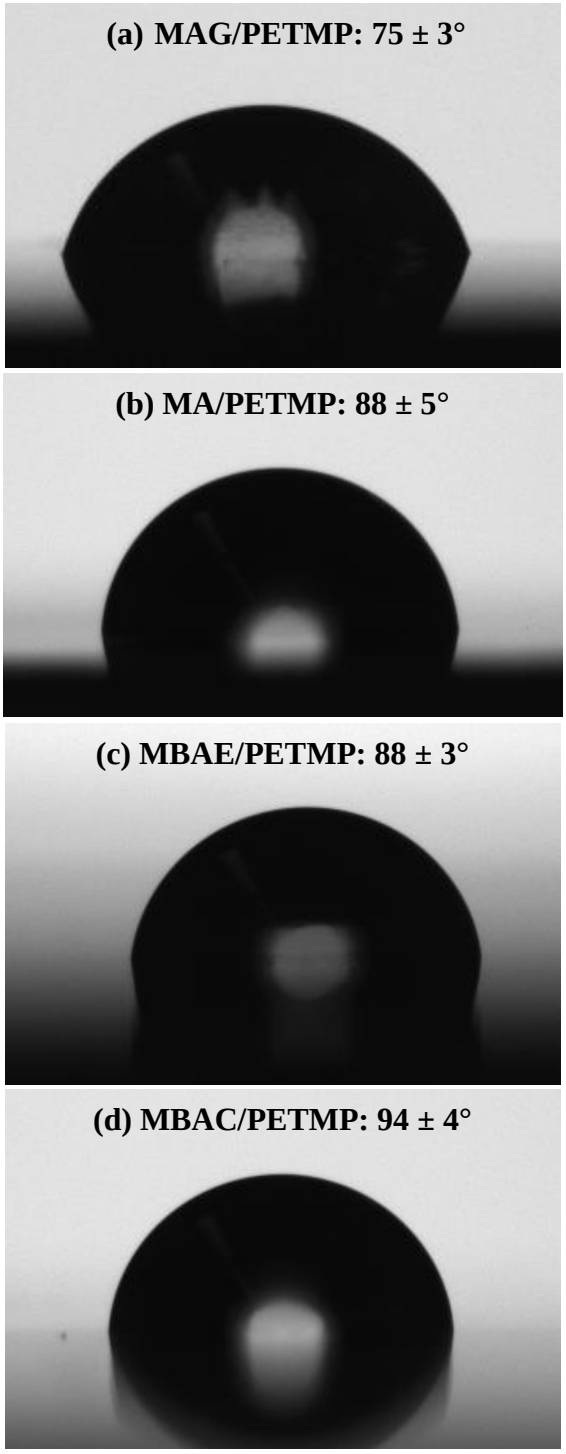

Figure 3-6. Static Water Contact Angles on MAG (a), MA (b), MBAE (c), and MBAC (d) Samples and Average Contact Angles for Each Substrate; $n \geq 3$..

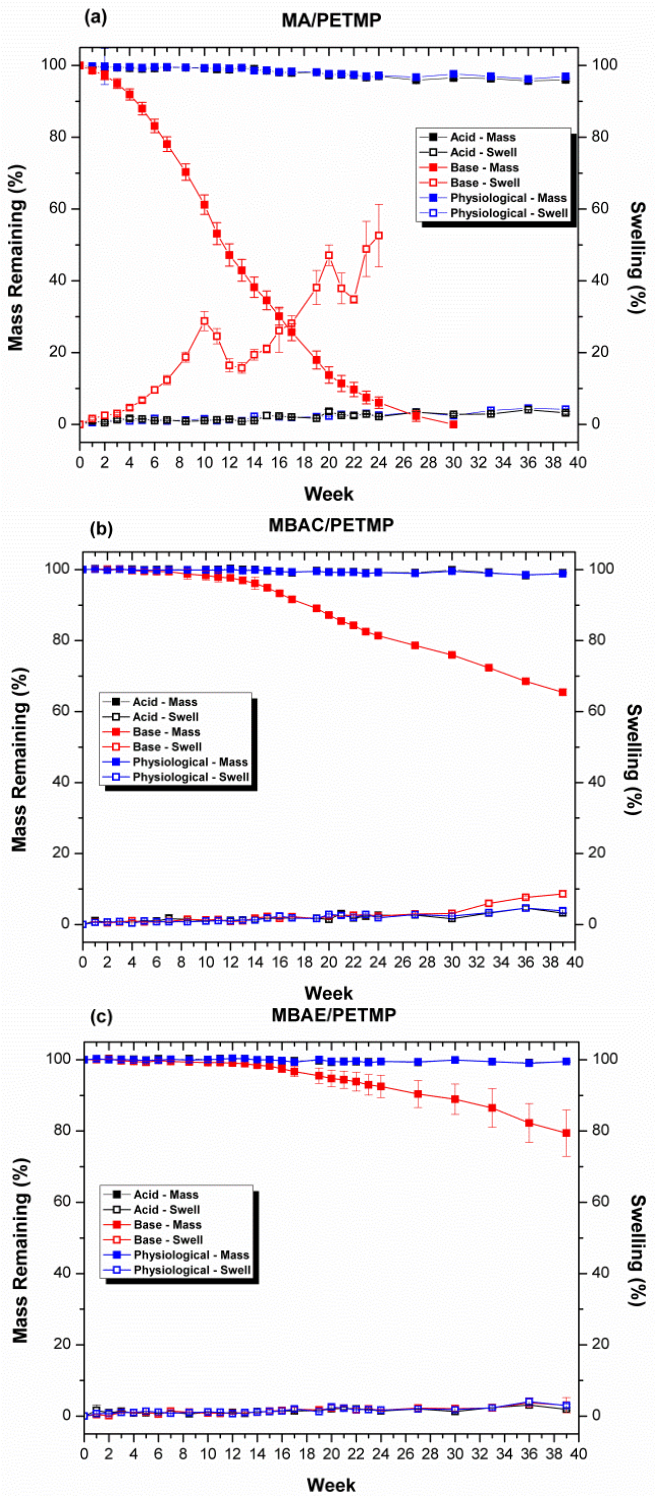

Figure 3-7. Hydrolytic Degradation and Swelling in PBS (a) MA/PETMP, (b) MBAC/PETMP, (c) MBAE/PETMP Under Basic, Acidic, and Physiological pH at 37 °C.

Previous reports have examined renewable resources in degradable polymers to affect a biological response as the polymer degrades. Salicylic acid-based poly(anhydride ester)s[143-144] and polyesters,[145-146] as well as ferulic acid-based poly(carbonate amide)s[51] and poly(anhydride ester)s[147] have been studied for the potential antimicrobial or antioxidant properties of their degradation products. Salicylic acid-based polymers have similarly been examined as an antioxidant coating in drug eluting stents,[148] while materials based on naturally-occurring biopolymers, such as modified dextran polymers[149] and melanin nanoparticles[150], have been utilized to efficiently scavenge hydrogen peroxide and other reactive oxygen or nitrogen species. Polymer peroxide scavenging may also be leveraged as a cue for polymer degradation and release of therapeutic.[149, 151] As these polymers and others[152] often show antioxidant properties as a result of the inherent radical scavenging ability of phenol moieties, functionalized magnolol thermosets which hydrolytically degrade to yield a phenol may similarly scavenge radicals and protect cells from oxidative stress. This may be particularly advantageous as protection in the local cellular environment from the response of the host immune system to a biomaterial. The crosslinking and modest hydrophobicity inherent to these polymer networks should also result in a slow, controllable degradation and a sustained release of the magnolol degradation products.

Degradation studies were again performed in acidic, basic, and physiological pH PBS media at physiological temperatures but with samples from the phenolic-functionalized thermosets. MA/PETMP began degrading within 2 weeks under basic conditions, had less than 50% mass remaining by week 12 and was fully degraded by

week 30. The MBAC/PETMP thermoset showed only 5% degradation at week 15 while MBAE/PETMP did not exhibit significant mass loss until after week 17 under identical conditions (Figure 3-7). Visually, the pellets display distinct differences both in size and surfaces even by week 10 (Figure A-19). There was no significant degradation observed for thermosets under acidic or neutral conditions during this time period – MA/PETMP had *ca.* 96% mass remaining under acidic and neutral conditions at 27 weeks while MBAC and MBAE thermosets still had *ca.* 99% mass remaining. The < 4% mass loss from MA/PETMP under acidic or neutral conditions may result, in part, from hydrolysis of the acetonide moiety that releases acetone but preserves the crosslinked polymer network. The stark difference in degradation behavior is likely a result of differences in the thermal response and plasticization of the polymers at physiological temperatures that initially leads to basic hydrolytic degradation of the pentaerythritol ester backbone. This hypothesis is supported by the results obtained from submersion DMA experiments and the observed T_gs of the dry material.

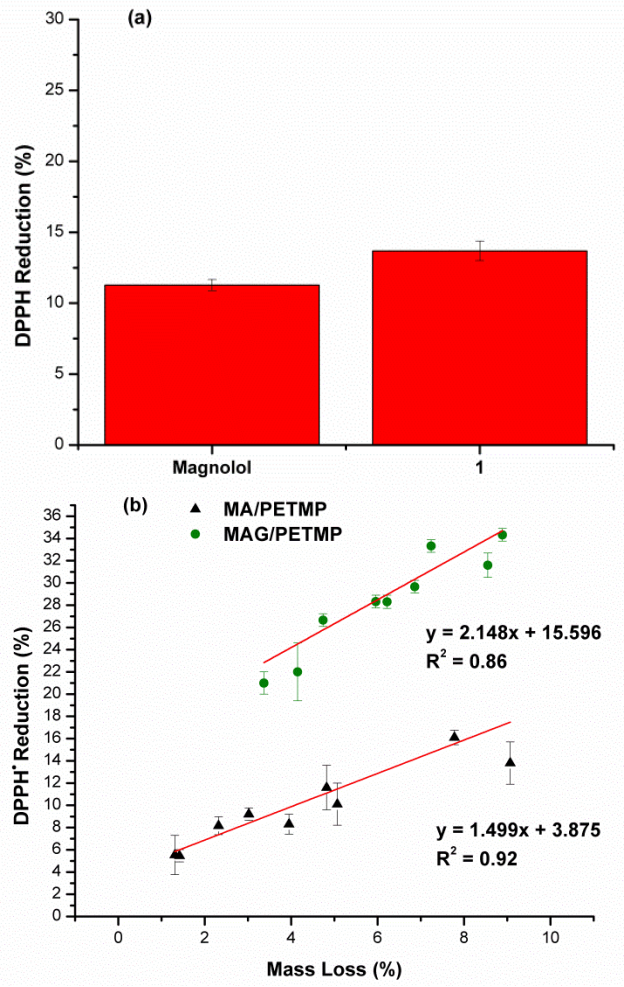

Figure 3-8. Radical Scavenging by DPPH$^{\bullet}$ Reduction. (a) Model Degradation Compound, **1**, Compared to Known Natural Product Antioxidant, Magnolol at Working Concentrations of 0.12×10^{-4} M. (b) Radical Scavenging of MAG/PETMP and MA/PETMP Degradation Products Compared to Mass Loss from the Thermosets.

We turned our attention toward translation of magnolol biological properties to the crosslinked networks. As a proof of principle, the radical scavenging ability of magnolol and a model degradation compound **1** – which would result from complete

hydrolysis of MA/PETMP, MAG/PETMP, and MBAC/PETMP – were assessed using the DPPH$^{\bullet}$ assay. Results in Figure 3-8 show that the model degradation compound contained similar radical scavenging ability to the unadulterated natural product. Additionally, as the thermosets degrade, the solubilized degradation fractions should contain analogous degradation products with phenol moieties that may scavengeradicals. Samples from the basic degradation of thermosets were prepared in the same manner as magnolol and model degradation compound **1** after lyophilization. DPPH$^{\bullet}$ reduction exhibited a linear relationship to percent mass loss from both MAG/PETMP and MA/PETMP thermosets while control samples from thermosets in which no degradation occurred showed no radical scavenging ability. In light of the controllable degradation of these samples, the release of radical scavenging degradation products could be used for the steady delivery of antioxidant supplementary to, or in replacement of, any additional therapeutic. It should be noted that for samples in which hydrolytic degradation would not lead to a phenol, such as the thermosets from **4**, there should be no significant antioxidant activity when comparing to MAG/PETMP or MA/PETMP for the same mass loss from the respective thermosets. DPPH$^{\bullet}$ reduction from MBAE/PETMP samples does not rise above background levels, however as previously mentioned, both MBAE/PETMP and MBAC/PETMP degraded at a sufficiently slower rates under basic conditions than either MA/PETMP or MAG/PETMP and thus samples from each thermoset could not be compared on an equivalent mass loss basis.

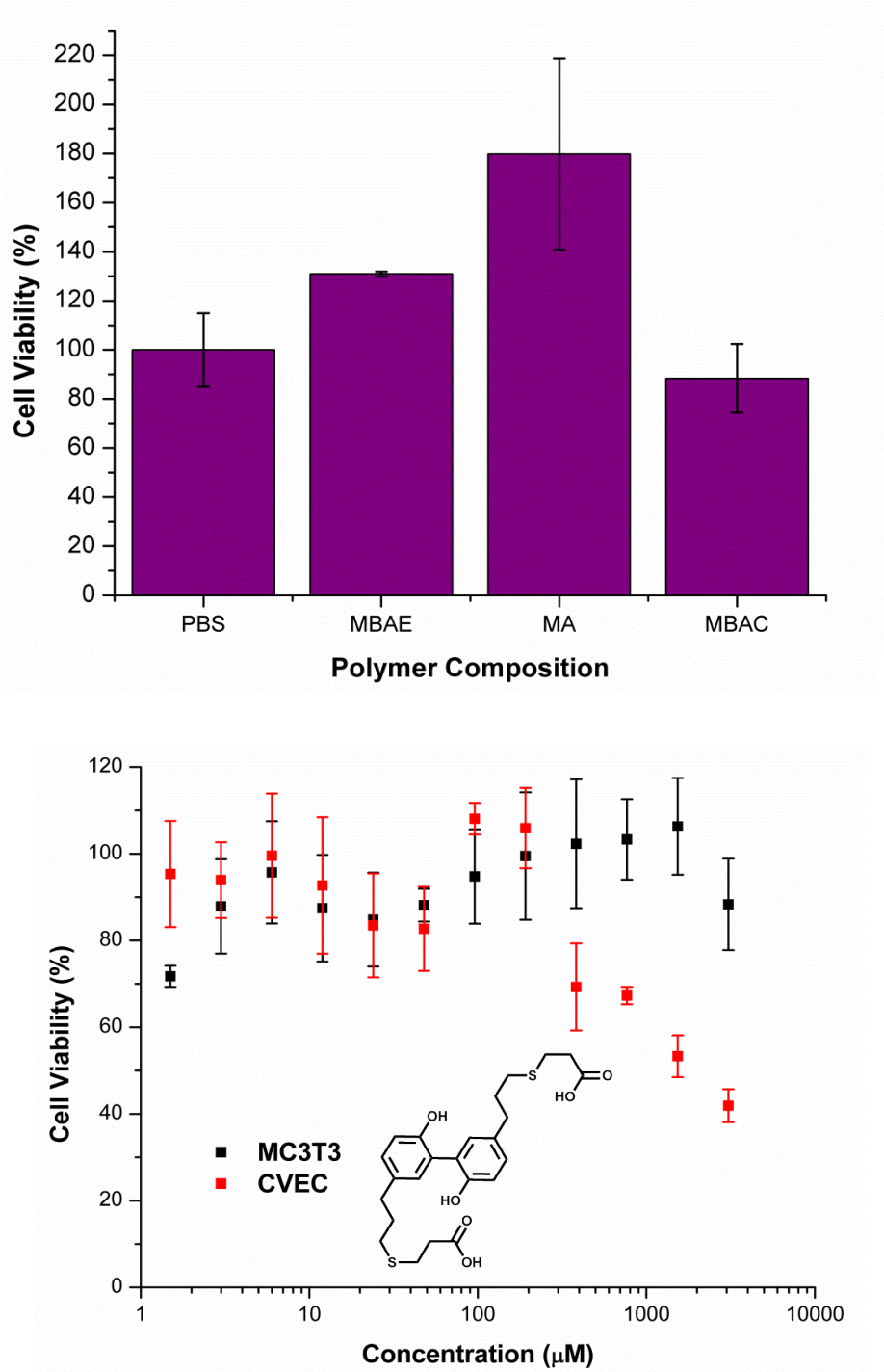

Figure 3-9. (Top) Cell Viability of Polymer Samples from Each Monomer (MBAE, MA, MBAC) and Control (PBS). Polymer Samples Were *ca*. 35 mg and MTS Assay Was Performed in Triplicate. (Bottom) MTS Assay of Model Degradation Compound Used in Antioxidant Assays.

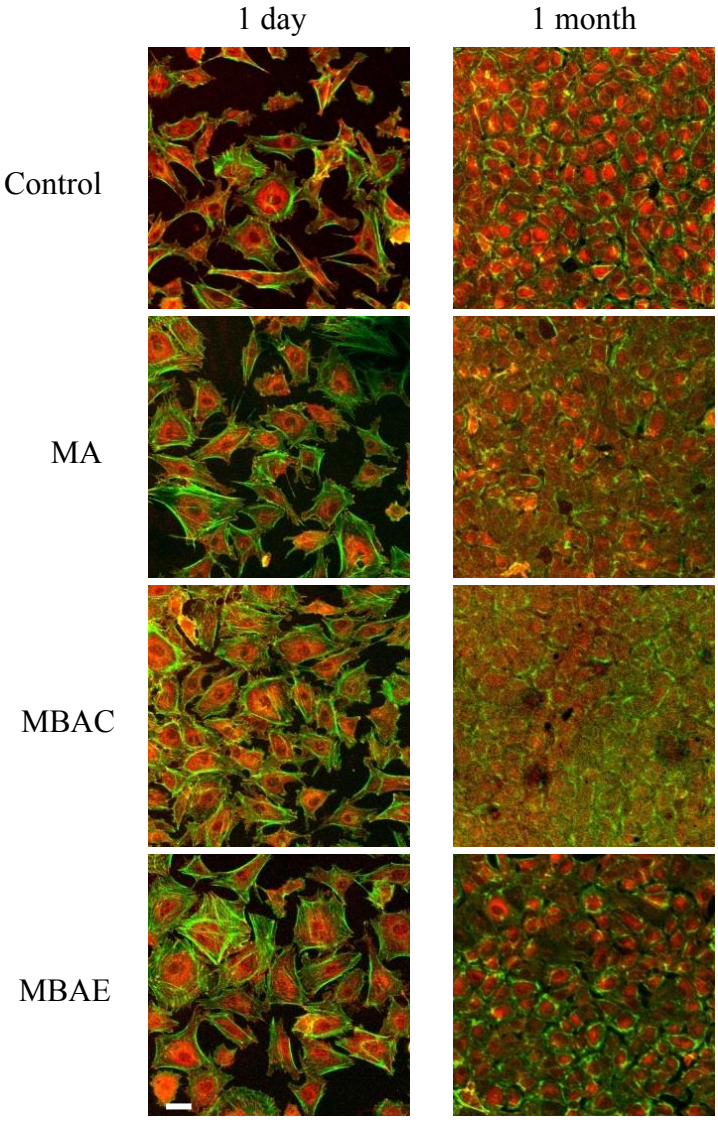

Figure 3-10. Laser Scanning Confocal Microscopy of Bovine Coronary Venular Endothelial Cells (CVECs) on Magnolol-Based Thermosets After 1 Day (Left) and 1 Month (Right). Cells Were Cultured on the Polymer or Gelatin (Control) Coated Glass Surface and Fixed with 4% Paraformaldehyde. Cytoskeleton and Focal Adhesions Were Visualized by Co-Staining with Phalloidin-Alexa488 (green) and Vinculin Antibody with Alexa647-Conjugated Secondary Antibody (Red). Scale Bar 30 μm.

To demonstrate valuable antioxidant activity *in vitro*, cytotoxicity assays were first performed on the polymer films and model degradation product, **1**. All thermosets showed high cell viability. **1** also allowed for good viability at mM concentrations (Figure 3-9) in several cell lines, namely MC3T3 fibroblasts and coronary venular endothelial cells (CVECs) that we have previously used in investigating poly(honokiol carbonate) as a culture surface in biomedical applications.[138] In order to determine adaptability of cells over longer periods of time to the thermosets, such as during placement of a biomaterial *in vivo*, CVECs were plated on thin films of the polymers and media was replaced every 2–3 days to allow for culturing up to one month. Cells were fixed and actin fibers and focal adhesions were visualized with phalloidin and appropriate antibody-fluorophore conjugate staining followed by imaging with confocal microscopy. The CVECs maintained a monolayer, showed good proliferation and adhesion to the thermosets during this time period, and were similar to the control film at both short and long time periods (Figure 3-10).

Antioxidant activity of **1** was then assessed using a reactive oxygen species (ROS) assay performed with *tert*-Butyl hydroperoxide (tBHP) in the presence of CVECs. Increasing concentrations of the model compound resulted in a general reduction of the ROS (Figure 3-11), however, the reduction was not as strong as that of magnolol (positive control) at a similar concentration – 10% reduction *vs.* 20% reduction in ROS. Although not essential for radical scavenging, the allylic moieties of magnolol may also participate in scavenging radical species. Accounting for all radical scavenging moieties in the substrates may help explain this difference between **1** and

magnolol, however the specific roles of the alkene and carboxylic acid moieties in the test compound were not further investigated for these *in vitro* studies.

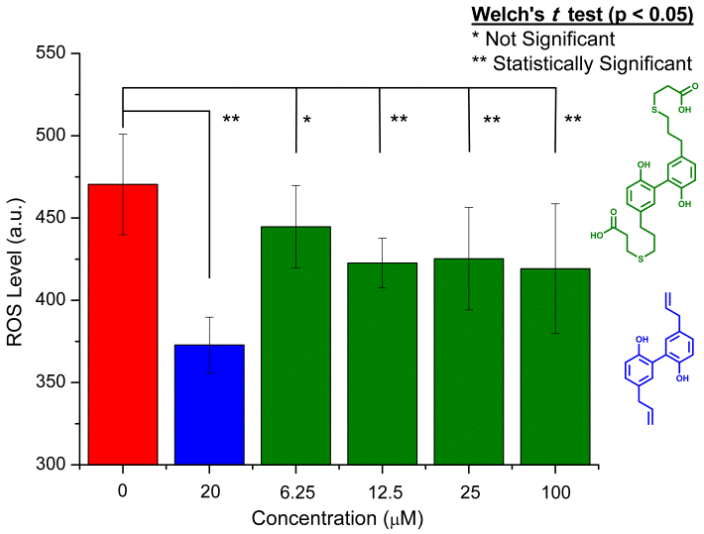

Figure 3-11. ROS Reduction Assay with CVECs in 1% FBS and 5 μM tBHP, Comparing Negative Control (Red), Magnolol (Positive Control, Blue), and Model Degradation Compound, (**1**) (Green). Data Are Presented as Mean ± Standard Deviation. Significance Respect to Negative Control Was Evaluated at $p < 0.05$ with Welch's *t* test.

3.5 Conclusions

In conclusion, we have developed a scalable, straightforward, and generally applicable route to renewable materials from the neolignan magnolol – a previously unexplored natural product in polymer production. The judicious choice of the highly-

functional starting material allowed for both direct thermoset synthesis and the development of a small library of monomers for solvent-free thiol-ene chemistry. The thermosets showed tunable thermomechanical properties and hydrolytic degradation rates that were influenced by the monomer design. Knowledge of the structure property relationships led to leveraging of the tunable thermomechanical properties in order to take advantage of the well-known, inherent radical scavenging and antioxidant properties of the natural product from which the polymer networks were synthesized. While no thermosets showed degradation under acidic and physiological pH, at basic pH, hydrolytic degradation occurred with drastically different rates on account of the thermomechanical properties and relative degree of crosslinking between the thermosets. Degradation products isolated from the thermosets synthesized from magnolol acetonide and magnolol displayed radical scavenging by the $DPPH^{\bullet}$ assay. These results were further corroborated by *in vitro* antioxidant assays with endothelial cells and a model degradation compound. This work lays a foundation for neolignan-based polymers wherein inherent biological properties of the natural product may be leveraged in degradable biomaterials and where straightforward, scalable chemical transformations are used to control the structure-property relationships for novel, bio-based polymers.

CHAPTER IV

OLEFIN MATERIALS *VIA* METATHESIS POLYMERIZATION OF MAGNOLOL DERIVATIVES

4.1. Overview

The natural product, magnolol – readily isolated from numerous *Magnolia* plants – was used in the synthesis of a small library of monomers for acyclic dience metathesis polymerization (ADMET). The phenolic moieties of magnolol provided synthetic handles with which to create a series of monomers with isopropylidene, ethylene, and propylene carbon spacers each prepared in one synthetic step. The olefin-containing polymers were produced in highest yields and thermomechanical properties when Grubbs 2nd generation (G2) catalyst was used at 1 mol%:monomer in dichloromethane or toluene. Thermal degradation temperatures were consistently ≥ 400 °C, yet the post polymerization modifications explored here resulted in drastic changes to the glass transitions and solubility of the materials. With the short synthetic sequence from natural product to modified polymer, magnolol is an interesting renewable resource that avoids both the need to install an α,ω-diene and lengthy synthetic procedure common to many new, renewably-sourced, functional materials produced *via* ADMET.

4.2 Introduction

Metathesis chemistry, in particular, ring-opening metathesis polymerization (ROMP) and acyclic diene metathesis (ADMET) polymerization have proven exceptional tools in the development of new polymers and polymer architectures from olefin-containing small molecules.[153-154] The controlled, living nature of ROMP affords monodisperse species that are diverse in their chemical and structural properties by either varying the functionality of a strained cyclic olefin monomer, polymerization scheme, or through post-polymerization modifications.[155] ADMET polymerization, an equilibrium polymerization process, has been important for the precise introduction of functional groups along a polymer backbone[156] and is superior to ROMP in monomer breadth given that any molecule containing two terminal olefins may polymerize *via* ADMET.[157] A natural interest in metathesis polymerization of renewable resources has emerged given the structural and chemical diversity which may be translated to the final polymer and yield emergent properties or new polymers for which there is no petrochemically-based equivalent.[5, 126] Renewable resources including oils, terpenes, sugars, and lignin have been explored in recent years as raw materials in an attempt to address both the fundamental[41,158] synthetic challenges and the practical design of new renewable monomers and polymers *via* ADMET[159] or ROMP.[160,161-162] However some drawbacks still exist including extensive synthetic procedures and/or the required installation of one or more alkene moieties to produce a viable monomer. For example, oils and fatty acid derivatives are common renewable resources that contain inherent

alkenes with which to perform metathesis polymerizations. The simple (often linear) hydrocarbon backbone of these oils, which may be appended to another core functionality, leads to polymers with sub-optimal thermomechanical properties and little chemical functionality or structural diversity.[30, 163-164] These monomers or polymers containing oils that do display varied structural or chemical diversity typically require multiple synthetic steps or rely on another incorporated component for varied polymer properties.[96, 165-167] To move forward in the use of renewable monomers in ADMET or ROMP, reducing the number of synthetic steps required to produce monomer, as well as taking advantage of those renewable resources which inherently contain the necessary chemical functionality for polymerization, is highly desired.

One class of natural products that may be amenable to metathesis chemistry and other polymerization techniques, but has not been well studied, is neolignans. Neolignans are secondary plant metabolites generated through the oxidative dimerization of phenylpropanoid units[57] and show potential in numerous biological applications.[76, 168-169] In particular, our group has recent interest in the polyphenolic neolignans honokiol[138] and magnolol. Honokiol and magnolol offer the opportunity to rapidly synthesize numerous monomers and polymers on account of the inherent alkene and phenol moieties. These inherent alkene moieties make the use of honokiol or magnolol for metathesis polymerization superior to other renewable resources that require installation of this necessary functional group.[170-175]

4.3 Experimental Section

4.3.1 Magnolol acetonide, MA

The synthesis was adapted from a previously reported procedure.[62] To a solution of magnolol (16.2128 g, 0.05965 mol) in 2,2-dimethoxypropane (70 mL) was added catalytic *p*-toluenesulfonic acid monohydrate (0.10 g). The reaction proceeded at room temperature overnight and was then concentrated, diluted with ether, and washed subsequently with aqueous sodium bicarbonate followed by water. The ether layer was then dried, filtered, and concentrated before purifying the orange-yellow oil by column chromatography (0→10% EtOAc in hexanes) to yield a clear oil (14.8780 g, 81% yield). ^{1}H NMR ($CDCl_3$, 500 MHz) δ 7.32 (d, *J* = 2.2 Hz, 2H), 7.16 (dd, *J* = 8.1, 2.2 Hz, 2H), 7.04 (d, *J* = 8.1 Hz, 2H), 6.03 (ddt, *J* = 16.8, 10.0, 6.7 Hz, 2H), 5.17 – 5.09 (m, 4H), 3.46 (d, *J* = 6.7 Hz, 2H), 1.65 (s, 6H) ppm; ^{13}C NMR (125 MHz) δ 150.16, 137.56, 136.86, 133.21, 128.80, 128.46, 123.26, 116.08, 115.40, 39.92, 25.25 ppm; ESI-MS $[M + Li]^+$ calculated: 313.1780, found: 313.1782.

4.3.2 Magnolol-O,O'-ethylether, MEE

To a 1 L flask containing magnolol (14.6742 g, 0.053995 mol) in acetonitrile (500 mL) with potassium carbonate (37.4 g, 0.270 mol) was added 1,2-dibromoethane (4.65 mL, 0.0539 mol). The solution was refluxed overnight before concentrating and taking up in dichloromethane. The salt was then filtered and the organic was washed

with water and brine before drying, filtering, and concentrating. The viscous oil obtained was then purified by column chromatography (10% EtOAc in hexanes) and extensively dried to yield a white powder (4.9642 g, 31% yield). ^{1}H NMR (500 MHz, $CDCl_3$) δ 7.18 (dd, *J* = 8.1, 2.2 Hz, 2H), 7.15 (d, *J* = 2.2 Hz, 2H), 7.08 (d, *J* = 8.1 Hz, 2H), 5.99 (ddt, *J* = 17.0, 10.1, 6.8 Hz, 2H), 5.10 (m, 4H), 4.41 (d, *J* = 8.9 Hz, 2H), 4.05 (d, *J* = 8.9 Hz, 2H), 3.41 (d, *J* = 6.8 Hz, 4H). ^{13}C NMR (125 MHz) δ 156.66, 137.54, 136.28, 132.00, 130.55, 129.73, 122.43, 116.05, 73.46, 39.78; ESI-MS $[M + Li]^+$ calculated: 299.1623, found: 299.1625

4.3.3 Magnolol-O,O'-propylether, MPE

To a round bottom flask equipped with a condenser was charged magnolol (13.819 g, 0.050849 mol) and acetonitrile (860 mL) followed by addition of potassium carbonate (60.199 g, 0.43556 mol) and 1,3-dibromopropane (5.3 mL, 0.052 mol). The solution was set to reflux overnight before concentrating the organic, taking up in dichloromethane and washing (x3) with water. The organic was dried, filtered, and concentrated and product was purified by column chromatography (5% EtOAc in hexanes) and extensively dried to yield a white powder (5.1280 g, 33% yield). ^{1}H NMR (500 MHz, $CDCl_3$) δ 7.13 (dd, *J* = 8.2, 2.3 Hz, 1H), 7.09 (d, *J* = 2.3 Hz), 7.03 (d, *J* = 8.2 Hz), 6.00 (ddt, *J* = 16.9, 10.0, 6.8 Hz), 5.15 – 5.05 (m), 4.36 – 4.30 (m), 3.42 – 3.36 (m), 1.99 (p, *J* = 5.4, 5.0 Hz); ^{13}C NMR (125 MHz) δ 155.62, 137.77, 134.73, 131.95, 130.19,

128.70, 117.82, 115.88, 71.35, 39.80, 30.24; ESI-MS $[M + Li]^+$ calculated: 313.1780, found: 313.1768

4.3.4 ADMET Polymerization Representative Procedure – G1

A solution of magnolol-O,O'-propylether (0.4431 g, 1.446 mmol) in DCM was degassed three times by freeze-pump-thaw cycles in a Schlenk flask. Grubbs 1st generation catalyst (0.0114 g, 0.0134 mmol, 1 mol% to monomer) in DCM (degassed) was then transferred to the monomer solution at 35 °C to achieve a total initial monomer concentration of 1M. The reaction was allowed to proceed overnight under dynamic vacuum before quenching with ethyl vinyl ether. The polymer was then precipitated into cold methanol three times and allowed to dry.

4.3.4.1 Poly(magnolol acetonide)

Yield: 16% ^{1}H NMR ($CDCl_3$) δ 7.47, 7.43, 7.37, 7.29, 7.18, 7.04, 6.47, 6.23, 5.80, 3.60, 3.45, 2.86, 2.59, 1.89, 1.64 ppm; ^{13}C NMR (125 MHz) δ 150.77, 135.19, 133.34, 130.47, 129.38, 128.77, 128.64, 128.27, 126.28, 126.13, 125.99, 125.80, 125.77, 125.66, 125.60, 123.39, 123.37, 123.20, 115.42, 76.91, 35.62, 35.19, 33.19, 25.26, 18.64; FTIR 3018.60, 2987.74, 2933.73, 2852.72, 1680.00, 1602.85, 1490.97, 1421.54, 1381.03, 1371.39, 1255.66, 1201.65, 1134.14, 1114.86, 1039.63, 964.41, 893.04, 840.96, 777.31, 717.52 cm^{-1}

4.3.4.2 Poly(magnolol ethylether), PMEE

Yield: 55% ^{1}H NMR ($CDCl_3$, 500 MHz) δ 7.18, 7.16, 7.07, 5.99, 5.75, 5.71, 5.13, 5.09, 5.07, 4.39, 4.03, 3.53, 3.39, 1.26 ppm; ^{13}C NMR (125 Hz) δ 156.66, 156.59, 137.53, 136.92, 136.26, 132.09, 132.01, 131.97, 130.61, 130.55, 130.49, 130.35, 129.70, 129.65, 129.62, 129.50, 129.47, 129.29, 122.50, 122.41, 116.05, 73.41 ppm; FTIR 3022.45, 2951.09, 2918.30, 2864.29, 1639.49, 1492.90, 1429.25, 1417.68, 1377.17, 1284.59, 1242.16, 1215.15, 1203.58, 1157.29, 1111.00, 1053.13, 1020.34, 975.98, 948.98, 912.33, 898.83, 877.61, 831.32, 794.67, 773.46, 719.45 cm^{-1}

4.3.4.2 Poly(magnolol propylether), PMPE

Yield: 75% ^{1}H NMR ($CDCl_3$, 500 MHz) δ 7.15, 7.12, 7.04, 6.38, 6.17, 6.02, 5.74, 5.09, 4.33, 3.53, 3.39, 1.99, 1.87 ppm; ^{13}C NMR (125 MHz) δ 155.51, 137.73, 135.42, 134.67, 131.85, 130.61, 130.15, 130.05, 129.29, 128.61, 128.56, 128.46, 117.78, 115.86, 71.30, 39.78, 38.50, 32.95, 30.21 ppm; FTIR 3018.60, 2931.80, 2883.58, 2113.98, 1637.56, 1604.77, 1492.90, 1456.26, 1421.54, 1384.89, 1267.23, 1211.30, 1118.71, 1056.99, 1033.85, 968.27, 937.40, 914.26, 889.18, 819.75, 763.81, 734.88 cm^{-1}

4.3.5 ADMET Polymerization Representative Procedure – G2

The polymerization was performed similarly to the method previously described, but the catalyst used was Grubbs 2nd generation: A solution of magnolol-O,O'-ethylether (0.4339 g, 1.484 mmol) in toluene was degassed three times by freeze-pump-thaw cycles in a Schlenk flask. Grubbs 2nd generation catalyst (0.0130 g, 15.3 μmol, 1 mol% to monomer) in toluene was then transferred to the monomer solution at 90 °C to achieve a total initial monomer concentration of 1M. The reaction was allowed to proceed overnight under dynamic vacuum before quenching with ethyl vinyl ether. The polymer was then precipitated into cold methanol three times and allowed to dry.

4.3.5.1 Poly(magnolol acetonide)

Yield: 68% ^{1}H NMR (500 MHz, $CDCl_3$) δ 7.73, 7.67, 7.50, 7.33, 7.17, 7.04, 6.53, 6.41, 6.23, 3.61, 1.88, 1.64 ppm; ^{13}C NMR (125 MHz) δ 151.44, 151.03, 150.68, 150.23, 150.05, 137.58, 137.02, 136.24, 135.22, 134.63, 133.63-132.87, 130.73-130.38, 130.11, 129.32-128.88, 128.76, 128.55, 128.38, 128.18, 127.92, 126.96-125.97, 125.74, 125.58, 123.67, 123.45, 123.37, 123.24, 115.66, 115.48, 40.12, 39.09, 38.70, 38.62 ppm; FTIR 3022.45, 2989.66, 2935.66, 1680.00, 1604.77, 1492.90, 1422.54, 1381.03, 1371.39, 1255.66, 1201.65, 1134.14, 1114.86, 1039.63, 972.12, 964.41, 893.04, 839.03, 777.31, 717.52 cm^{-1}

4.3.5.2 Poly(magnolol ethylether)

Yield: 93% ^{1}H NMR (500 MHz, $CDCl_3$) δ 7.49, 7.33, 7.21, 7.17, 7.07, 6.73, 6.48, 6.33, 6.19, 5.72, 5.58, 5.22, 5.08, 4.40, 4.03, 3.55, 3.39, 1.86, 1.67, 1.26 ppm; ^{13}C NMR (125 MHz) δ 157.46, 156.74, 156.55, 136.96, 136.39, 133.96, 131.94, 130.59, 129.60, 128.90, 128.38, 127.18, 126.55, 122.59, 122.50, 122.39, 116.04, 73.34, 39.74, 38.90, 38.57, 38.48, 18.62, 18.05 ppm; FTIR 3022.44, 2973.59, 2922.16, 2866.22, 1602.85, 1571.99, 1492.90, 1440.83, 1415.75, 1379.10, 1284.59, 1240.23, 1217.08, 1203.58, 1163.08, 1112.93, 1055.06, 1020.34, 966.34, 894.97, 829.39, 769.60, 719.45 cm^{-1}

4.3.5.3 Poly(magnolol propylether)

Yield: 78% ^{1}HNMR (500 MHz, DMSO-d_6) δ 7.58-6.90, 6.51-6.10, 5.72-5.43, 4.44-3.99, 3.54-3.37, 3.33-3.15, 1.93-1.70, 1.68-1.55 ppm; ^{13}C NMR (125 MHz) δ 156.24, 155.37, 134.62, 131.74, 131.48, 130.22, 129.41, 128.19, 117.84, 70.84, 37.47, 29.48 ppm; FTIR 3020.53, 2931.80, 2883.58, 1602.85, 1492.90, 1456.26, 1421.54, 1382.96, 1267.23, 1213.23, 1118.71, 1056.99, 1033.85, 964.41, 891.11, 819.75, 763.81, 717.52 cm^{-1}

4.3.6 Hydrogenation of ADMET Polymers

A solution of polymer (0.1061 g, 0.380 mmol alkene), *p*-toluenesulfonyl hydrazide (0.450 g, 2.34 mmol, 6.2 eq:alkene), and trace BHT in 3.5 mL of xylenes was degassed by freeze-pump-thaw cycles twice. The solution was then heated at 120 °C to produce a clear solution that was stirred until no more gas evolution occurred. The flask was then allowed to cool to room temperature and the solution was partially concentrated before precipitating the polymer into cold methanol twice.

4.3.6.1 Hydrogenated poly(magnolol acetonide)

^{1}HNMR (500 MHz, DMSO-d_6) δ 7.43-7.28, 7.28-7.07, 7.05-6.85, 3.00-2.76, 2.73-2.44, 2.02-1.78, 1.66-1.39, 1.33-1.16, 0.95-0.77 ppm; ^{13}C NMR (125 MHz) δ 149.24, 138.90, 138.67, 138.18, 132.45, 128.72, 128.45, 127.81, 122.77, 114.72, 36.74, 34.38, 32.71, 30.72, 24.69, 13.65.ppm; FTIR 2987.74, 2933.73, 2856.58, 1492.90, 1423.47, 1371.39, 1255.66, 1203.58, 1134.14, 1114.86, 1041.56, 974.05, 931.62, 894.94, 840.96, 810.10, 653.87, 584.43 cm^{-1}

4.3.6.2 Hydrogenated poly(magnolol ethylether)

^{1}HNMR (500 MHz, DMSO-d_6) δ 7.22-7.02, 4.32, 3.86, 2.60-2.50, 1.88, 1.55, 0.86 ppm, ^{13}C NMR (125 MHz) 155.92, 138.03, 137.77, 136.01, 131.32, 130.38, 129.84, 129.19, 122.09, 72.71, 36.59, 34.24, 32.74, 30.72, 24.24, 21.78, 21.11, 13.68 ppm; FTIR 3022.45, 2926.01 2856.58, 1595.13, 1492.90, 1440.83, 1415.75, 1379.10, 1327.03,

1284.59, 1273.02, 1240.23, 1217.08, 1202.58, 1163.08, 1141.86, 1112.93, 1055.06, 1020.34, 896.90, 885.33, 829.39, 769.60, 653.87 cm^{-1}

4.3.6.3 Hydrogenated poly(magnolol propylether)

^{1}HNMR (500 MHz, DMSO-d_6) δ 7.15-6.92, 4.26-4.07, 2.62-2.42, 1.90-1.71, 1.63-1.47, 1.32-1.22, 0.90-0.81.ppm; ^{13}C NMR (125 MHz) δ 155.08, 145.08, 142.12, 136.30, 136.02, 131.36, 130.38, 129.84, 129.30, 128.05, 127.12, 117.57, 70.57, 39.52, 36.63, 34.27, 33.36, 32.87, 30.86, 29.55, 21.11, 20.92, 20.55, 13.75 ppm; FTIR 3018.60, 2916.37, 2848.86, 1600.92, 1492.90, 1454.33, 1421.54, 1330.88, 1263.37, 1211.30, 1163.08, 1118.71, 1055.06, 1035.77, 941.26, 887.26, 815.89, 763.81, 651.91 cm^{-1}

4.3.7 Acetonide Deprotection of Poly(magnolol acetonide)

Poly(magnolol acetonide) (0.5430 g) was added to a flask containing trifluoroacetic acid in dichloromethane (1:1 v:v, 3 mL total) at room temperature. The reaction was stirred for 2 hours and concentrated. The polymer was then precipitated into methanol twice and dried. Yield: 81% ^{1}H NMR (500 MHz, DMSO-d_6) δ 9.29, 9.02, 7.33, 6.96, 6.80, 6.36, 6.18, 5.61, 3.22 ppm; ^{13}C NMR (125 MHz) ; FTIR 3325.42, 3024.51, 2965.68, 2933.85, 2900.10, 2875.02, 2835.48, 1780.37, 1674.28, 1606.77, 1493.93, 1417.74, 1373.38, 1219.06, 1203.63, 1135.16, 1113.94, 970.24, 891.15, 821.71, 723.34 cm^{-1}

4.3.8 General Procedure for Alkylether Deprotection of Poly(magnolol ethers)

To a 25 mL flask containing polymer (0.1146 g, 0.4120 mmol) was added dry dichloromethane (3 mL) at room temperature. The flask was then cooled in an ice bath before addition of boron tribromide (1M in DCM, 3.5 mL, 0.0035 mol) over 15 min. The reaction solution immediately turned blue and was allowed to stir overnight, followed by quenching with methanol. The solution was partially concentrated and polymer was then precipitated into ether. Further purification by precipitation was not possible as the polymer had extremely limited solubility in common organic solvents (DCM, DMF, THF, chloroform, benzene, and acetone).

4.4 Results and Discussion

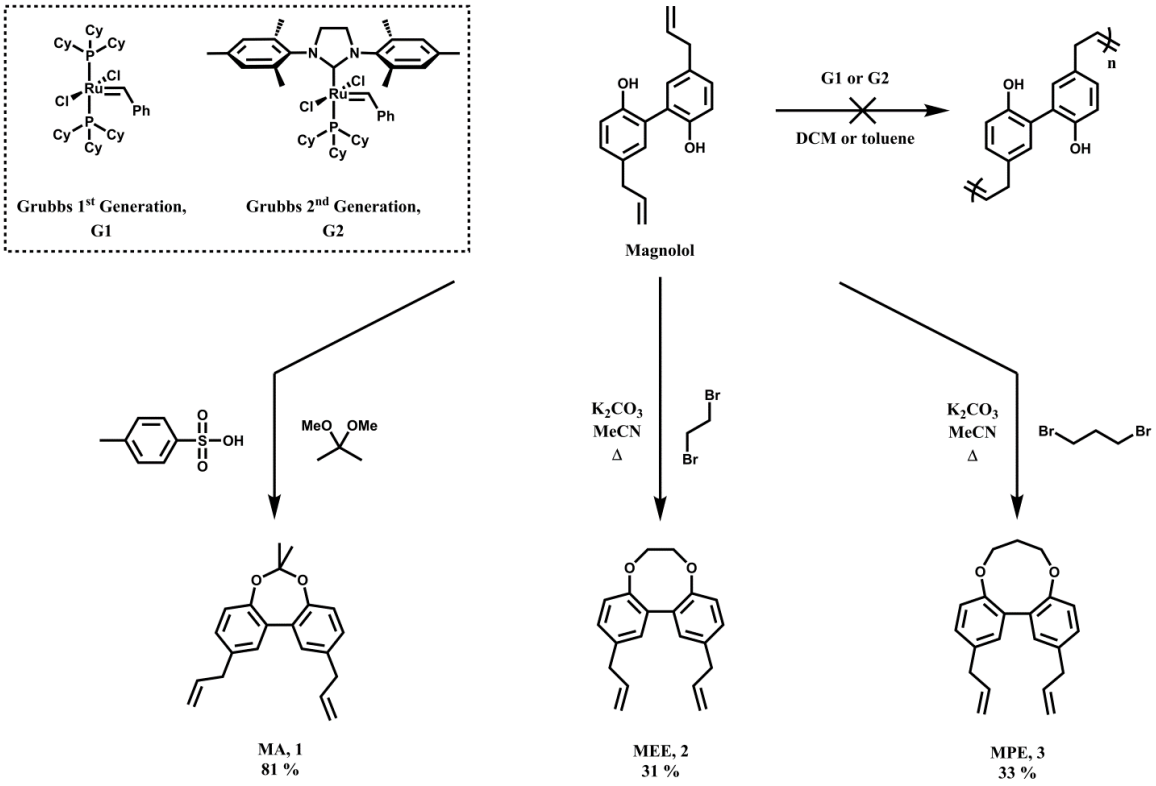

Figure 4-1. Synthetic Approach Toward Magnolol Monomers for ADMET Polymerization

Analogous to our previous studies in directly polymerizing magnolol *via* thiol-ene chemistry with a suitable multifunctional thiol compound, we were initially interested in whether the renewable resource could also polymerize *via* ADMET without any prior functionalization or monomer synthesis by exposing magnolol to Grubbs 1st (G1) and 2nd generation (G2) catalysts in dichloromethane or toluene. Unfortunately, no

polymer was isolated – insoluble black precipitate immediately formed upon catalyst addition. We expected that the biphenol moiety was playing a role in catalyst decomposition and subsequently synthesized a small library of monomers from magnolol each produced *via* a single step phenol functionalization reaction. The phenolic ethers were synthesized also to probe the effect of monomer rigidity on final polymer properties with a series of carbon spacer units (1-3) between the phenols (Figure 4-1). Specifically, the three monomers – magnolol acetonide (MA), magnolol ethylether (MEE), and magnolol propylether (MPE) – were designed to yield polymers with initial high thermomechanical properties by constricting rotation of the phenyl rings, yet would also allow for deprotection following polymerization. The synthesis of magnolol acetonide followed previous work, while magnolol ethylether and magnolol propylether were both synthesized by Williamson ether reactions involving weak base and alkyl dihalides at reflux. Larger size alkyl rings could not be synthesized, *i.e.* those ≥ 10-membered rings, and typically produced mono-functionalized product or dimer of magnolol. Additionally, attempts were made toward the synthesis of monomers for ROMP by first performing ring-closing metathesis on MA, MEE, and MPE under high dilution. A ring-closed monomer was produced only with MEE as the starting material in the presence of 5% Stewart-Grubbs catalyst at 90 °C in toluene (0.05 M) but contained a mixture of both *E*- & *Z*-olefin, along with the cross-metathesis adduct of MEE and isopropoxyphenylmethylene catalyst ligand. DFT calculations at the B3LYP/6-31G level further suggested that the E-isomer is the thermodynamically favored product by 17.2 kcal/mol in the case of MEE (Figure 4-2) and that the ring-

closed products from MA or MPE were sufficiently higher strain energy and endergonic products. However, there are continued efforts to investigate controlling the E/Z ratio with Z-selective catalysts to afford the desired Z-olefin monomer for ROMP.

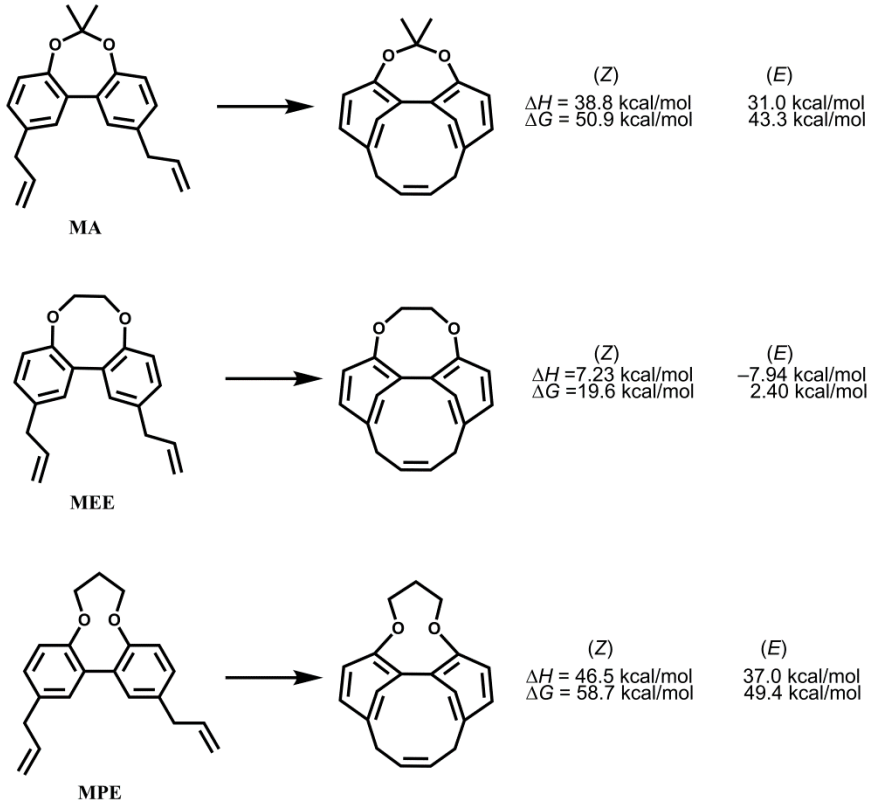

Figure 4-2. DFT Calculations (B3LYP/6-31G) Comparing Desired *Z*-Isomer and *E*-Isomer in the Attempted Syntheses of Ring-Closed Products Using Grubbs Catalysts for Use in ROMP.

Table 4-1. Thermal Analyses of Polymers Synthesized with G1 and G2 in DCM.

Monomer	**Grubbs 1st Gen.**[b]		**Grubbs 2nd Gen.**[b]	
	T_d (°C)	T_g (°C)	T_d (°C)	T_g (°C)
Magnolol[a]	–	–	–	–
MA	400	99	427	168
MEE	423	107	422	112
MPE	418	120	405	178

[a]Magnolol immediately formed black precipitate upon catalyst addition. [b]1 mol % catalyst at 1M $[monomer]_i$.

The monomers were next screened under various conditions in ADMET polymerization. G2 catalyst was more effective than G1 at producing high molecular weight polymers in DCM or toluene under dynamic vacuum in good yields. The resulting olefin-based polymers were thermally robust with onsets of thermal degradation ≥ 400 °C (Table 1) and T_gs ≥ 100 °C – up to *ca*. 180 °C in the case of poly(magnolol propylether), PMPE produced with 1 mol% G2 in DCM at 35 °C. Reaction times could be significantly short (1h) or left overnight with no noticeable change in molecular weight of the polymers when G2 was used. By ^{1}H NMR, it was noted that alkene isomerization[176] had occurred significantly with G2 catalyst – a well-known reaction for allylbenzene moieties in the presence of strong base and particularly with ruthenium catalysts such as those used in ADMET reactions.[177-178] The integration of α-protons in PMA was *ca*. 24% lower than what would be expected with no isomerization with G2 (Figure 4-3). Isomerization, as determined *via* NMR occurred irrespective of catalyst, solvent, and temperature conditions, but was more pronounced with G2 catalyst compared to G1. This isomerization may be a contributing factor to the high glass transition temperatures on account of increased rigidity along the polymer

backbone with increasing conjugation and reduced rotational freedom provided by one less methylene unit compared to the non-isomerized product. These high thermal properties along with the chemical functionality in the resulting polymers, served as starting points to further fine-tune the material properties through post-polymerization modification (PPM) of the protected phenolic moieties or olefin-containing backbone.

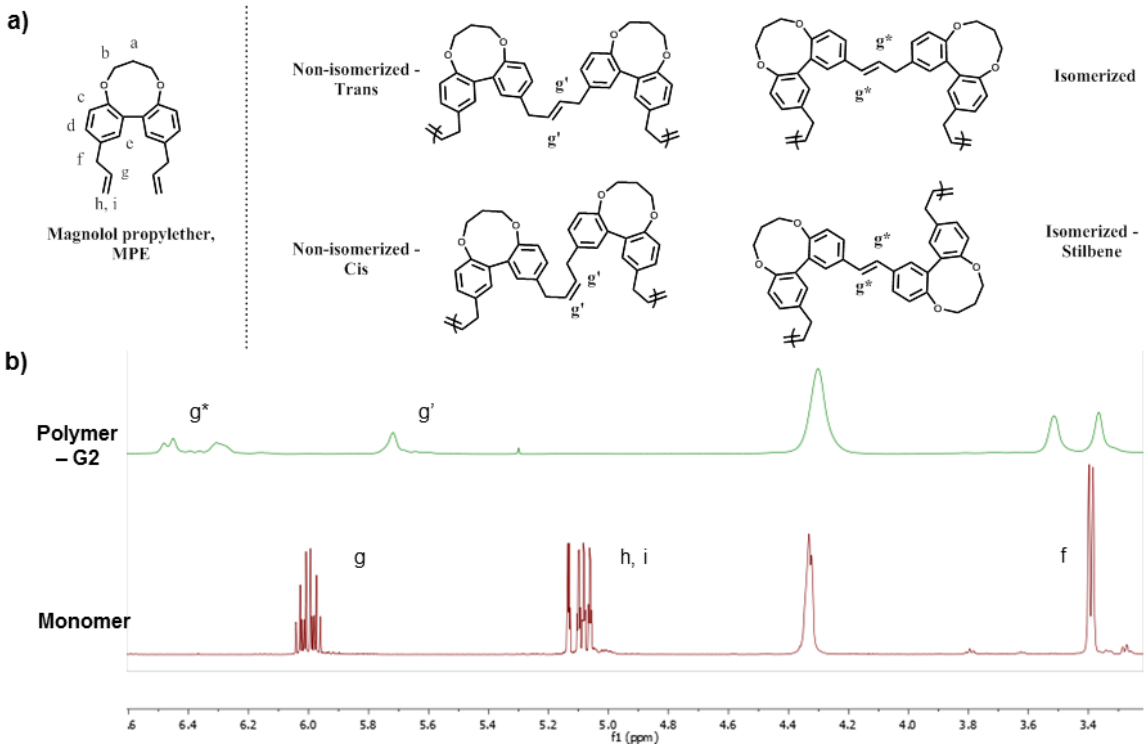

Figure 4-3. Isomerization of Allylbenzene Moiety During ADMET Polymerization with G2 catalyst. a) Monomer MPE and Possible Diads Resulting from Isomerization. b) ^{1}H NMR ($CDCl_3$, 500 MHz) Indicates No Remaining Terminal Alkenes in Product but Significant Isomerization Occurred as Evidenced by Resonances Labeled g^{*}.

Post-polymerization modification of ADMET-produced polymers can significantly alter their final properties including degradation[179], thermomechanical[180], solubility[181], and others.[182-183] Modifications are performed either on the olefin backbone, typically *via* reduction, or along a designed backbone functionality. In the case of the olefin-based magnolol polymers PMA, PMEE, and PMPE, we expected both phenol deprotection and olefin hydrogenation could provide convenient methods for further tuning thermomechanical properties. We then systematically explored both the removal of phenolic protecting groups with either Brønsted or Lewis acids as well as olefin reduction with a hydrogen source. As alcohols are non-solvents for the olefin polymers, a typical reduction with Pd/C, H_2, and alcohol solvent was not possible. Previous reports[184-186] have used *p*-toluenesulfonyl hydrazide as a hydrogen source for olefin reduction and this method was successful with magnolol polymers. (Figure 4-4) Specifically, when five to six equivalence of reagent:olefin in xylenes was used, NMR showed complete conversion of the isolated polymer. Temperatures near reflux of solvent (120 °C) were required in order to fully dissolve both polymer and reagent. Although the thermal degradation temperatures were unaffected, the T_gs (shown in Table 4-2) were significantly reduced: 63 °C and 57 °C for hydrogenated-PMEE and PMPE, respectively.

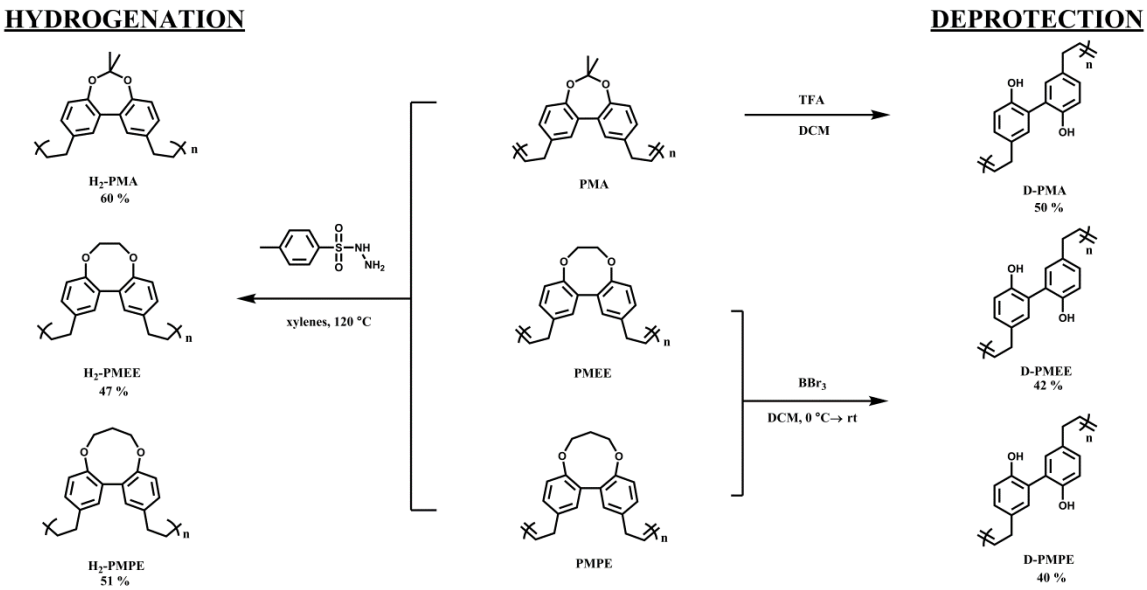

Figure 4-4. Post-Polymerization Modifications Yielding Hydrogenated Backbone or Phenol.

For phenolic deprotections, the most straightforward procedure involved exposing PMA to a 1:1 v:v trifluoroacetic acid/DCM solution at room temperature. Within ten minutes, the solution turned a cloudy deep-blue color and the isolated polymer was purified as a blue powder (Figure 4-5) after precipitation. ^{19}F NMR showed no fluorine resonances while ^{1}H NMR confirmed the presence of phenolic protons and loss of isopropylidene. The hypothesis for the color change involves the isomerization that had occurred during the synthesis of PMA using G2 and the decreased conformational constraints following post-polymerization modification. Specifically, PMA synthesized with G2 exhibits increased conjugation on account of the stilbene and styrenyl-moieties along the polymer backbone. In addition, following deprotection,

there is a thermodynamic driving force for the phenyl rings to rotate and increased conjugation may result through extending π-orbital overlap along the polymer backbone. This result was not unique to PMA: in the cases of PMEE and PMPE, both polymers were deprotected using BBr_3 and solutions changed to the characteristic blue after *ca*. 15 min. Notably, these polymers were significantly less soluble in common organic solvents including DMSO, chloroform, acetone, THF, DCM, chloroform, and benzene even with heating, and, as such, NMR analyses were limited. Thermal analyses, however, again showed distinct lowering of the glass transitions up to 100 °C *e.g.* PMPE displays a T_g *ca*. 155-180 °C that subsequently drops to *ca*. 85 °C upon ring-opening and PMEE displays a T_g *ca*. 112-130 °C that decreases to 83 °C.

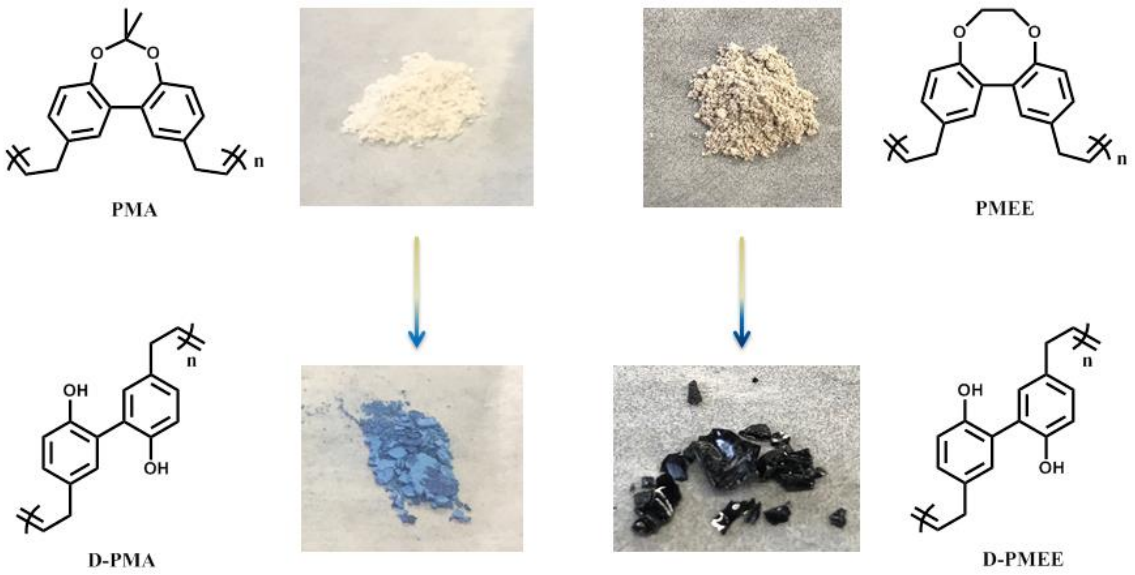

Figure 4-5. Deprotected Polymer Showing Distinct Color Change Potentially Resulting from Increased Conjugation in the Polymer Backbone. Structures are Idealized Repeat Units Resulting from No Isomerization.

Table 4-2. DSC Results from Hydrogenation or Deprotection of Magnolol Olefin Polymers

Parent Polymer	Hydrogenation – T_g (°C)	Phenol Deprotection – T_g (°C)
PMA	64	51
PMEE	63	85
PMPE	57	83

4.5 Conclusions

Herein we have introduced magnolol as a renewable resource amenable to metathesis chemistry through straightforward, one step reactions to monomers for ADMET polymerization. The small library of polymers displayed high thermal degradation temperatures and glass transition temperatures and, furthermore, these properties were fine-tuned through post polymerization modifications. The phenolic deprotections and hydrogenations produced new polymers that retained high thermal degradation temperatures while lowering the T_g by *ca*. 100 °C in some cases. Side reactions during the polymerization, namely allylbenzene isomerization, resulted in highly conjugated polymers that, upon phenolic deprotection reactions, displayed drastic color changes. Future work will look to further control isomerization and subsequent photophysical properties of the polymers, as well as further fine tuning thermomechanical properties through sequential post polymerization modifications. We

are also interested in tangential work toward the synthesis of monomers from magnolol for ring opening metathesis polymerization.

CHAPTER V

CONCLUSIONS AND FUTURE WORK

5.1 Conclusions

This dissertation has presented new renewable resources for the production of polymers that were initially studied in their fundamental properties for potential engineering and biomedical applications. Honokiol and magnolol are regioisomers belonging to the neolignan natural product class and have been examined in the academic and industrial communities for several decades in small molecule form for potential therapeutic applications. This work has laid a foundation to expand honokiol and magnolol use to include the production of renewable polymers with emergent properties. Both honokiol and magnolol contain phenolic and allylic moieties that are amenable to broad numbers and types of organic synthetic transformations and thus spurred the synthesis of chemically and structurally diverse monomers and polymers including polycarbonates, thermosets, and olefin-based materials. Polymer properties were controlled through the design of the monomer by the incorporation of various chemical functionalities or by the optimization of synthetic conditions employed in the polymer synthesis.

Chapter II focused on the direct synthesis of a polycarbonate from honokiol: poly(honokiol carbonate), PHC. Although under the conditions used in this study, polymers from magnolol were not obtained, PHC was synthesized with controllable M_n

through simple manipulation of the starting monomer concentration. PHC of all molecular weights examined were thermally and chemically robust, displaying thermal degradation temperatures above 450 °C and only modest chemical degradation with 1M sodium hydroxide solutions up to *ca.* 4 months. These properties were comparable to the well-known engineering polymer, BPA-PC. PHC thin films served as good substrates for cell growth over the course of a month and, as such, may allow for replacement of BPA-PC in food contact applications or in biomedical use where BPA-PC is restricted.

In Chapter III, thermosets were synthesized using the alkene moieties of magnolol or magnolol derivatives in thiol-ene reactions with a multifunctional thiol comonomer and photoinitiator. The design of the magnolol-based monomer library, including the incorporated chemical functionalities and total number of moieties involved in the polymerization, was crucial to the ultimate material properties. This design led to controllable thermomechanical characteristics as well as tunable degradation rates under basic aqueous conditions. More importantly, those thermosets that were designed to degrade and expose the phenolic moieties of the magnolol component displayed antioxidant/radical scavenging capabilities akin to what has been known for the unmodified natural product. Polymer films allowed for extended cell culture and model compounds displayed no cytotoxic effects. These results demonstrated that properties inherent to small natural products can be translated to polymeric materials and leveraged for biomedical applications. It was also demonstrated

that future biomedical applications are feasible given the short, straightforward synthetic sequences and solvent-free polymerization that is controlled *via* an external light source.

Chapter IV explored new olefin-based polymers produced *via* acyclic diene metathesis polymerization of functionalized magnolol monomers. The natural product was not amenable to direct metathesis chemistry with ruthenium catalysts and, as such, magnolol was protected by alkylation to form several tricyclic monomers that contained functionalities allowing post polymerization modification, *i.e.* they were removable after the polymer synthesis. The post polymerization modifications were not limited to deprotections and, additionally, included hydrogenation of the polymer backbone. Well-known allylbenzene isomerization was noted in the polymer backbone and, as a result, the stiff polymer chains displayed high glass transition temperatures, up to 180 °C. Through post polymerization modification the glass transition temperatures were significantly modified, up to 100 °C in some cases. This work expands the scope of natural product-based polymers synthesized *via* metathesis chemistry without requiring lengthy synthetic procedures or the need to install a terminal diene necessary for alkene metathesis.

5.2 Future Work

There is significant future potential for new monomers and polymers synthesized from renewable resources and the small subset of work done here with magnolol and

honokiol has only just begun. Future work should and will include developing a deeper understanding of those polymers already synthesized and exploring new applications in which they may prove well suited. Additionally, the chemical functionality inherent to magnolol and honokiol allows for expanding the polymer types and classes synthesized.

In the case of polycarbonates from honokiol or magnolol, a change in the synthesis of poly(honokiol carbonate) to replace phosgene-based carbonlyation reagents with non-toxic carbonylation chemistries would be in-line with the ideas of green and renewable chemistry. Currently, there are efforts towards CO fixation that yield diethyl carbonate or diphenol carbonate without the need for phosgene. Honokiol polymerization with diphenol carbonate has potential to better control molecular weights of the resulting polycarbonate, as well as increase molecular weights (compared to what has been achieved currently) by shifting the chemical equilibrium with the removal of byproduct, *i.e.* phenol, during polymerization. This polymerization chemistry would be significantly more energy intensive however as vacuum and temperatures in excess of 180 °C are typically required. An additional benefit of higher molecular weight poly(honokiol carbonate) *via* this route would be improved thermomemchanical properties. Aside from honokiol, magnolol-based polycarbonates *via* a ring opening polymerization scheme have been studied. The seven-membered cyclic carbonate monomer is unique in that there are very few examples in the literature of polymers synthesized from cyclic carbonates of this size. A 2,2'-biphenol moiety is required and currently there are no known examples of an organocatalytic ring opening polymerization of a seven-membered aromatic cyclic carbonate. Currently, it has been

shown that 4-methylbenzyl alcohol will initiate the monomers, magnolol carbonate and tetrahydromagnolol carbonate. Additionally, propagation does occur, however, polymer has not been isolated. Success in this endeavor may bring new insights for organocatalytic polymerization of medium size rings. Furthermore, post polymerization modification of these polycarbonates may be used to 1) adjust thermomechanical properties, 2) intra- or intermolecularly crosslink polymers, and 3) append biomedically-relevant moieties such as a drug or imaging agent.

Current work on the thermoset materials from Chapter III involves 3D printing applications. As these thermosets are synthesized *via* a photo-controlled process and are tunable in their thermomechanical, degradation, and antioxidant properties, biomedical devices such as a stent for cardiovascular applications or degradable orthopedic devices, including a bone screw or plate, are of interest. This collaborative work has initially focused on optimization of a resin composition for 3D printing (which may include multiple magnolol- or honokiol-based monomers), as well as, printing optimization, and material characterization. Eventual aims are to develop a prototype device and begin animal model studies.

The olefin-based materials of Chapter IV are currently the least understood from this dissertation: the photophysical properties resulting after phenol deprotection certainly necessitate thorough examination. In parallel to these investigations, further synthetic work would examine controlling allyl isomerization with the use of additives as well as performing sequential post polymerization modifications to a) further fine tune the thermomechanical properties that have been examined to date and b) to

investigate the role of the free phenol and isomerized backbone on the photophysical properties. Aside from the ADMET polymerization, tangential work would investigate the ring-closing metathesis reaction to selectively form monomers containing *Z*-isomer that may polymerize *via* ROMP.

Finally, in this student's opinion, honokiol and magnolol have a great opportunity that is not possible for all renewable resources in that many different polymer types are accessible from honokiol and magnolol in few synthetic steps. Toward that end, future work should also include the synthesis, characterization, and development of new polymer classes not explored here. For example, phenolic raw materials are a backbone for advanced materials in industries including aerospace, automotive, wind, construction, and electronics. The phenolic raw materials used in these industries are suitable for a myriad of thermoset chemistries based on benzoxazines, cyanate esters, and epoxy, among others. Honokiol and magnolol may similarly make for good renewable resources in the replacement and advancement of advanced materials based on the chemistries just listed.

REFERENCES

1. Philp, J. C.; Bartsev, A.; Ritchie, R. J.; Baucher, M.-A.; Guy, K., Bioplastics Science from a Policy Vantage Point. *New Biotechnology* **2013,** *30*, 635-646.

2. Rochman, C. M.; Browne, M. A.; Halpern, B. S.; Hentschel, B. T.; Hoh, E.; Karapanagioti, H. K.; Rios-Mendoza, L. M.; Takada, H.; Teh, S.; Thompson, R. C., Classify Plastic Waste as Hazardous. *Nature* **2013,** *494*, 169-171.

3. Borrelle, S. B.; Rochman, C. M.; Liboiron, M.; Bond, A. L.; Lusher, A.; Bradshaw, H.; Provencher, J. F., Opinion: Why We Need an International Agreement on Marine Plastic Pollution. *Proc. Natl. Acad. Sci. U.S.A.* **2017,** *114*, 9994-9997.

4. Schneiderman, D. K.; Hillmyer, M. A., 50th Anniversary Perspective: There Is a Great Future in Sustainable Polymers. *Macromolecules* **2017,** *50*, 3733-3749.

5. Zhu, Y.; Romain, C.; Williams, C. K., Sustainable Polymers from Renewable Resources. *Nature* **2016,** *540*, 354-362.

6. Ricapito, N. G.; Ghobril, C.; Zhang, H.; Grinstaff, M. W.; Putnam, D., Synthetic Biomaterials from Metabolically Derived Synthons. *Chem. Rev.* **2016,** *116*, 2664-2704.

7. Straathof, A. J. J., Transformation of Biomass into Commodity Chemicals Using Enzymes or Cells. *Chem. Rev.* **2013,** *114*, 1871-1908.

8. Wu, R.; Al-Azemi, T. F.; Bisht, K. S., Functionalized Polycarbonate Derived from Tartaric Acid: Enzymatic Ring-Opening Polymerization of a Seven-Membered Cyclic Carbonate. *Biomacromolecules* **2008,** *9*, 2921-2928.

9. Reano, A. F.; Pion, F.; Domenek, S.; Ducrot, P.-H.; Allais, F., Chemo-enzymatic Preparation and Characterization of Renewable Oligomers with Bisguaiacol Moieties: Promising Sustainable Antiradical/Antioxidant Additives. *Green Chem.* **2016**.

10. Martín, C.; Kleij, A. W., Terpolymers Derived from Limonene Oxide and Carbon Dioxide: Access to Cross-Linked Polycarbonates with Improved Thermal Properties. *Macromolecules* **2016**.

11. Byrne, C. M.; Allen, S. D.; Lobkovsky, E. B.; Coates, G. W., Alternating Copolymerization of Limonene Oxide and Carbon Dioxide. *J. Am. Chem. Soc.* **2004,** *126*, 11404-11405.

12. Wang, Y.; Fan, J.; Darensbourg, D. J., Construction of Versatile and Functional Nanostructures Derived from CO_2-based Polycarbonates. *Angew. Chem. Int. Ed.* **2015,** *54*, 10206-10210.

13. Tsai, F.-T.; Wang, Y.; Darensbourg, D. J., Environmentally Benign CO_2-Based Copolymers: Degradable Polycarbonates Derived from Dihydroxybutyric Acid and Their Platinum–Polymer Conjugates. *J. Am. Chem. Soc.* **2016,** *138*, 4626-4633.

14. Kamm, B., Production of Platform Chemicals and Synthesis Gas from Biomass. *Angew. Chem. Int. Ed.* **2007,** *46*, 5056-5058.

15. Bhagat, V.; Becker, M. L., Degradable Adhesives for Surgery and Tissue Engineering. *Biomacromolecules* **2017,** *18*, 3009-3039.

16. Badia, J. D.; Gil-Castell, O.; Ribes-Greus, A., Long-term Properties and End-of-life of Polymers from Renewable Resources. *Polymer Degradation and Stability* **2017,** *137*, 35-57.

17. Brannigan, R. P.; Dove, A. P., Synthesis, Properties and Biomedical Applications of Hydrolytically Degradable Materials Based on Aliphatic Polyesters and Polycarbonates. *Biomaterials Science* **2017,** *5*, 9-21.

18. Mahajan, N.; Gupta, P., New Insights into the Microbial Degradation of Polyurethanes. *RSC Adv.* **2015,** *5*, 41839-41854.

19. Steinbach, T.; Wurm, F. R., Poly(phosphoester)s: A New Platform for Degradable Polymers. *Angew. Chem. Int. Ed.* **2015,** *54*, 6098-6108.

20. Yoshida, S.; Hiraga, K.; Takehana, T.; Taniguchi, I.; Yamaji, H.; Maeda, Y.; Toyohara, K.; Miyamoto, K.; Kimura, Y.; Oda, K., A Bacterium that Degrades and Assimilates Poly(ethylene terephthalate). *Science* **2016,** *351*, 1196-1199.

21. Badia, J. D.; Ribes-Greus, A., Mechanical Recycling of Polylactide, Upgrading Trends and Combination of Valorization Techniques. *Eur. Polym. J.* **2016,** *84*, 22-39.

22. Quaranta, E.; Sgherza, D.; Tartaro, G., Depolymerization of Poly(bisphenol A carbonate) Under Mild Conditions by Solvent-free Alcoholysis Catalyzed by 1,8-diazabicyclo[5.4.0]undec-7-ene as a Recyclable Organocatalyst: A Route to Chemical Recycling of Waste Polycarbonate. *Green Chem.* **2017,** *19*, 5422-5434.

23. Hearon, K.; Nash, L. D.; Rodriguez, J. N.; Lonnecker, A. T.; Raymond, J. E.; Wilson, T. S.; Wooley, K. L.; Maitland, D. J., A High-Performance Recycling Solution for Polystyrene Achieved by the Synthesis of Renewable Poly(thioether) Networks Derived from d-Limonene. *Adv. Mater.* **2014,** *26*, 1552-1558.

24. Liu, T.; Hao, C.; Wang, L.; Li, Y.; Liu, W.; Xin, J.; Zhang, J., Eugenol-Derived Biobased Epoxy: Shape Memory, Repairing, and Recyclability. *Macromolecules* **2017**.

25. Klemm, D.; Heublein, B.; Fink, H.-P.; Bohn, A., Cellulose: Fascinating Biopolymer and Sustainable Raw Material. *Angew. Chem. Int. Ed.* **2005,** *44*, 3358-3393.

26. Greve, H.-H., Rubber, 2. Natural. In *Ullmann's Encyclopedia of Industrial Chemistry*, Wiley-VCH Verlag GmbH & Co. KGaA: 2000.

27. Erickson, B.; Nelson, J. E.; Winters, P., Perspective on Opportunities in Industrial Biotechnology in Renewable Chemicals. *Biotechnology Journal* **2012,** *7*, 176-185.

28. Li, C.; Zhao, X.; Wang, A.; Huber, G. W.; Zhang, T., Catalytic Transformation of Lignin for the Production of Chemicals and Fuels. *Chem. Rev.* **2015,** *115*, 11559-11624.

29. Besson, M.; Gallezot, P.; Pinel, C., Conversion of Biomass into Chemicals over Metal Catalysts. *Chem. Rev.* **2013,** *114*, 1827-1870.

30. Montero de Espinosa, L.; Meier, M. A. R., Plant Oils: The Perfect Renewable Resource for Polymer Science?! *Eur. Polym. J.* **2011,** *47*, 837-852.

31. Gandini, A.; Lacerda, T. M.; Carvalho, A. J. F.; Trovatti, E., Progress of Polymers from Renewable Resources: Furans, Vegetable Oils, and Polysaccharides. *Chem. Rev.* **2015,** *116*, 1637-1669.

32. Vilela, C.; Sousa, A. F.; Fonseca, A. C.; Serra, A. C.; Coelho, J. F. J.; Freire, C. S. R.; Silvestre, A. J. D., The Quest for Sustainable Polyesters - Insights into the Future. *Polym. Chem.* **2014,** *5*, 3119-3141.

33. Scott, A., Roquette Embraces Biobased Materials. *Chemical & Engineering News* **2012,** *90*.

34. AkzoNobel and Itaconix finalize first bio-based polymer application agreement. **2017**.

35. Scholten, E.; Dägele, D.; Haefner, S.; Schröder, H., Bacterial Strain and Process for the Fermentative Production of Organic Acids. Google Patents: 2013.

36. Fruchey, O. S.; Keen, B. T.; Albin, B. A.; Clinton, N. A.; Dunuwila, D.; Dombek, B. D., Processes for Producing Succinic Acid from Fermentation Broths Containing Diammonium Succinate. Google Patents: 2012.

37. Verwaal, R.; Wu, L.; Damveld, R. A.; Sagt, C. M. J., Succinic Acid Production in a Eukaryotic Cell. Google Patents: 2009.

38. Ahn, J. H.; Jang, Y.-S.; Lee, S. Y., Production of Succinic Acid by Metabolically Engineered Microorganisms. *Current Opinion in Biotechnology* **2016,** *42*, 54-66.

39. Wilbon, P. A.; Chu, F.; Tang, C., Progress in Renewable Polymers from Natural Terpenes, Terpenoids, and Rosin. *Macromol. Rapid Commun.* **2013,** *34*, 8-37.

40. Kristufek, S. L.; Yang, G.; Link, L. A.; Rohde, B. J.; Robertson, M. L.; Wooley, K. L., Synthesis, Characterization, and Cross-Linking Strategy of a Quercetin-Based Epoxidized Monomer as a Naturally-Derived Replacement for BPA in Epoxy Resins. *ChemSusChem* **2016**, n/a-n/a.

41. Pehere, A. D.; Xu, S.; Thompson, S. K.; Hillmyer, M. A.; Hoye, T. R., Diels–Alder Reactions of Furans with Itaconic Anhydride: Overcoming Unfavorable Thermodynamics. *Org. Lett.* **2016,** *18*, 2584-2587.

42. Winnacker, M.; Tischner, A.; Neumeier, M.; Rieger, B., New Insights into Synthesis and Oligomerization of ε-Lactams Derived from the Terpenoid Ketone (-)-Menthone. *RSC Adv.* **2015,** *5*, 77699-77705.

43. Iwata, T., Biodegradable and Bio-Based Polymers: Future Prospects of Eco-Friendly Plastics. *Angew. Chem. Int. Ed.* **2015,** *54*, 3210-3215.

44. Leslie Gunatilaka, A.; Begley, T. P., Natural Products in Plants: Chemical Diversity. In *Wiley Encyclopedia of Chemical Biology*, John Wiley & Sons, Inc.: 2007.

45. Mikami, K.; Lonnecker, A. T.; Gustafson, T. P.; Zinnel, N. F.; Pai, P. J.; Russell, D. H.; Wooley, K. L., Polycarbonates Derived from Glucose via an Organocatalytic Approach. *Journal of the American Chemical Society* **2013,** *135*, 6826-6829.

46. Lonnecker, A. T.; Lim, Y. H.; Felder, S. E.; Besset, C. J.; Wooley, K. L., Four Different Regioisomeric Polycarbonates Derived from One Natural Product, d-Glucose. *Macromolecules* **2016,** *49*, 7857-7867.

47. Lonnecker, A. T.; Lim, Y. H.; Wooley, K. L., Functional Polycarbonate of a d-Glucal-Derived Bicyclic Carbonate via Organocatalytic Ring-Opening Polymerization. *ACS Macro Lett.* **2017,** *6*, 748-753.

48. Link, L. A.; Lonnecker, A. T.; Hearon, K.; Maher, C. A.; Raymond, J. E.; Wooley, K. L., Photo-cross-linked Poly(thioether-co-carbonate) Networks Derived from the Natural Product Quinic Acid. *ACS Appl Mater Interfaces* **2014,** *6*, 17370-17375.

49. Kristufek, T. S.; Kristufek, S. L.; Link, L. A.; Weems, A. C.; Khan, S.; Lim, S.-M.; Lonnecker, A. T.; Raymond, J. E.; Maitland, D. J.; Wooley, K. L., Rapidly-cured Isosorbide-based Cross-linked Polycarbonate Elastomers. *Polym. Chem.* **2016,** *7*, 2639-2644.

50. Noel, A.; Borguet, Y. P.; Raymond, J. E.; Wooley, K. L., Poly(carbonate-amide)s Derived from Bio-Based Resources: Poly(ferulic acid-co-tyrosine). *Macromolecules* **2014,** *47*, 2974-2983.

51. Noel, A.; Borguet, Y. P.; Raymond, J. E.; Wooley, K. L., Poly(ferulic acid-co-tyrosine): Effect of the Regiochemistry on the Photophysical and Physical Properties en Route to Biomedical Applications. *Macromolecules* **2014,** *47*, 7109-7117.

52. He, X.; Fan, J.; Wooley, K. L., Stimuli-Triggered Sol–Gel Transitions of Polypeptides Derived from α-Amino Acid N-Carboxyanhydride (NCA) Polymerizations. *Chemistry – An Asian Journal* **2016,** *11*, 437-447.

53. Fan, J.; Li, R.; He, X.; Seetho, K.; Zhang, F.; Zou, J.; Wooley, K. L., Construction of a Versatile and Functional Nanoparticle Platform Derived from a Helical Diblock Copolypeptide-based Biomimetic Polymer. *Polym. Chem.* **2014,** *5*, 3977-3981.

54. El-Seedi, H. R.; El-Said, A. M. A.; Khalifa, S. A. M.; Göransson, U.; Bohlin, L.; Borg-Karlson, A.-K.; Verpoorte, R., Biosynthesis, Natural Sources, Dietary Intake, Pharmacokinetic Properties, and Biological Activities of Hydroxycinnamic Acids. *Journal of Agricultural and Food Chemistry* **2012,** *60*, 10877-10895.

55. Miean, K. H.; Mohamed, S., Flavonoid (Myricetin, Quercetin, Kaempferol, Luteolin, and Apigenin) Content of Edible Tropical Plants. *Journal of Agricultural and Food Chemistry* **2001,** *49*, 3106-3112.

56. Jensen, H. D.; Krogfelt, K. A.; Cornett, C.; Hansen, S. H.; Christensen, S. B., Hydrophilic Carboxylic Acids and Iridoid Glycosides in the Juice of American and European Cranberries (Vaccinium macrocarpon and V. oxycoccos), Lingonberries (V. vitis-idaea), and Blueberries (V. myrtillus). *Journal of Agricultural and Food Chemistry* **2002,** *50*, 6871-6874.

57. Pan, J.-Y.; Chen, S.-L.; Yang, M.-H.; Wu, J.; Sinkkonen, J.; Zou, K., An Update on Lignans: Natural Products and Synthesis. *Nat. Prod. Rep.* **2009,** *26*, 1251-1292.

58. Saleem, M.; Kim, H. J.; Ali, M. S.; Lee, Y. S., An Update on Bioactive Plant Lignans. *Nat. Prod. Rep.* **2005,** *22*, 696-716.

59. Teponno, R. B.; Kusari, S.; Spiteller, M., Recent Advances in Research on Lignans and Neolignans. *Nat. Prod. Rep.* **2016,** *33*, 1044-1092.

60. Lee, Y. J.; Lee, Y. M.; Lee, C. K.; Jung, J. K.; Han, S. B.; Hong, J. T., Therapeutic Applications of Compounds in the Magnolia Family. *Pharmacol. Ther.* **2011,** *130*, 157-176.

61. Shen, C.-C.; Ni, C.-L.; Shen, Y.-C.; Huang, Y.-L.; Kuo, C.-H.; Wu, T.-S.; Chen, C.-C., Phenolic Constituents from the Stem Bark of Magnolia officinalis. *Journal of Natural Products* **2009,** *72*, 168-171.

62. Amblard, F.; Delinsky, D.; Arbiser, J. L.; Schinazi, R. F., Facile Purification of Honokiol and Its Antiviral and Cytotoxic Properties. *J. Med. Chem.* **2006,** *49*, 3426-3427.

63. Chen, L.; Zhang, Q.; Yang, G.; Fan, L.; Tang, J.; Garrard, I.; Ignatova, S.; Fisher, D.; Sutherland, I. A., Rapid Purification and Scale-Up of Honokiol and Magnolol Using

High-Capacity High-Speed Counter-Current Chromatography. *J. Chromatogr. A* **2007,** *1142*, 115-122.

64. Peng, A.; Hewitson, P.; Ye, H.; Zu, L.; Garrard, I.; Sutherland, I.; Chen, L.; Ignatova, S., Sample Injection Strategy to Increase Throughput in Counter-current Chromatography: Case Study of Honokiol Purification. *J. Chromatogr. A* **2016,** *1476*, 19-24.

65. Peng, A.; Ye, H.; Shi, J.; He, S.; Zhong, S.; Li, S.; Chen, L., Separation of Honokiol and Magnolol by Intermittent Counter-current Extraction. *J. Chromatogr. A* **2010,** *1217*, 5935-5939.

66. Srinivas, J.; Singh, P. P.; Varma, Y. K.; Hyder, I.; Kumar, H. M. S., Concise Total Synthesis of Honokiol via Kumada Cross Coupling. *Tetrahedron Lett.* **2014,** *55*, 4295-4297.

67. Agharahimi, M. R.; LeBel, N. A., Synthesis of (-)-Monoterpenylmagnolol and Magnolol. *J. Org. Chem.* **1995,** *60*, 1856-1863.

68. Wright, A. M.; O'Neil, G. W., Total Synthesis of Honokiol by Selective Samarium-mediated Allylic Benzoate Reduction. *Tetrahedron Lett.* **2016,** *57*, 3441-3443.

69. Harada, K.; Arioka, C.; Miyakita, A.; Kubo, M.; Fukuyama, Y., Efficient Synthesis of Neurotrophic Honokiol Using Suzuki–Miyaura Reactions. *Tetrahedron Lett.* **2014,** *55*, 6001-6003.

70. Subba Reddy, B. V.; Nageshwar Rao, R.; Siva Senkar Reddy, N.; Somaiah, R.; Yadav, J. S.; Subramanyam, R., A Short and Efficient Synthesis of Honokiol via Claisen Rearrangement. *Tetrahedron Lett.* **2014,** *55*, 1049-1051.

71. Pulvirenti, L.; Muccilli, V.; Cardullo, N.; Spatafora, C.; Tringali, C., Chemoenzymatic Synthesis and α-Glucosidase Inhibitory Activity of Dimeric Neolignans Inspired by Magnolol. *Journal of Natural Products* **2017,** *80*, 1648-1657.

72. Bernaskova, M.; Schoeffmann, A.; Schuehly, W.; Hufner, A.; Baburin, I.; Hering, S., Nitrogenated Honokiol Derivatives Allosterically Modulate GABAA Receptors and Act as Strong Partial Agonists. *Bioorganic & Medicinal Chemistry* **2015,** *23*, 6757-6762.

73. Fuchs, A.; Baur, R.; Schoeder, C.; Sigel, E.; Mueller, C. E., Structural Analogues of the Natural Products Magnolol and Honokiol as Potent Allosteric Potentiators of GABAA Receptors. *Bioorg. Med. Chem.* **2014,** *22*, 6908-6917.

74. Ma, L.; Chen, J.; Wang, X.; Liang, X.; Luo, Y.; Zhu, W.; Wang, T.; Peng, M.; Li, S.; Jie, S.; Peng, A.; Wei, Y.; Chen, L., Structural Modification of Honokiol, a Biphenyl Occurring in Magnolia officinalis: the Evaluation of Honokiol Analogues as

Inhibitors of Angiogenesis and for Their Cytotoxicity and Structure-Activity Relationship. *J. Med. Chem.* **2011,** *54*, 6469-6481.

75. Li, Y.; Yuan, X.; Rong, X.; Gao, Y.; Qiu, Z.; Zhang, Z.; Zhou, D.; Li, W., Design, Synthesis and Biological Evaluation of a Hybrid Compound of Berberine and Magnolol for Improvement of Glucose and Lipid Metabolism. *RSC Adv.* **2016,** *6*, 81924-81931.

76. Kantham, S.; Chan, S.; McColl, G.; Miles, J. A.; Veliyath, S. K.; Deora, G. S.; Dighe, S. N.; Khabbazi, S.; Parat, M.-O.; Ross, B. P., Effect of the Biphenyl Neolignan Honokiol on Aβ42-Induced Toxicity in Caenorhabditis elegans, Aβ42 Fibrillation, Cholinesterase Activity, DPPH Radicals, and Iron(II) Chelation. *ACS Chemical Neuroscience* **2017,** *8*, 1901-1912.

77. Bang, K. H.; Kim, Y. K.; Min, B. S.; Na, M. K.; Rhee, Y. H.; Lee, J. P.; Bae, K. H., Antifungal Activity of Magnolol and Honokiol. *Archives of Pharmacal Research* **2000,** *23*, 46-49.

78. Sakaue, Y.; Domon, H.; Oda, M.; Takenaka, S.; Kubo, M.; Fukuyama, Y.; Okiji, T.; Terao, Y., Anti-biofilm and Bactericidal Effects of Magnolia Bark-derived Magnolol and Honokiol on Streptococcus mutans. *Microbiology And Immunology* **2016,** *60*, 10-16.

79. Vavilala, D. T.; Ponnaluri, V. K.; Kanjilal, D.; Mukherji, M., Evaluation of Anti-HIF and Anti-angiogenic Properties of Honokiol for the Treatment of Ocular Neovascular Diseases. *PloS ONE* **2014,** *9*, e113717.

80. Woodbury, A.; Yu, S. P.; Chen, D.; Gu, X.; Lee, J. H.; Zhang, J.; Espinera, A.; García, P. S.; Wei, L., Honokiol for the Treatment of Neonatal Pain and Prevention of Consequent Neurobehavioral Disorders. *Journal of Natural Products* **2015**.

81. Holmberg, A. L.; Reno, K. H.; Wool, R. P.; Epps, T. H., III, Biobased Building Blocks for the Rational Design of Renewable Block Polymers. *Soft Matter* **2014,** *10*, 7405-7424.

82. Miller, S. A., Sustainable Polymers: Replacing Polymers Derived from Fossil Fuels. *Polym. Chem.* **2014,** *5*, 3117-3118.

83. Kanetaka, Y.; Yamazaki, S.; Kimura, K., Preparation of Poly(ether ketone)s Derived from 2,5-Furandicarboxylic Acid by Polymerization in Ionic Liquid. *Macromolecules* **2016,** *49*, 1252-1258.

84. Yuan, L.; Wang, Z.; Trenor, N. M.; Tang, C., Robust Amidation Transformation of Plant Oils into Fatty Derivatives for Sustainable Monomers and Polymers. *Macromolecules* **2015,** *48*, 1320-1328.

85. Winkler, M.; Lacerda, T. M.; Mack, F.; Meier, M. A. R., Renewable Polymers from Itaconic Acid by Polycondensation and Ring-Opening-Metathesis Polymerization. *Macromolecules* **2015,** *48*, 1398-1403.

86. Weinhouse, C.; Anderson, O. S.; Bergin, I. L.; Vandenbergh, D. J.; Gyekis, J. P.; Dingman, M. A.; Yang, J. Y.; Dolinoy, D. C., Dose-Dependent Incidence of Hepatic Tumors in Adult Mice following Perinatal Exposure to Bisphenol A. *Environ. Health Persp.* **2014,** *122*, 485-491.

87. Mauck, S. C.; Wang, S.; Ding, W.; Rohde, B. J.; Fortune, C. K.; Yang, G.; Ahn, S.-K.; Robertson, M. L., Biorenewable Tough Blends of Polylactide and Acrylated Epoxidized Soybean Oil Compatibilized by a Polylactide Star Polymer. *Macromolecules* **2016,** *49*, 1605-1615.

88. Poussard, L.; Mariage, J.; Grignard, B.; Detrembleur, C.; Jérôme, C.; Calberg, C.; Heinrichs, B.; De Winter, J.; Gerbaux, P.; Raquez, J. M.; Bonnaud, L.; Dubois, P., Non-Isocyanate Polyurethanes from Carbonated Soybean Oil Using Monomeric or Oligomeric Diamines To Achieve Thermosets or Thermoplastics. *Macromolecules* **2016,** *49*, 2162-2171.

89. Leibfarth, F. A.; Hawker, C. J., The Emerging Utility of Ketenes in Polymer Chemistry. *J. Polym. Sci. A Polym. Chem.* **2013,** *51*, 3769-3782.

90. Fuji, M.; Akita, M.; Tanaka, T. Polycarbonate Copolymer and Method of Producing The Same. US 9193823 B2, 2015.

91. Mülhaupt, R., Green Polymer Chemistry and Bio-based Plastics: Dreams and Reality. *Macromol. Chem. Phys.* **2013,** *214*, 159-174.

92. Isikgor, F. H.; Becer, C. R., Lignocellulosic biomass: a sustainable platform for the production of bio-based chemicals and polymers. *Polymer Chemistry* **2015,** *6*, 4497-4559.

93. Japu, C.; Martinez de Ilarduya, A.; Alla, A.; Garcia-Martin, M. a. G.; Galbis, J. A.; Munoz-Guerra, S., Bio-based PBT Copolyesters Derived from d-Glucose: Influence of Composition on Properties. *Polym. Chem.* **2014,** *5*, 3190-3202.

94. Ragauskas, A. J.; Williams, C. K.; Davison, B. H.; Britovsek, G.; Cairney, J.; Eckert, C. A.; Frederick, W. J.; Hallett, J. P.; Leak, D. J.; Liotta, C. L.; Mielenz, J. R.; Murphy, R.; Templer, R.; Tschaplinski, T., The Path Forward for Biofuels and Biomaterials. *Science* **2006,** *311*, 484-489.

95. Laurichesse, S.; Avérous, L., Chemical Modification of Lignins: Towards Biobased Polymers. *Prog. Polym. Sci.* **2014,** *39*, 1266-1290.

96. Shearouse, W. C.; Lillie, L. M.; Reineke, T. M.; Tolman, W. B., Sustainable Polyesters Derived from Glucose and Castor Oil: Building Block Structure Impacts Properties. *ACS Macro Lett.* **2015,** *4*, 284-288.

97. Li, Q.; Zhu, W.; Li, C.; Guan, G.; Zhang, D.; Xiao, Y.; Zheng, L., A Non-phosgene Process to Homopolycarbonate and Copolycarbonates of Isosorbide Using Dimethyl Carbonate: Synthesis, Characterization, and Properties. *J. Polym. Sci. A Polym. Chem.* **2013,** *51*, 1387-1397.

98. Yokoe, M.; Aoi, K.; Okada, M., Biodegradable Polymers Based on Renewable Resources. VII. Novel Random and Alternating Copolycarbonates from 1,4:3,6-Dianhydrohexitols and Aliphatic Diols. *J. Polym. Sci. A Polym. Chem.* **2003,** *41*, 2312-2321.

99. Chatti, S.; Kricheldorf, H. R.; Schwarz, G., Copolycarbonates of isosorbide and various diols. *J. Polym. Sci. A Polym. Chem.* **2006,** *44*, 3616-3628.

100. Oliver, S.; Vittorio, O.; Cirillo, G.; Boyer, C., Enhancing the Therapeutic Effects of Polyphenols with Macromolecules. *Polym. Chem.* **2016,** *7*, 1529-1544.

101. Mou, Z.; Feng, S.; Chen, E. Y. X., Bio-based difuranic polyol monomers and their derived linear and cross-linked polyurethanes. *Polymer Chemistry* **2016,** *7*, 1593-1602.

102. Xu, J.; Feng, E.; Song, J., Renaissance of Aliphatic Polycarbonates: New Techniques and Biomedical Applications. *J. Appl. Polym. Sci.* **2014,** *131*, 1.

103. Azechi, M.; Matsumoto, K.; Endo, T., Anionic Ring-opening Polymerization of a Five-membered Cyclic Carbonate having a Glucopyranoside Structure. *J. Polym. Sci. A Polym. Chem.* **2013,** *51*, 1651-1655.

104. Besset, C. J.; Lonnecker, A. T.; Streff, J. M.; Wooley, K. L., Polycarbonates from the polyhydroxy natural product quinic acid. *Biomacromolecules* **2011,** *12*, 2512-2517.

105. Kelly, E. A.; Opanashuk, L. A.; Majewska, A. K., The Effects of Postnatal Exposure to Low-dose Bisphenol-A on Activity-dependent Plasticity in the Mouse Sensory Cortex. *Front. Neuroanat.* **2014,** *8*, 117.

106. Dolinoy, D. C.; Huang, D.; Jirtle, R. L., Maternal Nutrient Supplementation Counteracts Bisphenol A-induced DNA Hypomethylation in Early Development. *Proc. Natl. Acad. Sci. U.S.A.* **2007,** *104*, 13056-13061.

107. Pillai, V. B.; Samant, S.; Sundaresan, N. R.; Raghuraman, H.; Kim, G.; Bonner, M. Y.; Arbiser, J. L.; Walker, D. I.; Jones, D. P.; Gius, D.; Gupta, M. P., Honokiol Blocks and Reverses Cardiac Hypertrophy in Mice by Activating Mitochondrial Sirt3. *Nat. Commun.* **2015,** *6*, 6656.

108. Wang, X.; Duan, X.; Yang, G.; Zhang, X.; Deng, L.; Zheng, H.; Deng, C.; Wen, J.; Wang, N.; Peng, C.; Zhao, X.; Wei, Y.; Chen, L., Honokiol Crosses BBB and BCSFB, and Inhibits Brain Tumor Growth in Rat 9L Intracerebral Gliosarcoma Model and Human U251 Xenograft Glioma Model. *PloS ONE* **2011,** *6*, e18490.

109. Wang, H.; Liao, Z.; Sun, X.; Shi, Q.; Huo, G.; Xie, Y.; Tang, X.; Zhi, X.; Tang, Z., Intravenous Administration of Honokiol Provides Neuroprotection and Improves Functional Recovery after Traumatic Brain Injury through Cell Cycle Inhibition. *Neuropharmacology* **2014,** *86*, 9-21.

110. Munroe, M. E.; Businga, T. R.; Kline, J. N.; Bishop, G. A., Anti-Inflammatory Effects of the Neurotransmitter Agonist Honokiol in a Mouse Model of Allergic Asthma. *J. Immunol.* **2010,** *185*, 5586-5597.

111. Qiu, N.; Cai, L.-l.; Xie, D.; Wang, G.; Wu, W.; Zhang, Y.; Song, H.; Yin, H.; Chen, L., Synthesis, Structural and in vitro Studies of Well-dispersed Monomethoxy-poly(ethylene glycol)-honokiol Conjugate Micelles. *Biomed. Mater.* **2010,** *5*, 065006.

112. Xie, Y.; Long, Q.; Wu, Q. J.; Shi, S.; Dai, M.; Liu, Y.; Liu, L.; Gong, C.; Qian, Z.; Wei, Y.; Zhao, X., Improving Therapeutic Effect in Ovarian Peritoneal Carcinomatosis with Honokiol Nanoparticles in a Thermosensitive Hydrogel Composite. *RSC Adv.* **2012,** *2*, 7759-7771.

113. Feng, L.; Zhu, W.; Li, C.; Guan, G.; Zhang, D.; Xiao, Y.; Zheng, L., A High-molecular-weight and High-Tg Poly(ester carbonate) Partially Based on Isosorbide: Synthesis and Structure-property Relationships. *Polym. Chem.* **2015,** *6*, 633-642.

114. Puglisi, C.; Sturiale, L.; Montaudo, G., Thermal Decomposition Processes in Aromatic Polycarbonates Investigated by Mass Spectrometry. *Macromolecules* **1999,** *32*, 2194-2203.

115. Maharana, T.; Mohanty, B.; Negi, Y. S., Melt–solid Polycondensation of Lactic Acid and its Biodegradability. *Prog. Polym. Sci.* **2009,** *34*, 99-124.

116. Kuroda, S.-i.; Terauchi, K.; Nogami, K.; Mita, I., Degradation of Aromatic Polymers—I. Rates of Crosslinking and Chain Scission During Thermal Degradation of Several Soluble Aromatic Polymers. *Eur. Polym. J.* **1989,** *25*, 1-7.

117. Haidar, B.; Smith, T. L., Time Dependence of the Storage Modulus of Polycarbonate Following Temperature Jumps within the Glassy State. *Macromolecules* **1990,** *23*, 3710-3712.

118. Sinha Ray, S.; Yamada, K.; Okamoto, M.; Ogami, A.; Ueda, K., New Polylactide/Layered Silicate Nanocomposites. 3. High-Performance Biodegradable Materials. *Chem. Mater.* **2003,** *15*, 1456-1465.

119. Lai, S.-M.; Hsu, R.-C.; Hsieh, C.-Y.; Chiu, F.-C., Comparisons of Polycarbonate and Polycarbonate/Carbon Nanotube Nanocomposites and their Microcellular Foams Prepared using Supercritical Carbon Dioxide. *J. Mater. Sci.* **2015,** *50*, 2272-2283.

120. Gibbs, J. H.; DiMarzio, E. A., Nature of the Glass Transition and the Glassy State. *J. Chem. Phys.* **1958,** *28*, 373-383.

121. Adam, G. A.; Hay, J. N.; Parsons, I. W.; Haward, R. N., Effect of Molecular Weight on the Thermal Properties of Polycarbonates. *Polymer* **1976,** *17*, 51-57.

122. Nagy, J. A.; Benjamin, L.; Zeng, H.; Dvorak, A. M.; Dvorak, H. F., Vascular Permeability, Vascular Hyperpermeability and Angiogenesis. *Angiogenesis* **2008,** *11*, 109-119.

123. Engler, A. J.; Sen, S.; Sweeney, H. L.; Discher, D. E., Matrix Elasticity Directs Stem Cell Lineage Specification. *Cell* **2006,** *126*, 677-689.

124. Lim, S.-M.; Trzeciakowski, J. P.; Sreenivasappa, H.; Dangott, L. J.; Trache, A., RhoA-induced Cytoskeletal Tension Controls Adaptive Cellular Remodeling to Mechanical Signaling. *Integr. Biol.* **2012,** *4*, 615-627.

125. Fertier, L.; Koleilat, H.; Stemmelen, M.; Giani, O.; Joly-Duhamel, C.; Lapinte, V.; Robin, J.-J., The Use of Renewable Feedstock in UV-curable Materials – A New Age for Polymers and Green Chemistry. *Prog. Polym. Sci.* **2013,** *38*, 932-962.

126. Kristufek, S. L.; Wacker, K. T.; Tsao, Y.-Y. T.; Su, L.; Wooley, K. L., Monomer Design Strategies to Create Natural Product-based Polymer Materials. *Nat. Prod. Rep.* **2017,** *34*, 433-459.

127. Anastas, P.; Eghbali, N., Green Chemistry: Principles and Practice. *Chem. Soc. Rev.* **2010,** *39*, 301-312.

128. Hoyle, C. E.; Bowman, C. N., Thiol–Ene Click Chemistry. *Angew. Chem. Int. Ed.* **2010,** *49*, 1540-1573.

129. Hoyle, C. E.; Lowe, A. B.; Bowman, C. N., Thiol-Click Chemistry: A Multifaceted Toolbox for Small Molecule and Polymer Synthesis. *Chem. Soc. Rev.* **2010,** *39*, 1355-1387.

130. Lowe, A. B., Thiol-ene "Click" Reactions and Recent Applications in Polymer and Materials Synthesis: A First Update. *Polym. Chem.* **2014,** *5*, 4820-4870.

131. Yoshimura, T.; Shimasaki, T.; Teramoto, N.; Shibata, M., Bio-based Polymer Networks by Thiol–ene Photopolymerizations of Allyl-etherified Eugenol Derivatives. *Eur. Polym. J.* **2015,** *67*, 397-408.

132. Donovan, B. R.; Cobb, J. S.; Hoff, E. F. T.; Patton, D. L., Thiol-ene Adhesives from Clove Oil Derivatives. *RSC Adv.* **2014,** *4*, 61927-61935.

133. Lorenzini, C.; Haider, A.; Kang, I.-K.; Sangermano, M.; Abbad-Andalloussi, S.; Mazeran, P.-E.; Lalevée, J.; Renard, E.; Langlois, V.; Versace, D.-L., Photoinduced Development of Antibacterial Materials Derived from Isosorbide Moiety. *Biomacromolecules* **2015,** *16*, 683-694.

134. Modjinou, T.; Versace, D.-L.; Abbad-Andallousi, S.; Bousserrhine, N.; Babinot, J.; Langlois, V.; Renard, E., Antibacterial Networks Based on Isosorbide and Linalool by Photoinitiated Process. *ACS Sustain. Chem. Eng.* **2015,** *3*, 1094-1100.

135. Firdaus, M.; Montero de Espinosa, L.; Meier, M. A. R., Terpene-Based Renewable Monomers and Polymers via Thiol–Ene Additions. *Macromolecules* **2011,** *44*, 7253-7262.

136. Firdaus, M.; Meier, M. A. R., Renewable Polyamides and Polyurethanes Derived from Limonene. *Green Chem.* **2013,** *15*, 370-380.

137. Yang, G.; Kristufek, S. L.; Link, L. A.; Wooley, K. L.; Robertson, M. L., Synthesis and Physical Properties of Thiol–Ene Networks Utilizing Plant-Derived Phenolic Acids. *Macromolecules* **2015,** *48*, 8418-8427.

138. Wacker, K. T.; Kristufek, S. L.; Lim, S.-M.; Kahn, S.; Wooley, K. L., Bio-based Polycarbonates Derived from the Neolignan Honokiol. *RSC Adv.* **2016,** *6*, 81672-81679.

139. Zhao, C.; Liu, Z.-Q., Comparison of Antioxidant Abilities of Magnolol and Honokiol to Scavenge Radicals and to Protect DNA. *Biochimie* **2011,** *93*, 1755-1760.

140. Amorati, R.; Zotova, J.; Baschieri, A.; Valgimigli, L., Antioxidant Activity of Magnolol and Honokiol: Kinetic and Mechanistic Investigations of Their Reaction with Peroxyl Radicals. *J. Org. Chem.* **2015,** *80*, 10651-10659.

141. Scherer, R.; Godoy, H. T., Antioxidant Activity Index (AAI) by the 2,2-diphenyl-1-picrylhydrazyl Method. *Food Chem.* **2009,** *112*, 654-658.

142. Hill, L. W., Calculation of Crosslink Density in Short Chain Networks. *Progress in Organic Coatings* **1997,** *31*, 235-243.

143. Erdmann, L.; Macedo, B.; Uhrich, K. E., Degradable Poly(anhydride ester) Implants: Effects of Localized Salicylic Acid Release on Bone. *Biomaterials* **2000,** *21*, 2507-2512.

144. Carbone-Howell, A. L.; Stebbins, N. D.; Uhrich, K. E., Poly(anhydride-esters) Comprised Exclusively of Naturally Occurring Antimicrobials and EDTA: Antioxidant and Antibacterial Activities. *Biomacromolecules* **2014,** *15*, 1889-1895.

145. Chandorkar, Y.; Bhagat, R. K.; Madras, G.; Basu, B., Cross-Linked, Biodegradable, Cytocompatible Salicylic Acid Based Polyesters for Localized, Sustained Delivery of Salicylic Acid: An In Vitro Study. *Biomacromolecules* **2014,** *15*, 863-875.

146. Chandorkar, Y.; Bhaskar, N.; Madras, G.; Basu, B., Long-Term Sustained Release of Salicylic Acid from Cross-Linked Biodegradable Polyester Induces a Reduced Foreign Body Response in Mice. *Biomacromolecules* **2015,** *16*, 636-649.

147. Ouimet, M. A.; Griffin, J.; Carbone-Howell, A. L.; Wu, W.-H.; Stebbins, N. D.; Di, R.; Uhrich, K. E., Biodegradable Ferulic Acid-Containing Poly(anhydride-ester): Degradation Products with Controlled Release and Sustained Antioxidant Activity. *Biomacromolecules* **2013,** *14*, 854-861.

148. Jabara, R.; Chronos, N.; Robinson, K., Novel Bioabsorbable Salicylate-based Polymer as a Drug-eluting Stent Coating. *Catheterization and Cardiovascular Interventions* **2008,** *72*, 186-194.

149. Broaders, K. E.; Grandhe, S.; Frechet, J. M., A Biocompatible Oxidation-Triggered Carrier Polymer with Potential in Therapeutics. *J. Am. Chem. Soc.* **2011,** *133*, 756-758.

150. Liu, Y.; Ai, K.; Ji, X.; Askhatova, D.; Du, R.; Lu, L.; Shi, J., Comprehensive Insights into the Multi-Antioxidative Mechanisms of Melanin Nanoparticles and Their Application To Protect Brain from Injury in Ischemic Stroke. *J. Am. Chem. Soc.* **2017,** *139*, 856-862.

151. Lux, C. D.; Joshi-Barr, S.; Nguyen, T.; Mahmoud, E.; Schopf, E.; Fomina, N.; Almutairi, A., Biocompatible Polymeric Nanoparticles Degrade and Release Cargo in Response to Biologically Relevant Levels of Hydrogen Peroxide. *J. Am. Chem. Soc.* **2012,** *134*, 15758-15764.

152. Wattamwar, P. P.; Mo, Y.; Wan, R.; Palli, R.; Zhang, Q.; Dziubla, T. D., Antioxidant Activity of Degradable Polymer Poly(trolox ester) to Suppress Oxidative Stress Injury in the Cells. *Adv. Funct. Mater.* **2010,** *20*, 147-154.

153. Grubbs, R. H., 4.03 - Living Ring-Opening Olefin Metathesis Polymerization. In *Polymer Science: A Comprehensive Reference*, Möller, K. M., Ed. Elsevier: Amsterdam, 2012; pp 21-29.

154. Berda, E. B.; Wagener, K. B., 5.09 - Advances in Acyclic Diene Metathesis Polymerization. In *Polymer Science: A Comprehensive Reference*, Möller, K. M., Ed. Elsevier: Amsterdam, 2012; pp 195-216.

155. Moerdyk, J. P.; Bielawski, C. W., 4.20 - Architectures of Polymers Synthesized using ROMP. In *Polymer Science: A Comprehensive Reference*, Möller, K. M., Ed. Elsevier: Amsterdam, 2012; pp 523-550.

156. Li, H.; Rojas, G.; Wagener, K. B., Precision Long-Chain Branched Polyethylene via Acyclic Diene Metathesis Polymerization. *ACS Macro Lett.* **2015,** *4*, 1225-1228.

157. Caire da Silva, L.; Rojas, G.; Schulz, M. D.; Wagener, K. B., Acyclic Diene Metathesis Polymerization: History, Methods and Applications. *Prog. Polym. Sci.* **2017,** *69*, 79-107.

158. Bai, Y.; Clark, J. H.; Farmer, T. J.; Ingram, I. D. V.; North, M., Wholly Biomass Derivable Sustainable Polymers by Ring-opening Metathesis Polymerisation of Monomers Obtained from Furfuryl Alcohol and Itaconic Anhydride. *Polym. Chem.* **2017,** *8*, 3074-3081.

159. Lv, A.; Li, Z.-L.; Du, F.-S.; Li, Z.-C., Synthesis, Functionalization, and Controlled Degradation of High Molecular Weight Polyester from Itaconic Acid via ADMET Polymerization. *Macromolecules* **2014,** *47*, 7707-7716.

160. Strick, B. F.; Delferro, M.; Geiger, F. M.; Thomson, R. J., Investigations into Apopinene as a Biorenewable Monomer for Ring-Opening Metathesis Polymerization. *ACS Sustain. Chem. Eng.* **2015,** *3*, 1278-1281.

161. Peng, Y.; Decatur, J.; Meier, M. A. R.; Gross, R. A., Ring-Opening Metathesis Polymerization of a Naturally Derived Macrocyclic Glycolipid. *Macromolecules* **2013,** *46*, 3293-3300.

162. Gao, W.; Hagver, R.; Shah, V.; Xie, W.; Gross, R. A.; Ilker, M. F.; Bell, C.; Burke, K. A.; Coughlin, E. B., Glycolipid Polymer Synthesized from Natural Lactonic Sophorolipids by Ring-Opening Metathesis Polymerization. *Macromolecules* **2007,** *40*, 145-147.

163. Hibert, G.; Grau, E.; Pintori, D.; Lecommandoux, S.; Cramail, H., ADMET Polymerization of α,ω-Unsaturated Glycolipids: Synthesis and Physico-chemical Properties of the Resulting Polymers. *Polym. Chem.* **2017,** *8*, 3731-3739.

164. Rybak, A.; Meier, M. A. R., Acyclic Diene Metathesis with a Monomer from Renewable Resources: Control of Molecular Weight and One-Step Preparation of Block Copolymers. *ChemSusChem* **2008,** *1*, 542-547.

165. Barbara, I.; Flourat, A. L.; Allais, F., Renewable Polymers Derived from Ferulic Acid and Biobased Diols via ADMET. *Eur. Polym. J.* **2015,** *62*, 236-243.

166. Llevot, A.; Grau, E.; Carlotti, S.; Grelier, S.; Cramail, H., Dimerization of Abietic Acid for the Design of Renewable Polymers by ADMET. *Eur. Polym. J.* **2015,** *67*, 409-417.

167. Lebarbé, T.; More, A. S.; Sane, P. S.; Grau, E.; Alfos, C.; Cramail, H., Bio-Based Aliphatic Polyurethanes Through ADMET Polymerization in Bulk and Green Solvent. *Macromol. Rapid Comm.* **2014,** *35*, 479-483.

168. Buckler, J. N.; Banwell, M. G.; Kordbacheh, F.; Parish, C. R.; Santiago, F. S.; Khachigian, L. M., Developing Neolignans as Proangiogenic Agents: Stereoselective Total Syntheses and Preliminary Biological Evaluations of the Four Guaiacylglycerol 8-O-4′-Coniferyl Ethers. *ACS Omega* **2017,** *2*, 7375-7388.

169. Wang, D.; Jin, Q.; Xiang, H.; Wang, W.; Guo, N.; Zhang, K.; Tang, X.; Meng, R.; Feng, H.; Liu, L.; Wang, X.; Liang, J.; Shen, F.; Xing, M.; Deng, X.; Yu, L., Transcriptional and Functional Analysis of the Effects of Magnolol: Inhibition of Autolysis and Biofilms in Staphylococcus aureus. *PloS ONE* **2011,** *6*, e26833.

170. Luleburgaz, S.; Abuaf, M.; Tunca, U.; Hizal, G.; Durmaz, H., Synthesis of Poly(vitamin C) through ADMET. *Macromol. Rapid Comm.* **2017,** *38*, n/a-n/a.

171. Lillie, L. M.; Tolman, W. B.; Reineke, T. M., Structure/Property Relationships in Copolymers Comprising Renewable Isosorbide, Glucarodilactone, and 2,5-Bis(hydroxymethyl)furan Subunits. *Polym. Chem.* **2017,** *8*, 3746-3754.

172. Hollande, L.; Jaufurally, A. S.; Ducrot, P.-H.; Allais, F., ADMET Polymerization of Biobased Monomers Deriving from Syringaresinol. *RSC Adv.* **2016,** *6*, 44297-44304.

173. Firdaus, M.; Meier, M. A. R., Renewable Co-polymers Derived from Vanillin and Fatty Acid Derivatives. *Eur. Polym. J.* **2013,** *49*, 156-166.

174. Vlaminck, L.; Lingier, S.; Hufendiek, A.; Du Prez, F. E., Lignin Inspired Phenolic Polyethers Synthesized via ADMET: Systematic Structure-property Investigation. *Eur. Polym. J.* **2017,** *95*, 503-513.

175. Ding, R.; Xia, Y.; Mauldin, T. C.; Kessler, M. R., Biorenewable ROMP-based Thermosetting Copolymers from Functionalized Castor Oil Derivative with Various Cross-linking Agents. *Polymer* **2014,** *55*, 5718-5726.

176. Hassam, M.; Taher, A.; Arnott, G. E.; Green, I. R.; van Otterlo, W. A. L., Isomerization of Allylbenzenes. *Chem. Rev.* **2015,** *115*, 5462-5569.

177. Llevot, A.; Grau, E.; Carlotti, S.; Grelier, S.; Cramail, H., ADMET Polymerization of Bio-based Biphenyl Compounds. *Polym. Chem.* **2015,** *6*, 7693-7700.

178. Hong, S. H.; Sanders, D. P.; Lee, C. W.; Grubbs, R. H., Prevention of Undesirable Isomerization during Olefin Metathesis. *J. Am. Chem. Soc.* **2005,** *127*, 17160-17161.

179. Lv, A.; Cui, Y.; Du, F.-S.; Li, Z.-C., Thermally Degradable Polyesters with Tunable Degradation Temperatures via Postpolymerization Modification and Intramolecular Cyclization. *Macromolecules* **2016,** *49*, 8449-8458.

180. Vlaminck, L.; De Bruycker, K.; Turunc, O.; Du Prez, F. E., ADMET and TAD Chemistry: A Sustainable Alliance. *Polym. Chem.* **2016,** *7*, 5655-5663.

181. Kreye, O.; Tóth, T.; Meier, M. A. R., Introducing Multicomponent Reactions to Polymer Science: Passerini Reactions of Renewable Monomers. *J. Am. Chem. Soc.* **2011,** *133*, 1790-1792.

182. Becker, G.; Ackermann, L.-M.; Schechtel, E.; Klapper, M.; Tremel, W.; Wurm, F. R., Joining Two Natural Motifs: Catechol-Containing Poly(phosphoester)s. *Biomacromolecules* **2017,** *18*, 767-777.

183. de Espinosa, L. M.; Meier, M. A. R.; Ronda, J. C.; Galià, M.; Cádiz, V., Phosphorus-containing Renewable Polyester-Polyols via ADMET Polymerization: Synthesis, Functionalization, and Radical Crosslinking. *J. Polym. Sci. A Polym. Chem.* **2010,** *48*, 1649-1660.

184. Gaines, T. W.; Trigg, E. B.; Winey, K. I.; Wagener, K. B., High Melting Precision Sulfone Polyethylenes Synthesized by ADMET Chemistry. *Macromol. Chem. Phys.* **2016,** *217*, 2351-2359.

185. Thompson, D.; Yamakado, R.; Wagener, K. B., Extending the Methylene Spacer Length of ADMET Hydroxy-Functionalized Polymers. *Macromol. Chem. Phys.* **2014,** *215*, 1212-1217.

186. Wu, Z.; Grubbs, R. H., Synthesis of Narrow Dispersed Linear Polyethylene and Block Copolymers from Polycyclobutene. *Macromolecules* **1994,** *27*, 6700-6703.

APPENDIX

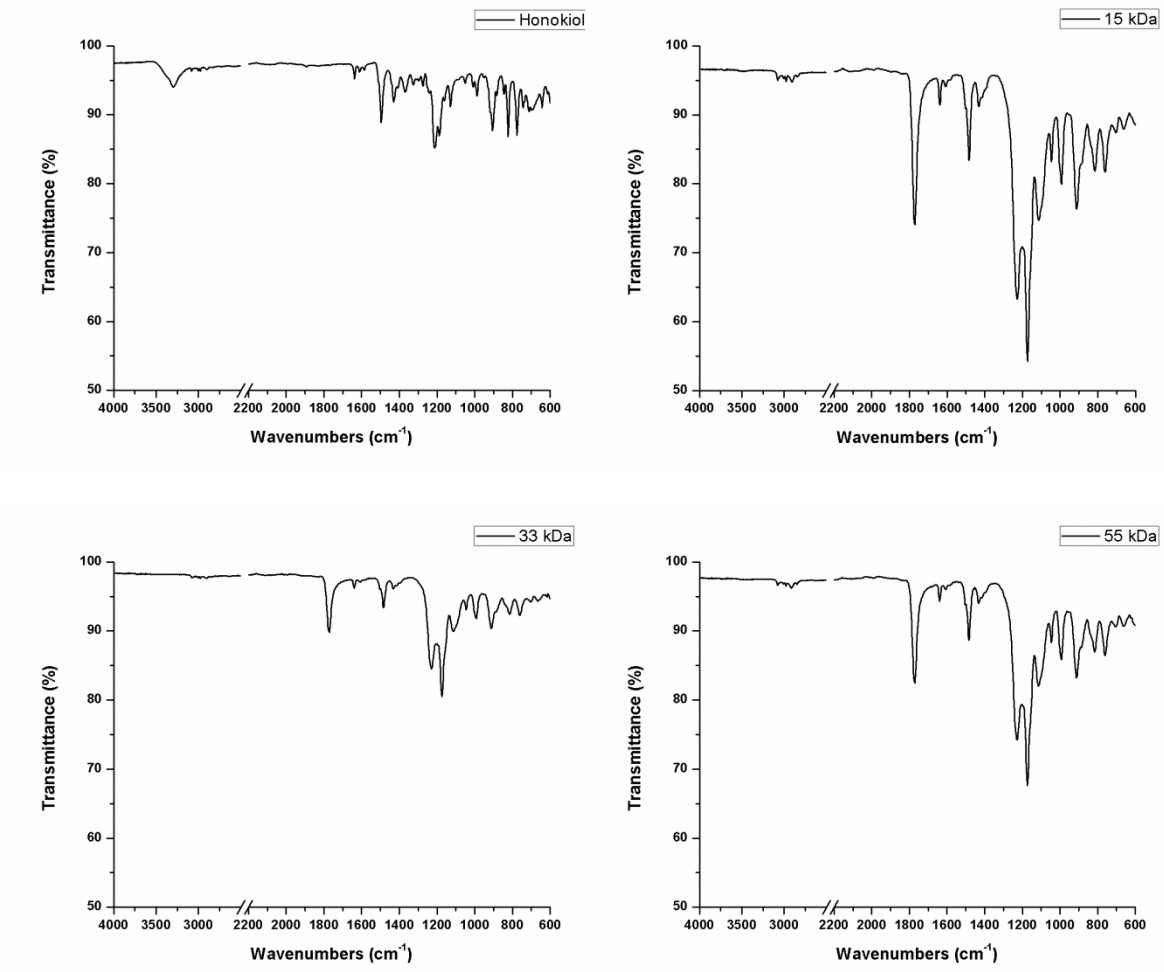

Figure A-1. ATR-FTIR spectra comparing PHC and honokiol.

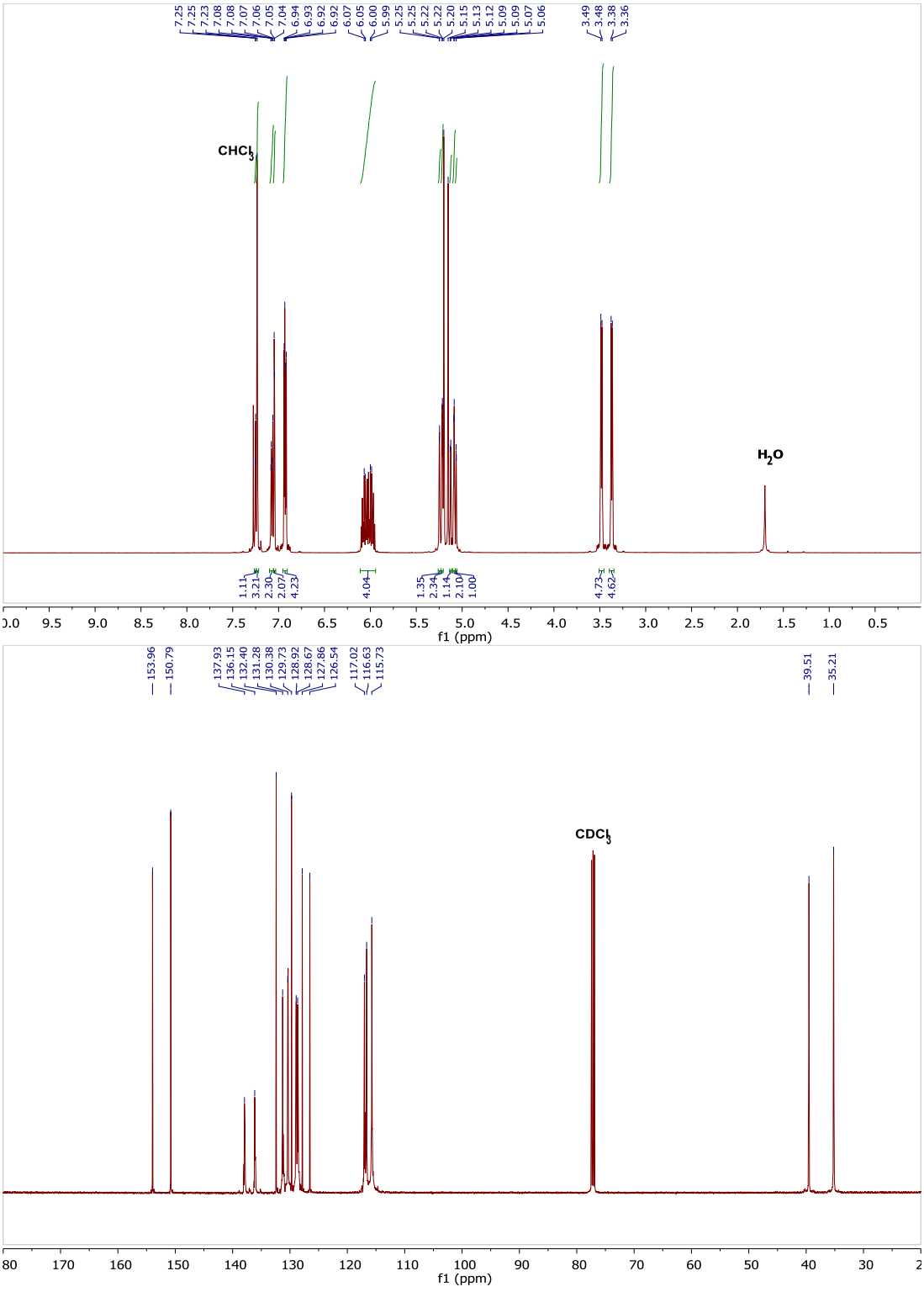

Figure A-2. ^{1}H (500 MHz) and ^{13}C (125 MHz) NMR spectra for honokiol.

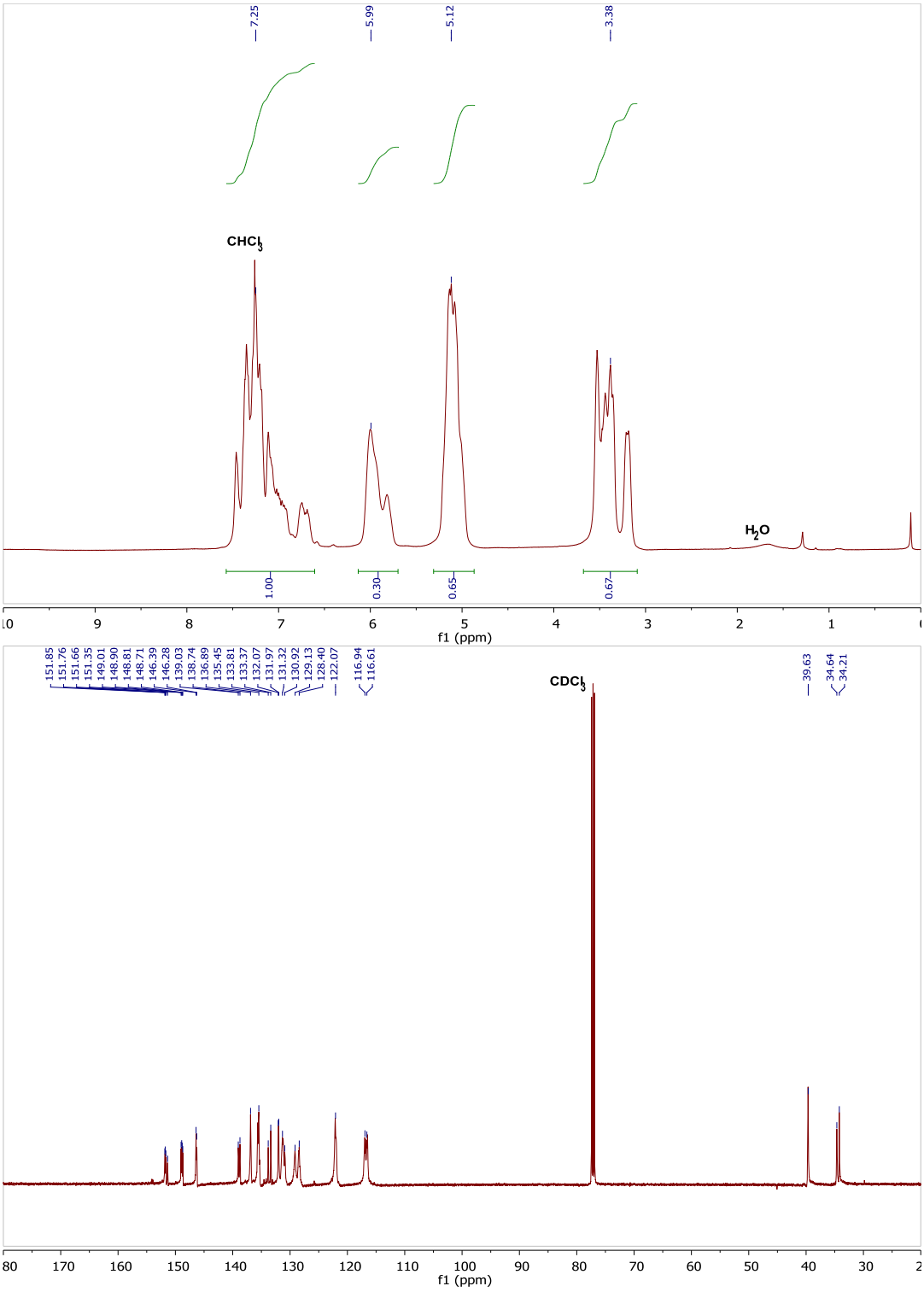

Figure A-3. ^{1}H (500 MHz) and ^{13}C (125 MHz) NMR spectra for poly(honokiol carbonate) having a M_n of 15 kDa.

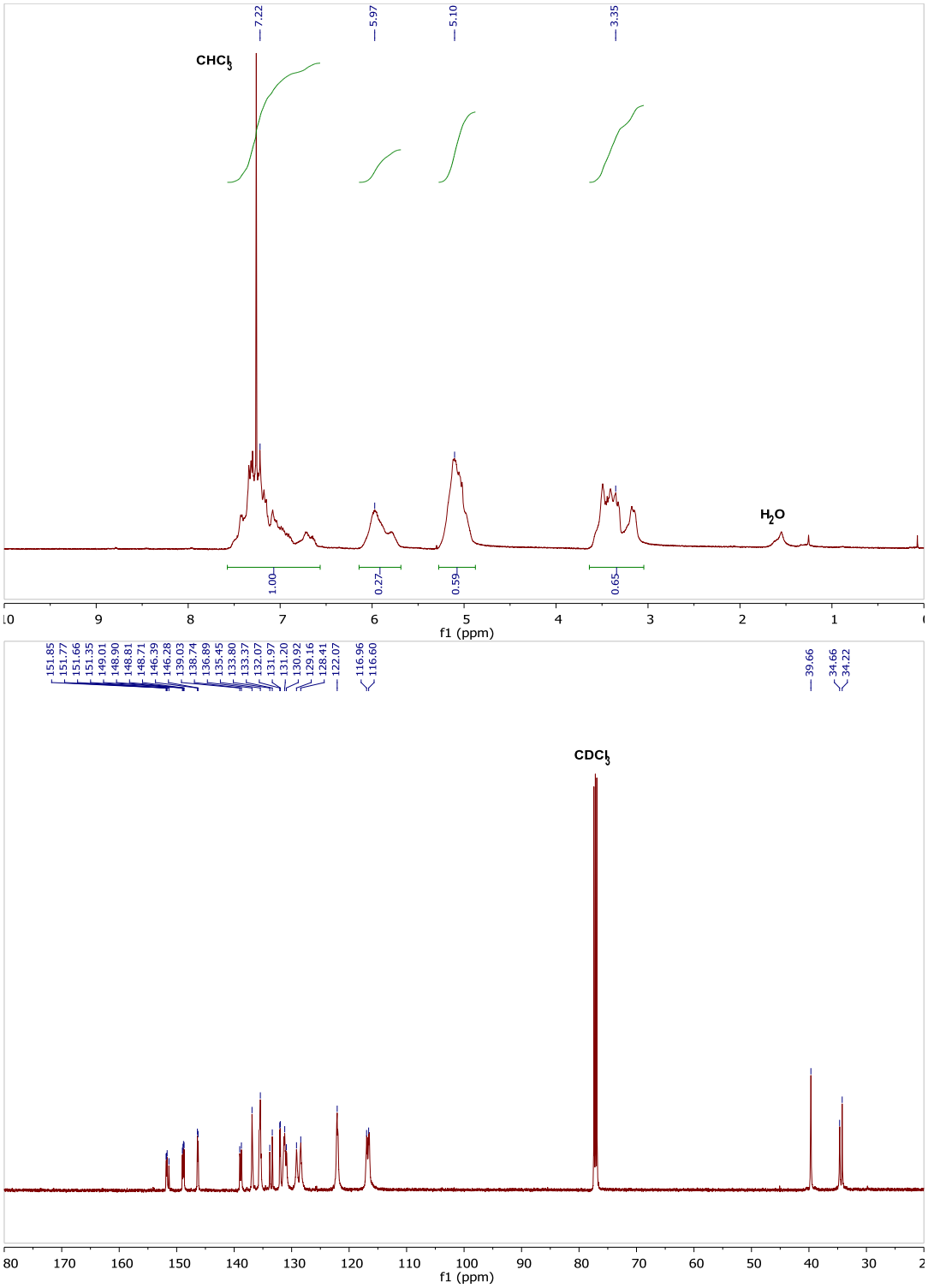

Figure A-4. ^{1}H (500 MHz) and ^{13}C (125 MHz) NMR spectra for poly(honokiol carbonate) having a M_n of 33 kDa.

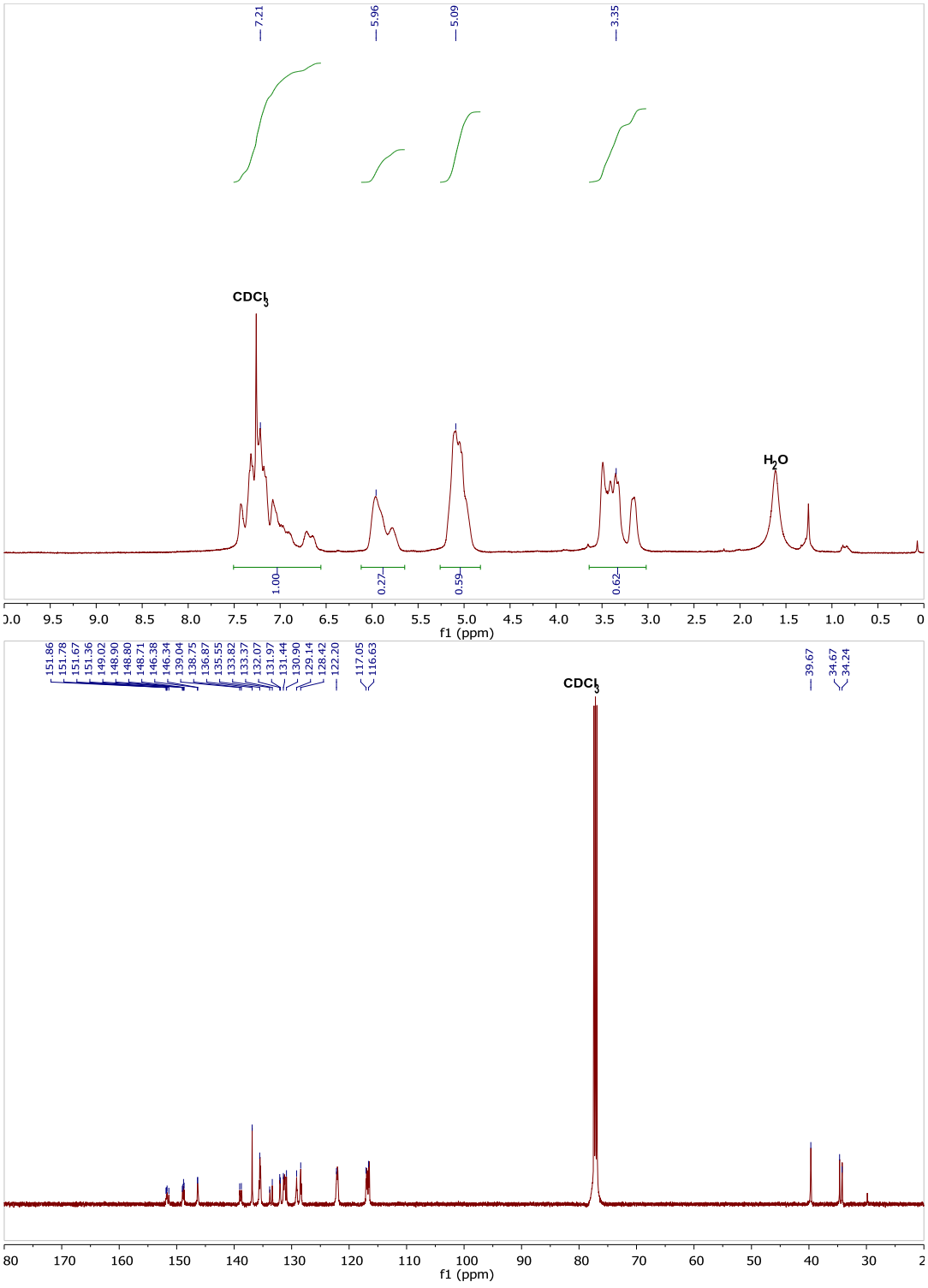

Figure A-5. ^{1}H (500 MHz) and ^{13}C (125 MHz) NMR spectra for poly(honokiol carbonate) having a M_n of 55 kDa.

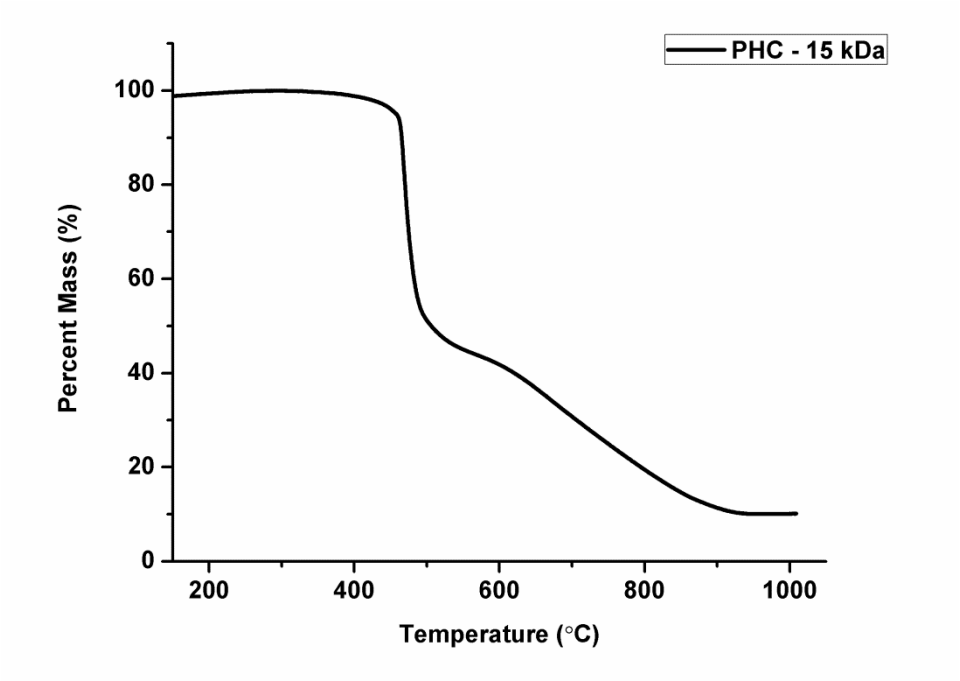

Figure A-6. TGA – Thermal degradation of PHC having a M_n of 15 kDa.

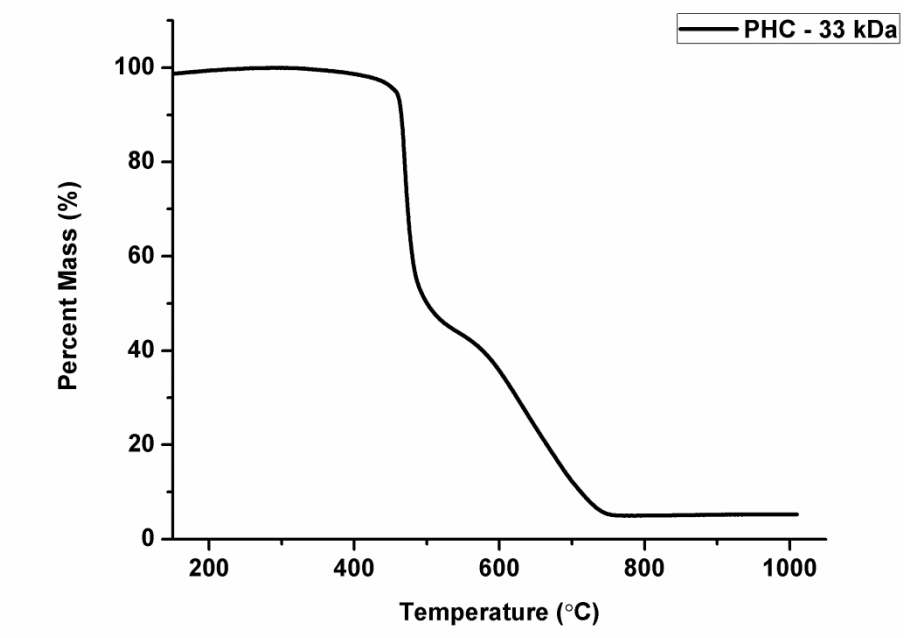

Figure A-7. TGA – Thermal degradation of PHC having a M_n of 33 kDa.

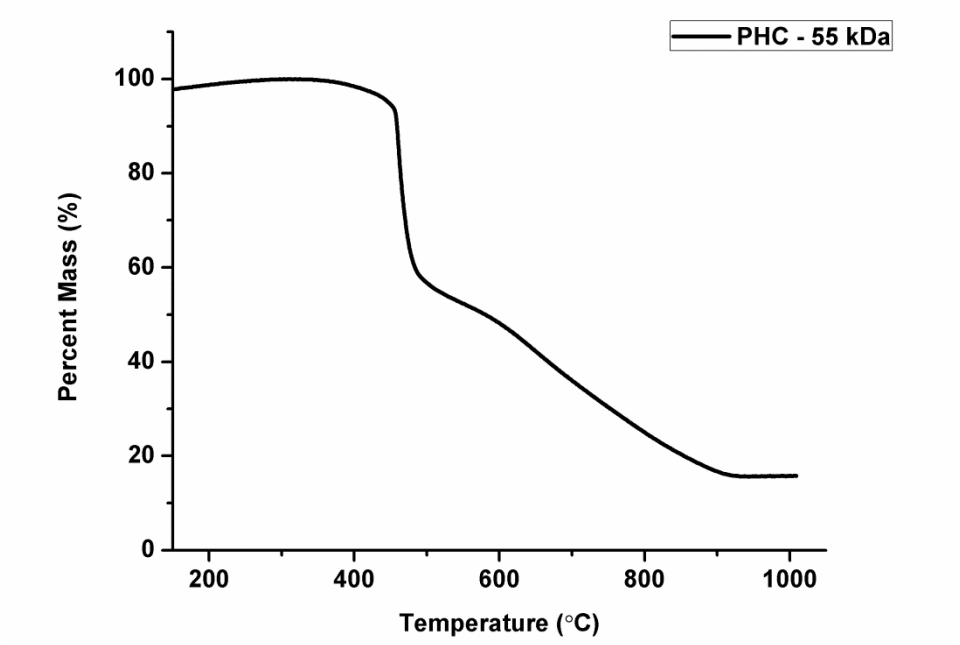

Figure A-8. TGA – Thermal degradation of PHC having a M_n of 55 kDa.

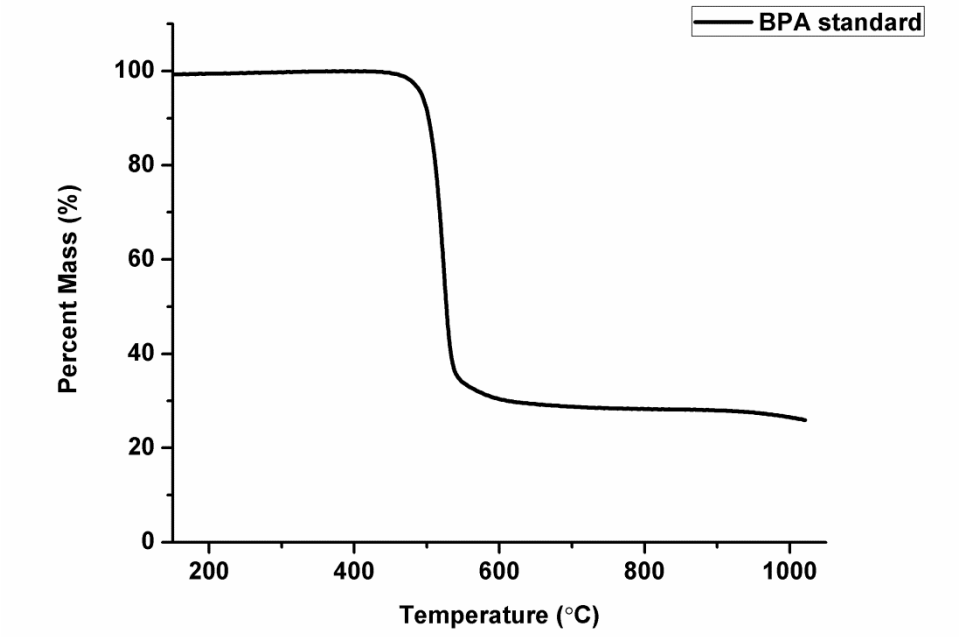

Figure A-9. TGA – Thermal degradation of poly(BPA carbonate) having a M_n of 21 kDa.

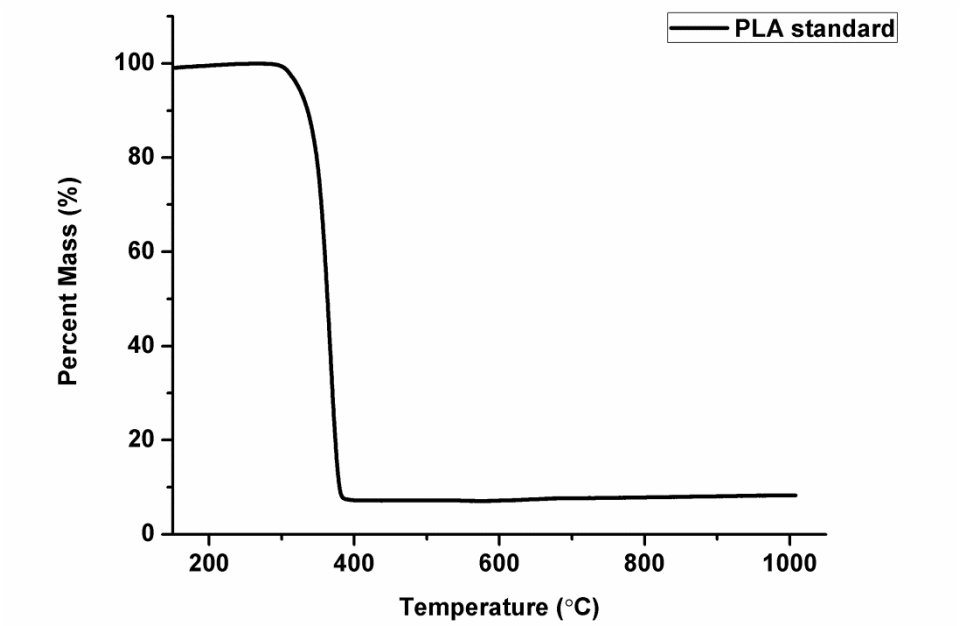

Figure A-10. TGA – Thermal degradation of poly(lactic acid) having a M_n of 30 kDa.

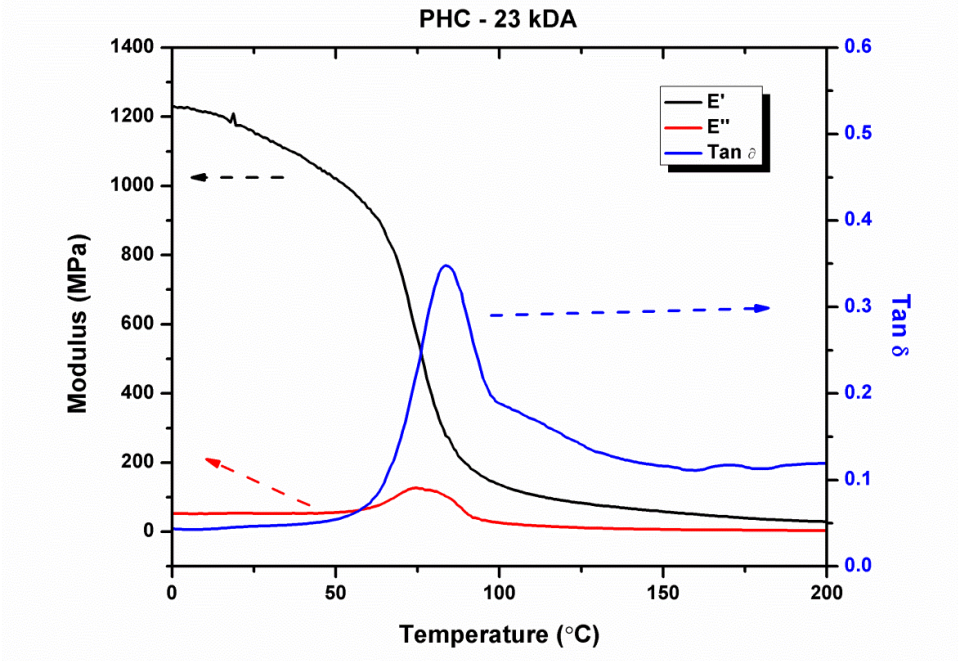

Figure A-11. DMA – Representative dynamic mechanical analysis of PHC having a M_n of 23 kDa.

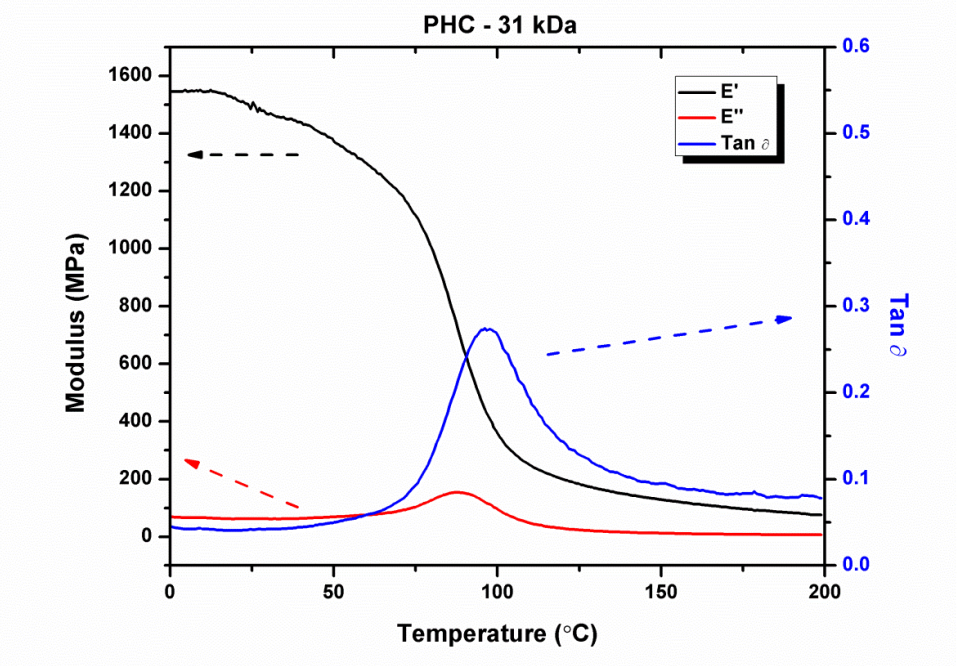

Figure A-12. DMA – Representative dynamic mechanical analysis of PHC having a M_n of 31 kDa.

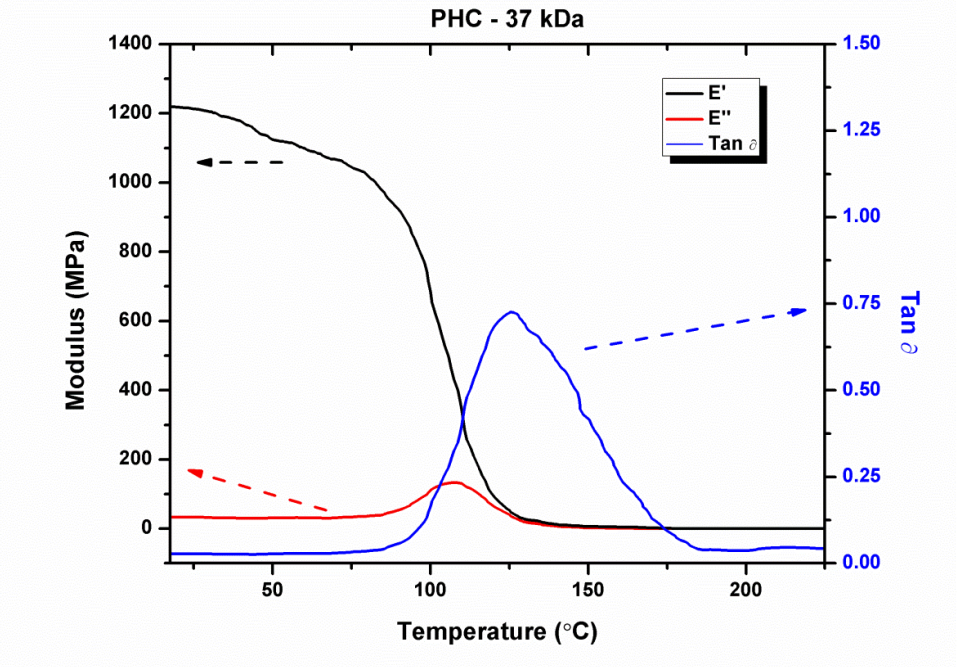

Figure A-13. DMA – Representative dynamic mechanical analysis of PHC having a M_n of 37 kDa.

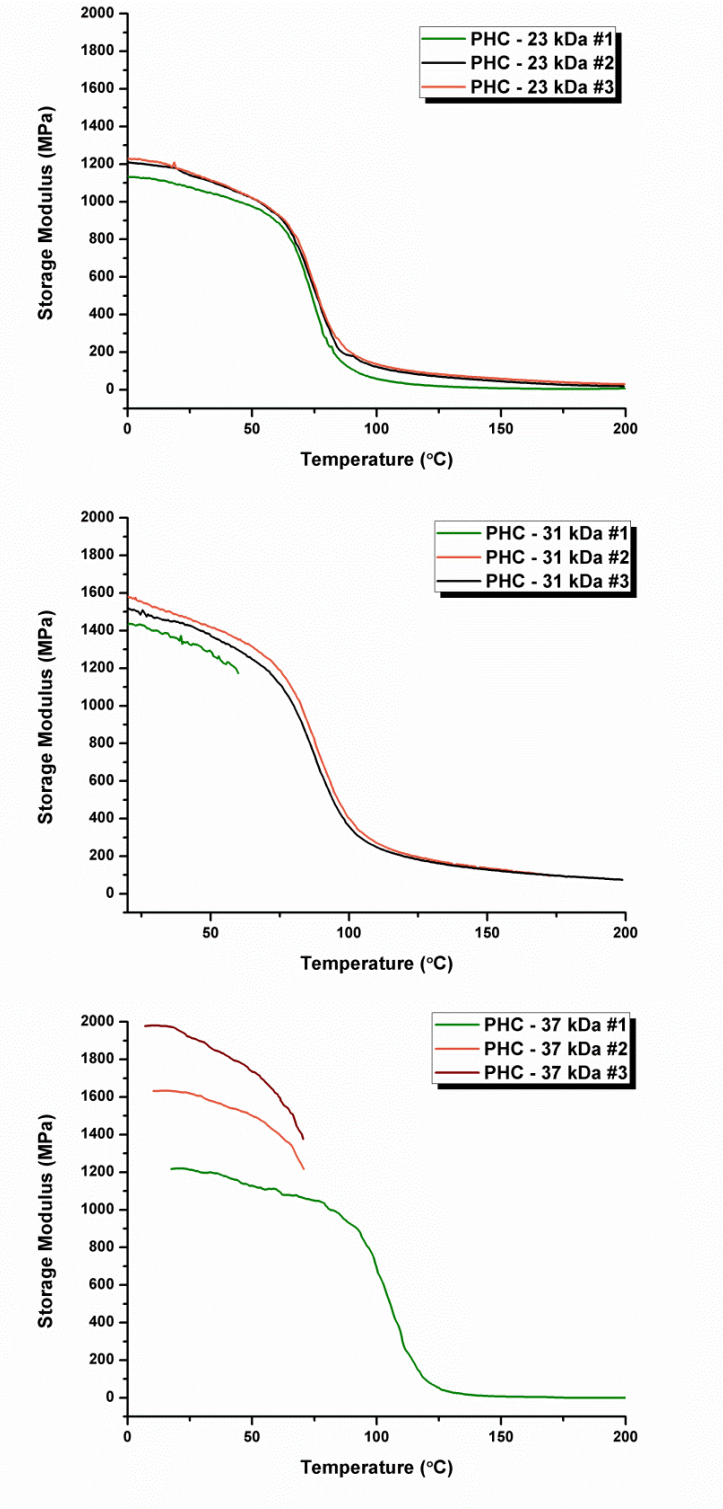

Figure A-14. DMA – Composite of storage moduli traces collected for each of the PHC samples having M_n values of (a) 23 kDa, (b) 31 kDa, (c) 37 kDa.

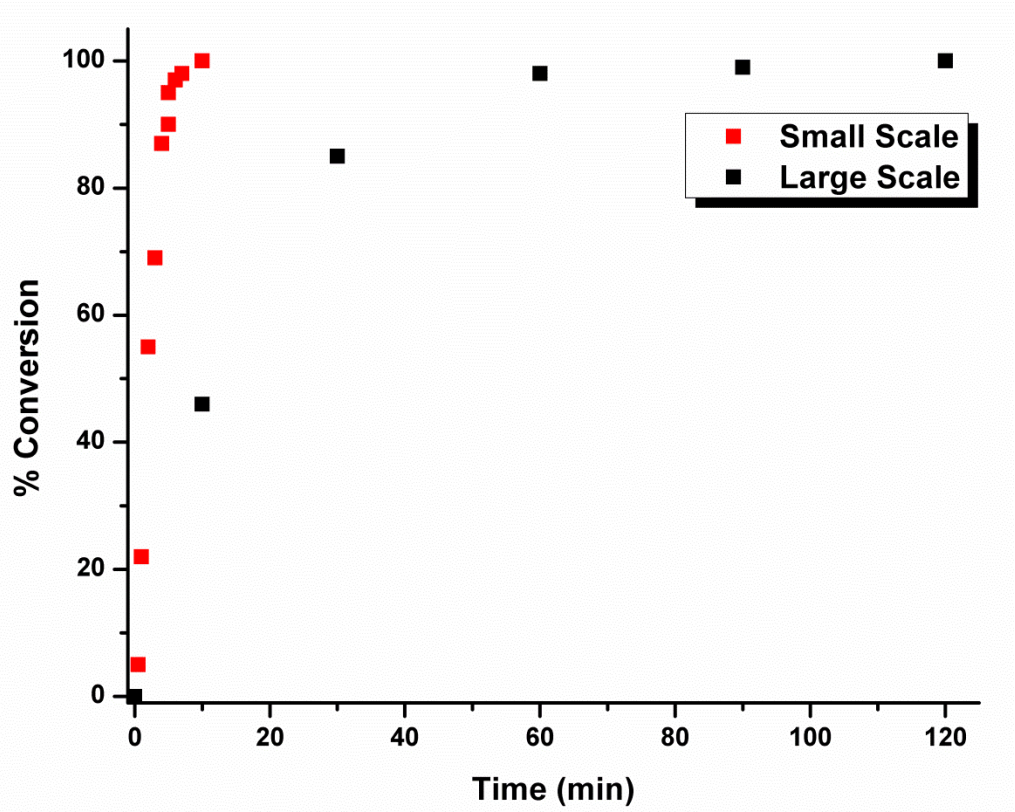

Figure A-15. Reaction kinetics for the synthesis of **1**. Both reactions were performed under identical conditions (*vide supra*) with either *ca.* 100 mg (small scale) and *ca*. 2.0 g (large scale) of starting material, magnolol

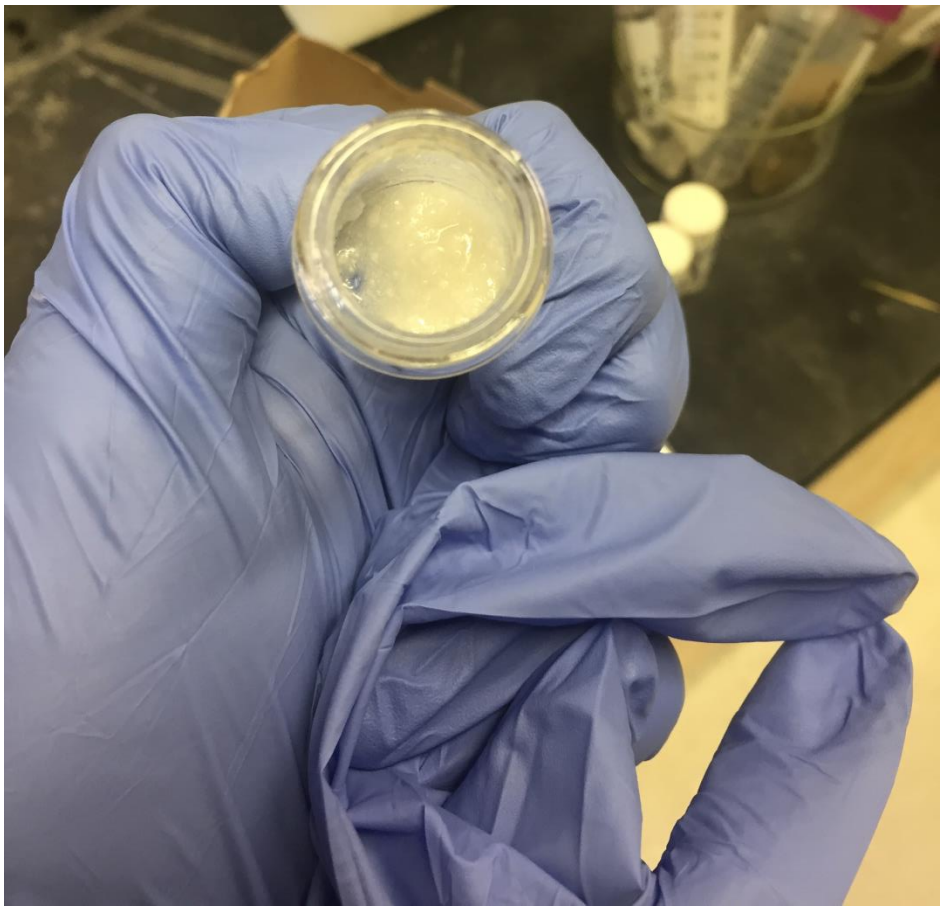

Figure A-16. Magnolol, PETMP, and DMPA mixture at room temperature.

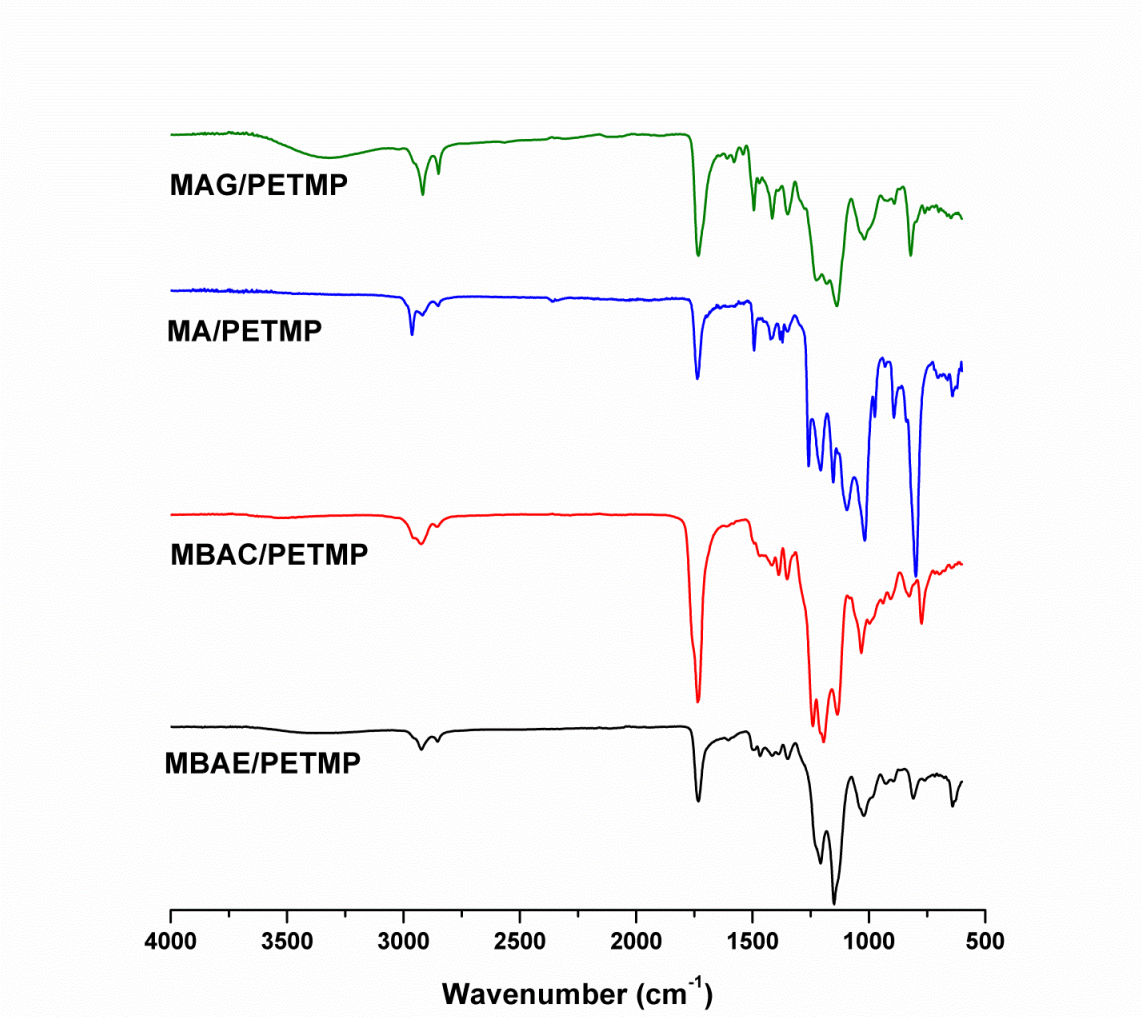

Figure A-17. ATR-FTIR of magnolol thermosets.

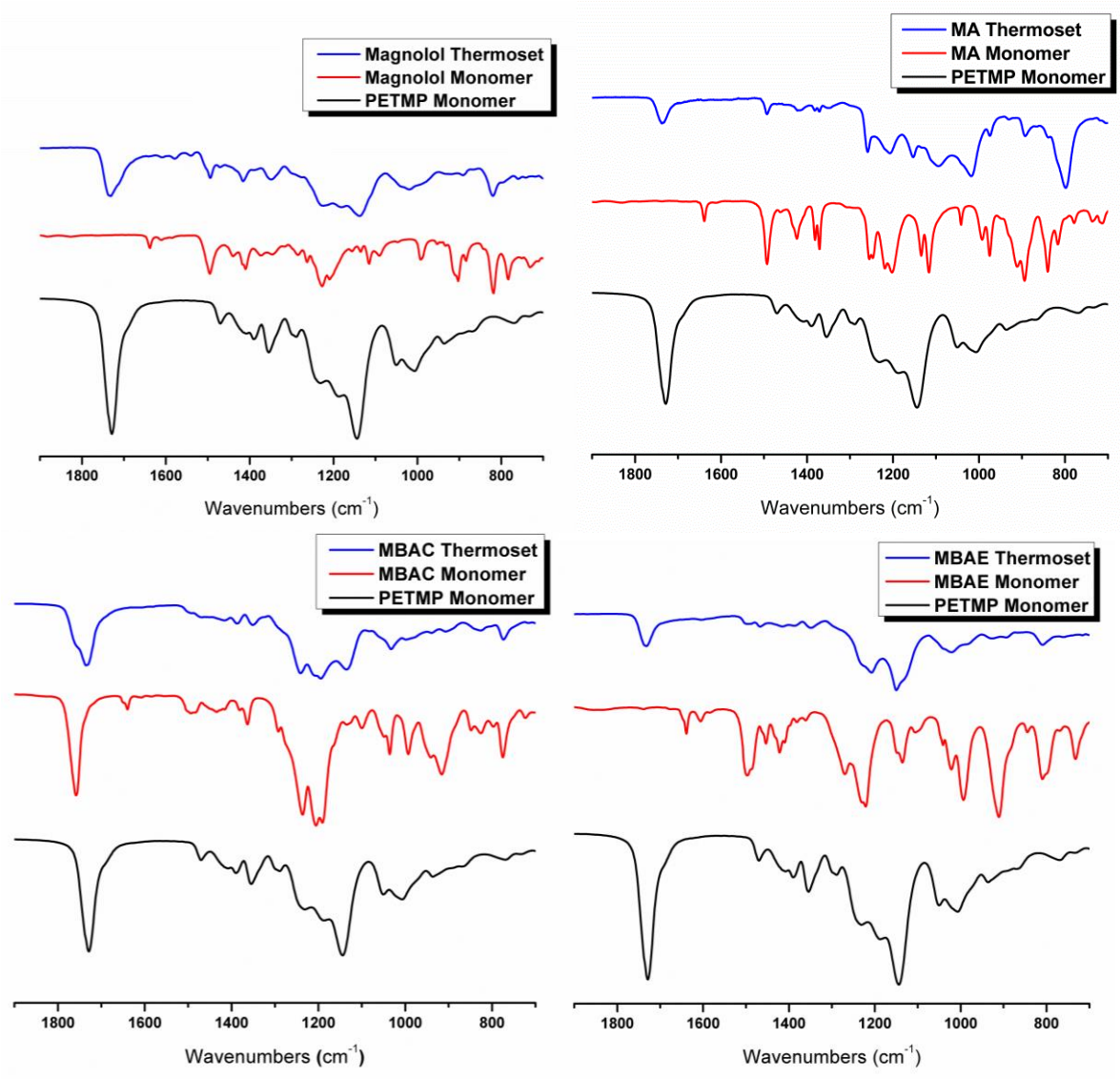

Figure A-18. FTIR comparisons of monomers to thermosets.

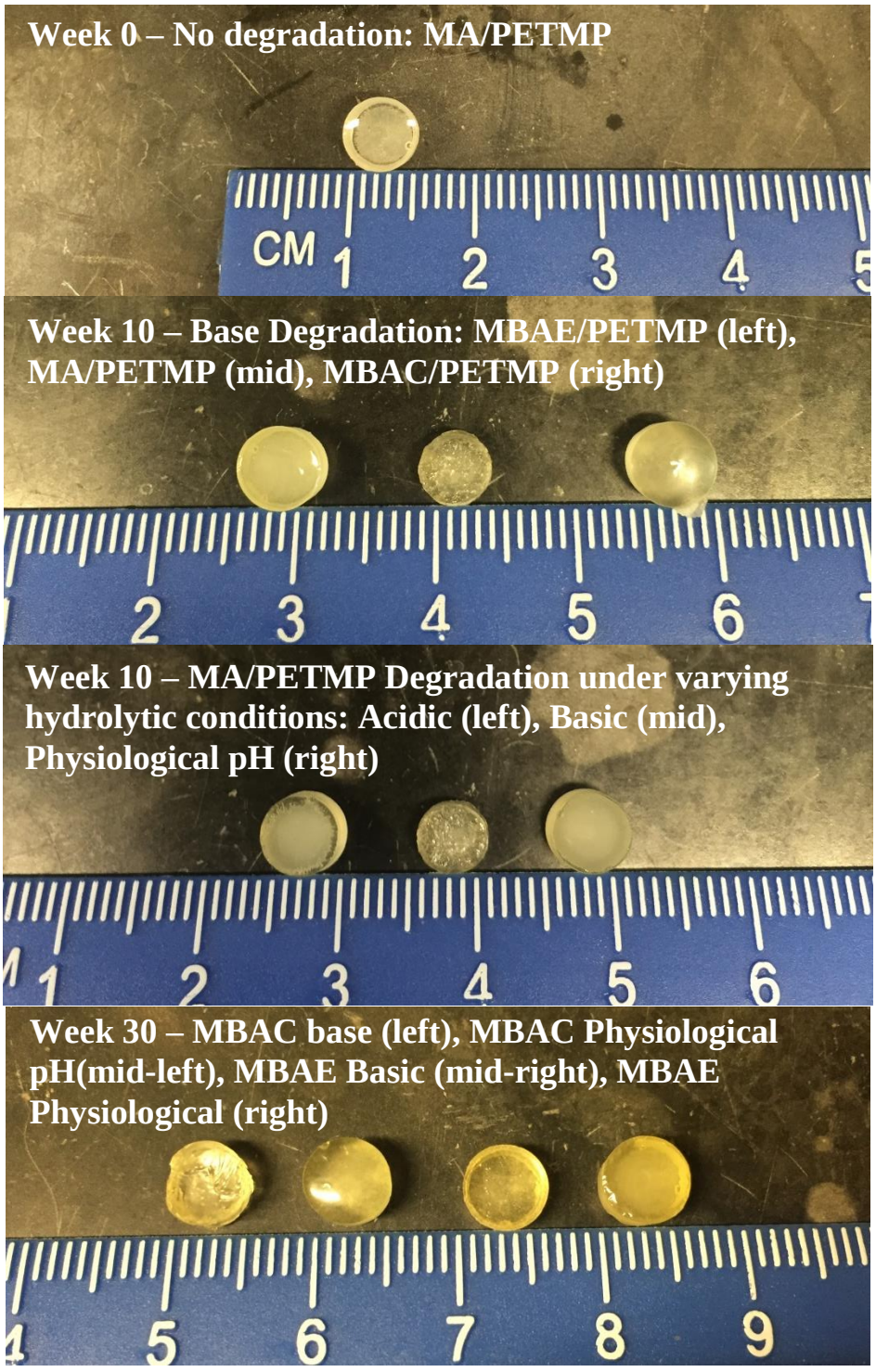

Figure A-19. Pellet degradation at 0, 10, and 30 weeks, comparing different thermoset compositions and hydrolytic conditions.

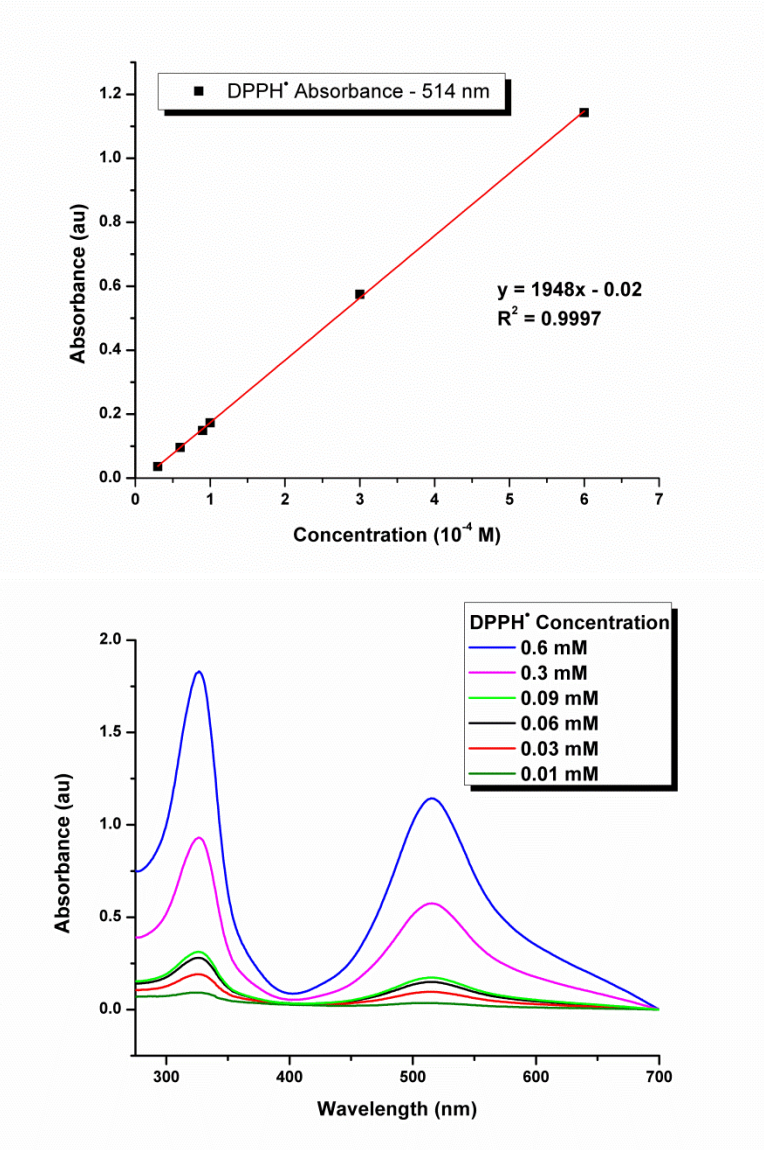

Figure A-20. UV-vis DPPH• calibration curve (upper) and DPPH• spectra (lower) in methanol.